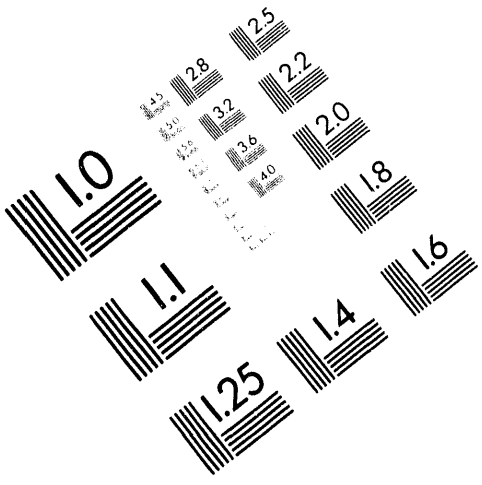

Association for Information and Image Management

1100 Wayne Avenue, Suite 1100
Silver Spring, Maryland 20910

301/587-8202

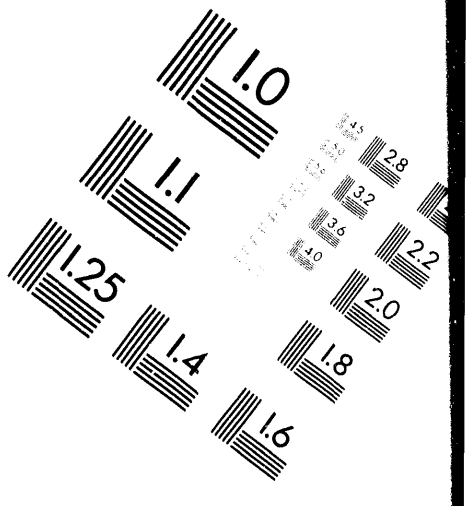

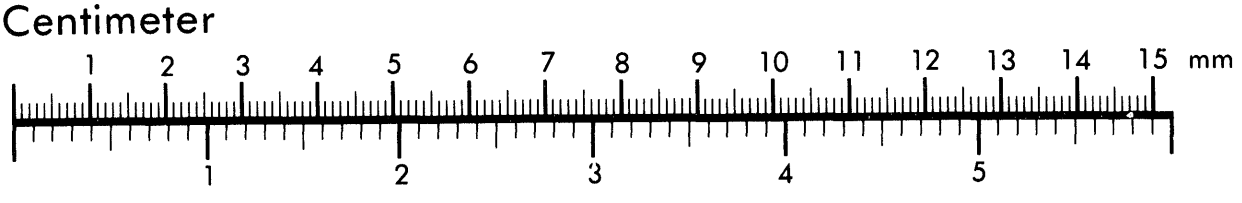

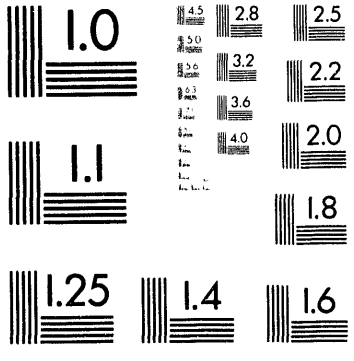

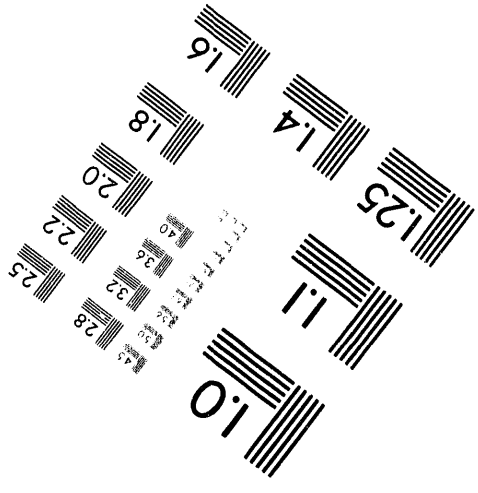

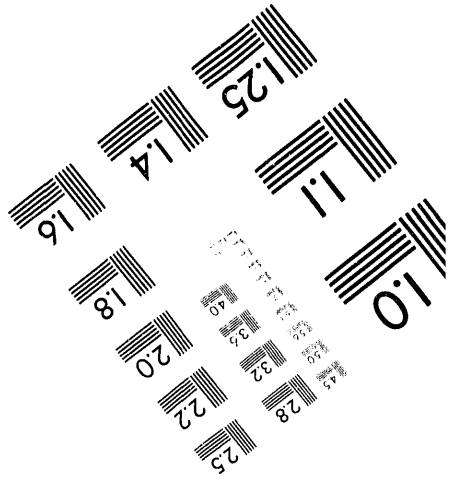

1 of 1

10/5-9-94 (1) CONF-930767--8

SLAC-PUB-6450
March 1994
M

POLARIZATION PHENOMENA IN QUANTUM CHROMODYNAMICS*

Stanley J. Brodsky
Stanford Linear Accelerator Center
Stanford University, Stanford, California 94309

ABSTRACT

I discuss a number of interrelated hadronic spin effects which test fundamental features of perturbative and non-perturbative QCD. For example, the anomalous magnetic moment of the proton and the axial coupling g_A on the nucleon are shown to be related to each other for fixed proton radius, independent of the form of the underlying three-quark relativistic quark wavefunction. The renormalization scale and scheme ambiguities for the radiative corrections to the Bjorken sum rule for the polarized structure functions can be eliminated by using commensurate scale relations with other observables. Other examples include (a) new constraints on the shape and normalization of the polarized quark and gluon structure functions of the proton at large and small $x_{\rm bj}$; (b) consequences of the principle of hadron helicity retention in high x_F inclusive reactions; (c) applications of hadron helicity conservation to high momentum transfer exclusive reactions; and (d) the dependence of nuclear structure functions and shadowing on virtual photon polarization. I also discuss the implications of a number of measurements which are in striking conflict with leading-twist perturbative QCD predictions, such as the extraordinarily large spin correlation A_{NN} observed in large angle proton-proton scattering, the anomalously large $\rho\pi$ branching ratio of the J/ψ, and the rapidly changing polarization dependence of both J/ψ and continuum lepton pair hadroproduction observed at large x_F. The azimuthal angular dependence of the Drell-Yan process is shown to be highly sensitive to the projectile distribution amplitude, the fundamental valence light-cone wavefunction of the hadron.

Invited Lectures presented at the
SLAC Summer Institute on Particle Physics:
Spin Structure in High Energy Processes
Stanford, California — July 26–August 6, 1993

* Work supported by the Department of Energy, contract DE–AC03–76SF00515.

1 Introduction and Overview

A central goal in the study of quantum chromodynamics is to understand the non-perturbative structure of hadrons in terms of their quark and gluon degrees of freedom. The polarization properties of the nucleons are described globally in terms of their magnetic moments and axial coupling constants. Additional constraints on nucleon spin structure are obtained from exclusive processes, particularly the ratio of helicity-changing (Pauli) and helicity-conserving (Dirac) form factors.

The most direct tool and sensitive test for probing the quark and gluon substructure of the proton is polarized-lepton polarized-target deep inelastic scattering. By using a combination of polarized light nuclear targets, experimentalists are now able to extract detailed information on the shape and magnitude of the helicity-dependent nucleon structure functions for each quark flavor: $\Delta u(x,Q^2), \Delta d(x,Q^2), \Delta s(x,Q^2)$. A combined analysis of recent SMC deuteron target data from CERN and ^{3}He data from the SLAC E142 experiment by Ellis and Karliner[1] gives the value

$$\Delta\Sigma = \Delta u + \Delta d + \Delta s = 0.27 \pm 0.11 \tag{1}$$

for the percentage of proton helicity carried by the sum of all quarks (and anti-quarks) in the nucleon, and the individual integrated values

$$\Delta u = 0.82 \pm 0.04,\ \Delta d = -0.44 \pm 0.04,\ \Delta s = -0.11 \pm 0.04\ . \tag{2}$$

Thus the helicities of the up quarks in the proton are highly correlated with that of the proton, whereas the down and strange quarks are anti-aligned.

In a naive non-relativistic three quark model of the proton, one would expect $\Delta\Sigma = 1$. As I will discuss below and in Section 10, relativistic binding of the quarks reduces the prediction of a three-quark model for $\Delta\Sigma$ by 25%. In contrast, in the Skyrme model, in which the nucleon emerges as a spin-$\frac{1}{2}$ topological soliton of an effective chiral Lagrangian, one predicts $\Delta\Sigma \sim 0(1/N_c)$ due to the decoupling of the SU(3) flavor-singlet axial current.[2] In more conventional descriptions, one can obtain a small value for $\Delta\Sigma$ if the gluon polarization in the nucleon is large and positive. The negative value for the strange quark helicity Δs can then be generated through perturbative QCD radiative corrections; *i.e.* the gluon anomaly.

However it should be emphasized that the extracted values for $\Delta\Sigma$ and Δs are somewhat uncertain because of higher twist corrections, Regge extrapolations, QCD radiative corrections, and other uncertainties which I will discuss in Sections 6–9. I will report results from the most recent experiments, including a new and preliminary analysis from the SMC experiment using polarized muons scattering on polarized proton targets in Section 5. The SLAC-Yale, EMC, and recent SLAC E142 measurements are reviewed in detail in this volume by Emlyn Hughes.[3]

Theory predicts that the polarization-dependent measures of the nucleons are interrelated in subtle ways; for example, the first moment of the nucleon structure functions are related to the nucleon axial couplings through the Bjorken and Ellis-Jaffe sum rules, and the anomalous magnetic moments are related through the Drell-Hearn-Gerasimov sum rule to logarithmic integrals of spin-dependent photoabsorption cross sections. In fact, as emphasized by Ioffe *et al.*,[4] the DHG sum rule is the analytic extension of the Bjorken sum rule evaluated at zero photon virtuality. This relation provides important constraints on the magnitude of the coherent higher-twist contributions to the Bjorken and Ellis-Jaffe sum rules at low Q^2. I review the DHG constraint in Section 7.

Polarization-sensitive scattering experiments can also test dynamical principles such as perturbative QCD factorization and hadron helicity conservation by tracing the flow of particle helicities through the reactions and measuring spin correlations. Although much of the observed phenomena can be understood within standard QCD mechanisms, there are a number of extraordinary experimental anomalies, such as the large and sudden jump in the spin-spin correlation A_{NN} observed in large angle elastic proton-proton scattering, the violation of hadron helicity conservation observed in vector-pseudoscalar decays of the J/ψ, and the striking pattern of polarizations seen in massive lepton hadroproduction, both in the continuum, and at the J/ψ. In Section 17 I discuss recent work with Brandenburg, Khoze and Müller which shows how azimuthal correlations in the Drell-Yan process can provide direct information on hadron structure at the amplitude level.

A simple language for encoding the helicity structure of relativistic composite hadrons is given by the light-cone Fock expansion. In this framework, the hadron eigenstate is written as a sum over free quark and gluon Fock states with the same global quantum numbers. The projection on the n-particle Fock state is the

light-cone wavefunction

$$\psi_n(x_i, k_{\perp i}, \lambda_i) \; . \tag{3}$$

Here

$$x_i = \frac{k_i^+}{P^+} = \frac{k_i^0 + k_i^z}{P^0 + P^z} \tag{4}$$

is the longitudinal light-cone fraction, the $k_{\perp i}$ are the relative transverse momenta, and the λ_i are the quark and gluon helicities. The wavefunction $\psi_n(x_i, k_{\perp i}, \lambda_i)$ is the probability amplitude for the hadron to be in this n-particle Fock state at fixed light-cone time $\tau = t - z/c$ with particle momenta $p_i^+ = x_i P^+$ and $p_{\perp i} = x_i P_\perp + k_{\perp i}$.

The central advantage of the light-cone description is that it allows a wavefunction interpretation of hadrons as composite systems of a relativistic quantum field theory. One is not restricted to states of fixed particle number; all quantum fluctuations consistent with conservation laws and global symmetries are allowed.[5] The description of the hadron is boost invariant, since the wavefunction $\psi_n(x_i, k_{\perp i}, \lambda_i)$ is independent of the hadron four-momentum. Form factors are simple convolutions of the light-cone wavefunctions. More generally the light-cone wavefunctions act as the interpolators between hadron matrix amplitudes and quark and gluon scattering amplitudes. A more complete discussion is given in the Appendix.

Thus given the light-cone Fock wavefunctions, one can compute form factors, polarized and unpolarized structure functions, decay constants, exclusive amplitudes, higher twist matrix element coefficients, etc. In principle, one can determine the light-cone wavefunctions for both bound states and continuum scattering states in QCD by diagonalizing the light-cone Hamiltonian as an eigenvalue problem on the free light-cone Fock basis:

$$H_{LC} \, |\Psi\rangle = M^2 \, |\Psi\rangle \; , \tag{5}$$

$$\langle m | H_{LC} | n \rangle \, \langle n | \Psi \rangle = M^2 \, \langle m | \Psi \rangle \; . \tag{6}$$

In fact this has been done on a discrete basis assuming periodic boundary conditions for a number of simpler quantum field theories such as QCD(1+1) and QED(1+1). Recently, Klebanov and Dalley[6] have used the discretized light-cone quantization (DLCQ) method to solve more complicated theories such as

QCD(1+1) with adjoint matter representations. There also has been strong progress in solving field theories displaying spontaneous symmetry breaking. The complications of the equal-time vacuum is replaced by constraint equations for the non-dynamical zero modes of the theory.

The use of light-cone wavefunctions also allows one to study relations between the magnetic moment and the axial coupling of the nucleon which follow from its underlying relativistic quark substructure. For example, Schlumpf and I[7] have found that the relationship between μ_p and g_A is controlled by the kinematics of the Melosh transformation connecting the rest frame wavefunction to the light-cone, and it is essentially independent of the dynamical form of the light-cone wave function. At large proton radius, μ_p and g_A are given by the usual nonrelativistic formulae. At small radius, μ_p becomes equal to the Dirac moment, as demanded by the Drell-Hearn-Gerasimov sum rule. In addition, as $R_1 \to 0$, the constituent quark helicities become completely disoriented and $g_A \to 0$. At the physical radius $R_1 = 0.76$ fm, one obtains the experimental values for both μ_p and g_A, and the helicity carried by the valence u and d quarks are each reduced by a factor $\simeq 0.75$ relative to their non-relativistic values. Thus for the proton's empirical size $M_p R_1 = 3.63$, the three-quark model predicts $\Delta u = 1$, $\Delta d = -1/4$, and $\Delta\Sigma = \Delta u + \Delta d = 0.75$. Although the gluon contribution $\Delta G = 0$ in this model, the general sum rule[2]

$$\frac{1}{2}\Delta\Sigma + \Delta G + L_z = \frac{1}{2} \tag{7}$$

is still satisfied, since the Melosh transformation effectively contributes to L_z. It should be emphasized that deep inelastic polarized structure function and $g_1(x, Q^2)$ and its sum rules actually measure the quark helicity content of the nucleon, not the rest frame quark spin projection S_z^q.

Although the Q^2 evolution of deep inelastic structure functions is well understood from perturbative QCD, we only have general constraints on the perturbative and nonperturbative dynamics which control the shape of the helicity-dependent quark and gluon distributions. For example, in order to insure positivity of fragmentation functions, the distribution functions $G_{a/b}(x)$ must behave as an odd or even power of $(1-x)$ at $x \to 1$ according to the relative statistics of a and b.[8] Thus the gluon distribution of a nucleon must have the behavior: $G_{g/N}(x) \sim (1-x)^{2k}$ at $x \to 1$ to ensure correct crossing to the fragmentation

function $D_{N/g}(z)$. On the other hand, in the $x \to 1$ limit, a constituent of the proton is far off-shell and the leading behavior in the hadron wavefunctions is dominated by perturbative QCD contributions to the interaction kernel. We thus may use the minimally connected tree-graphs to characterize the threshold dependence of the structure functions. The gluon distribution of a hadron is often assumed to be radiatively generated from the QCD evolution of the quark structure functions beginning at an initial scale Q_0^2. The evolution is incoherent; *i.e.* each quark in the hadron radiates gluons independently. However, as can be seen in the light–cone Hamiltonian approach, the higher Fock components of a bound state in QCD contain gluons at any resolution scale. Furthermore, the exchange of gluon quanta between the bound-state constituents provides an interaction potential whose energy–dependent part generates a non-trivial non-additive contribution to the full gluon distribution $G_{g/H}(x, Q_0^2)$. In Sections 11 and 12 I will discuss recent work by Burkardt and Schmidt and myself[9] which develops analytic representations of polarized quark and gluon distributions in the nucleon. The analysis incorporates general constraints obtained from the requirements of color coherence of gluon couplings at $x \sim 0$ and the helicity retention properties of perturbative QCD couplings at $x \sim 1$.

One of the most important tests of QCD is the Bjorken sum rule. An essential part of the QCD analysis is the evaluation of the perturbative radiative corrections to structure function moments. However, there is considerable uncertainty in the radiative corrections, particularly at low momentum transfer due to scale ambiguities, scheme dependence, and higher twist corrections. In these lectures I will discuss a new approach based on work with Hung Jung Lu[10] in which the scale and scheme dependence of perturbative QCD predictions can be eliminated by relating observables to each other. For example we show in Section 15 that perturbatively calculable observables in QCD, including the annihilation ratio $R_{e^+e^-}$, the heavy quark potential, and radiative corrections to structure function sum rules, are related to each other at fixed relative scales. QCD can thus be tested in a new and precise way by checking that the radiative corrections to the Bjorken sum rule and the radiative corrections to the annihilation cross section track both in their relative normalization and in their commensurate scale dependence.

Although the net correlation of the quark helicity with the proton helicity in inclusive reactions is apparently small, the spin correlations of large angle elastic

pp scattering nevertheless display a dramatic structure at the highest measured energies $\sqrt{s} \sim 5\ GeV$.[11] These measurements are in strong conflict with the expectations of perturbative QCD which predicts a smooth power-law fall-off for exclusive helicity amplitude with increasing momentum transfer.[12] The strong polarization correlations observed in pp scattering are clearly of fundamental interest, since the microscopic QCD mechanisms that underlie the spin correlations between the incident and final hadrons must involve the coherent transfer of helicity information through their common quark and gluon constituents. The implications of the spin correlation measurements will be discussed in Section 18.

A basic but non-trivial property of the gauge couplings of PQCD is "hadron helicity retention": a projectile hadron tends to transfer its helicity to its leading particle fragments. A particularly interesting consequence is the prediction that the J/ψ and the continuum lepton pairs produced in pion-nucleus collisions will be longitudinally polarized at large x_F. Helicity retention also provides important constraints on the shape of the gluon and quark helicity distributions. In the large x_F domain, with $Q^2(1-x)$ fixed, leading twist and multi-parton higher twist processes can be of equal importance.[13] In the case of large momentum transfer exclusive reactions, the underlying chiral structure of perturbative QCD predicts that sum of hadron helicities in the initial state must equal that of the final state.[14] Although hadron helicity conservation appears to be empirically satisfied in most reactions, the most interesting cases are its dramatic failures such as the large branching ratio for $J/\psi \to \rho\pi$. I will discuss the implications of this failure of perturbative QCD predictions in Section 17.

In these lectures I will give a survey of just a few of the many areas of polarization studies possible in hadron physics. Although most of the topics discussed in these lectures are concerned with quark or gluon helicity, there are also interesting linear polarization predicted by the theory, such as in Υ decays, or in the planar correlations of four-jet events in e^+e^- annihilation. In addition, the oblateness[15] of a gluon jet can be used to determine its axis of linear polarization. One of the most promising areas in the future of polarization studies will be the analysis of spin transfer from the initial electron to the final state hadrons and jets in e^+e^- annihilation.

2 Helicity Structure Functions of the Nucleon

The distributions of quark helicities in a polarized nucleon are directly determined from measurements of deep inelastic polarized-lepton-polarized nucleon scattering. The key measure is the cross section asymmetry for parallel versus antiparallel lepton and nucleon longitudinal polarizations:

$$A_1 = \frac{\sigma_T^{\gamma^* p}(\uparrow\downarrow) - \sigma_T^{\gamma^* p}(\uparrow\uparrow)}{\sigma_T^{\gamma^* p}(\uparrow\downarrow) + \sigma_T^{\gamma^* p}(\uparrow\uparrow)}. \tag{8}$$

One can then identify the leading-twist helicity structure function

$$g_1(x,Q^2) = A_1(x,Q^2)F_1(x,Q^2) = \frac{A_1(x,Q^2)F_2(x,Q^2)}{2x[1+R(x,Q^2)]} \tag{9}$$

where $R = \sigma_L^{\gamma^* p}/\sigma_T^{\gamma^* p}$. As usual $Q^2 = -q^2$ and $2M\nu = 2p\cdot q$, and $x = x_{\rm bj} = Q^2/2p\cdot q$.

The g_1 structure function has a simple probabilistic interpretation in the parton model. In the Bjorken limit with fixed $x_{\rm bj}$,

$$g_1(x,Q^2) = \tfrac{1}{2}\Sigma_q e_q^2[q_\uparrow(x,Q^2) - q_\downarrow(x,Q^2)] \tag{10}$$

where $q_\uparrow(x,Q^2) = G_{q_\uparrow/p_\uparrow}(x,Q^2) + G_{\bar{q}_\uparrow/p_\uparrow}(x,Q^2)$ is the number distribution of quarks (plus antiquarks) with helicity aligned with that of the proton. The deep inelastic kinematics sets the light-cone momentum fraction $x = k^+/p^+$ of the struck quark in the hadron wavefunction equal to the Bjorken variable $x_{\rm bj}$. The individual up and down quark helicity distributions in the proton $u(x,Q^2)$ and $d(x,Q^2)$ can then be obtained, modulo small nuclear and isospin-symmetry corrections, by combining proton target and deuteron or ^{3}He data.

It is also apparent from the light-cone Fock-space description of the proton (see Appendix) that the integral of the quark helicity distributions can be obtained at low Q^2 from forward matrix elements of the axial current:

$$\langle p|A_\mu^q|p\rangle = \langle p|\bar{q}\gamma_\mu\gamma_5 q|p\rangle = \Delta q\ S_\mu(p), \tag{11}$$

where S_μ is the proton spin vector. The notation Δq sums both the quark and antiquark contributions in the proton.

The axial current of the quarks can also be written

$$\overline{q}\gamma_\mu\gamma_5 q = \overline{q}_R\gamma_\mu q_R - \overline{q}_L\gamma_\mu q_L, \tag{12}$$

where $R, L = \frac{1}{2}(1 \pm \gamma_5)$ projects the right- and left-handed chiral components of the quark fields. For massless quarks, chirality coincides with helicity. If we choose the Drell-Yan light-cone frame with $Q^+ = 0$ and the $\mu = +$ component of the axial current, then its matrix element in the light-cone Fock space is diagonal in particle number. The axial current matrix element thus measures the first moment of the quark helicity distributions:

$$\Delta q = \int_0^1 dx[q_\uparrow(x, Q^2) - q_\downarrow(x, Q^2)]. \tag{13}$$

Note that this moment has zero anomalous dimensions. The axial coupling of the nucleon measured in β-decay $n \to p e^- \overline{\nu}_e$, together with isospin symmetry, thus determines

$$\Delta u - \Delta d = g_A = 1.2573 \pm 0.0002. \tag{14}$$

Similarly hyperon decay plus $SU(3)$ symmetry determines the combination

$$\Delta u + \Delta d - 2\Delta s = 0.59 \pm 0.02. \tag{15}$$

A discussion of the uncertainties in these values due to the assumption of isospin and $SU(3)$-flavor symmetry has been discussed by Lipkin.[16] The neutron values are obtained from isospin symmetry.

3 The Bjorken Sum Rule

Much of our understanding of the helicity structure of hadrons comes from rigorous constraints, such as the Bjorken sum rule for the integral of the spin dependent structure functions, and the Drell-Hearn-Gerasimov sum rule, which relates the anomalous magnetic moment of a composite system to an integral over the photoabsorption cross section. In fact, as we will discuss below, the DHG and Bjorken sum rules can be regarded as low and high Q^2 limits of one fundamental measure.

The most celebrated application of current algebra is the Bjorken sum rule[17] for polarized lepton–polarized nucleon scattering. The sum rule is based on the fact that the matrix element of the commutator of the electromagnetic currents for polarized protons is given by the proton matrix element of the axial current. For the isospin-changing proton-neutron difference, this gives

$$\int_0^1 dx[g_1^p(x, Q^2) - g_1^n(x, Q^2)] = \frac{1}{6}\, g_A \left[1 - \frac{\alpha_s(Q^2)}{\pi} + \ldots\right]. \tag{16}$$

The Bjorken sum rule has the remarkable feature of relating the first moment of the helicity-dependent structure functions of the nucleons, which are measured at high Q^2, to a nearly static quantity, the axial coupling constant g_A which is measured at $Q^2 \sim 0$ in the β decay of the neutron: This sum rule has played an historic role in high energy physics, providing the first hint that the structure functions must become essentially Q^2–independent at fixed $x = \frac{Q^2}{2p\cdot q}$. Bjorken's derivation was based on current algebra, with the essential ansatz that the current commutators have the same structure as the currents of free quarks. However, as in the case of the Bjorken scaling of the parton model, the Bjorken sum rule is only a first approximation; radiative corrections of leading twist (powers of α_s) and higher twist (powers of $1/Q^2$) also appear. In practice, there are a host of important theoretical issues that must be understood to actually test the Bjorken sum rule. In the following I will make a brief survey of some of the underlying physics.

The radiative corrections to the Bjorken sum rule reflect the fact that gluon radiation induced by the scattering process $eq \to eq$ depolarize the quark helicity. According to perturbative QCD, deep inelastic lepton-nucleon scattering at high Q^2 can be identified with lepton scattering on effectively free quark currents of the target. A crucial assumption is that the large distance effects of confinement of the quarks in the final state can be neglected—the important invariant length scales which are probed in the forward virtual Compton amplitude are of order $1/Q$. The Bjorken-scaling of the structure functions is then equivalent to the impulse approximation; *i.e.* the absence of final-state interactions of the outgoing quark with the spectators of the target nucleon. In light-cone gauge $A^+ = 0$ the final state gluon interactions between the active and spectator system give corrections

of order $\ell_\perp^2/Q^2$, since the exchanged gluon momenta $\ell_\perp^2$ are finite. However, the contributions from gluons associated with vertex corrections and gluons emitted from the struck quark with momenta $\ell^2 \sim Q^2$ are only logarithmically suppressed. Thus one obtains a perturbative series in powers of $\alpha_s(Q)$ from the leading order corrections. The leading twist corrections are universal since they are the same whether the target is a quark or a hadron. The lowest order correction in α_s was first obtained by Kodaira.[18] The perturbative QCD corrections have now been evaluated by Larin, Tkachev, and Vermaseran[19] through order $\alpha_s^3(Q)$ in $\overline{MS}$ scheme.

The numerical value of the perturbative corrections to any finite order depends on the choice of renormalization scheme *e.g.*, $\overline{MS}$ and on the choice of renormalization scale. In Section 15 I will discuss recent work done with Hung Jung Lu[10] in which we show that the scale ambiguity can be consistently resolved for any choice of scheme through the first two orders of perturbation theory by using the methods of Ref. 20. We also show that the scale and scheme ambiguity of the leading twist PQCD radiative corrections can be eliminated by relating these corrections to the radiative corrections for other observables. These "commensurate scale relations" greatly diminish the uncertainty in the perturbative QCD corrections. In addition, we note that the radiative corrections to the Bjorken sum rule are identical to those of the Gross-Llewellyn Smith sum rule—up to small corrections of order $\alpha_s^3(Q^2)$.

Thus a basic test of QCD can be made by considering the ratio of the Gross-Llewellyn Smith, and Bjorken sum rules:[21]

$$R_{GLLS/Bj}(Q^2,\epsilon) = \frac{3\int_\epsilon^1 dx \left[F_3^{\nu p}(x,Q^2) - F_3^{\bar\nu p}(x,Q^2)\right]}{\frac{6}{g_A}\int_\epsilon^1 dx \left[g_1^p(x,Q^2) - g_1^n(x,Q^2)\right]}. \tag{17}$$

Since the Regge behavior of the two sum rules is similar, the empirical extrapolation to $\epsilon \to 0$ should be relatively free of systematic error. Moreover, PQCD predicts

$$R_{GLLS/Bj}(Q^2,\epsilon\to 0) = 1 + \mathcal{O}\left(\alpha_s^3(Q)\right) + \mathcal{O}\left(\frac{\Lambda_{QCD}^2}{Q^2}\right), \tag{18}$$

i.e. hard relativistic corrections to the ratio of the sum rules only enter at three loops. Thus measurements of the *ratio* of the sum rules could provide a remarkably

complication-free test of QCD—any significant deviation from $R_{GLLS/Bj}(Q^2,\epsilon\to 0) = 1$ must be due to higher twist effects which should vanish rapidly with increasing Q^2.

4 The Ellis-Jaffe Sum Rule

The Bjorken sum rule applies to the isospin-non-singlet proton-neutron difference, and it is thus insensitive to the helicity carried by strange quarks in the proton. We can also apply the same analysis to the proton alone:

$$\int_0^1 dx\, g_1^p(x,Q^2) = \tfrac{1}{2}\left[\frac{4}{9}\Delta u + \frac{1}{9}\Delta d + \frac{1}{9}\Delta s\right]\left[1 + \mathcal{O}\frac{\alpha_s(Q)}{\pi} + \ldots\right]. \tag{19}$$

The radiative corrections to this sum rule are only known to order α_s.[22] If one assumes that the strange quark contribution Δs in the proton is small, then the above result gives the original Ellis-Jaffe sum rule.[23]

One also obtains a non-zero contribution to the sea quark helicities if the gluons in the nucleon are polarized.[24] This contribution arises from the quark loop contribution to $g^*\gamma^* \to g^*\gamma^*$ in the forward virtual Compton amplitude; *i.e.* from the scattering of the leptons on the quarks arising from the gluon's substructure:

$$\Delta q = -\frac{\alpha_s(Q^2)}{2\pi}\,\Delta g(Q^2). \tag{20}$$

The result is independent of the scale Q since the product $\alpha_s(Q^2)\Delta g(Q^2)$ is a renormalization-group invariant. However, the actual value for $\Delta g(Q^2)$ depends on the internal non-perturbative structure of the proton. Since it is isospin-invariant, the gluon anomaly contribution cancels in the evaluation of the Bjorken sum rule.

The "gluon anomaly" contribution adds to any "intrinsic" sea-quark polarization inherent to higher Fock states in the bound state wavefunction.[25] The anomaly contribution only arises if the gluon virtuality is large compared to the mass of the sea quark; thus the analysis requires the introduction of a minimum transverse momentum cutoff for the gluons, which is a gauge-dependent separation of scales.[26] As noted by Carlitz, Collins, and Mueller,[27] it is possible in principle

to physically isolate the anomaly contribution by demanding a coincident high p_T jet in the nucleon fragmentation regime.

In the next section I will discuss theoretical constraints on the shape of the quark and gluon helicity distributions which follow from general QCD principles.

5 Comparison of Experiment and Theory for the QCD Helicity Sum Rules

A complete discussion of the SLAC-Yale, EMC, and the most recent SLAC E142 and CERN SMC measurements of the polarized structure functions of the nucleons can be found in Emlyn Hughes' contribution to this volume and in a recent presentation of the SMC data by Vernon Hughes.[28] I will only summarize the main results here.[29]

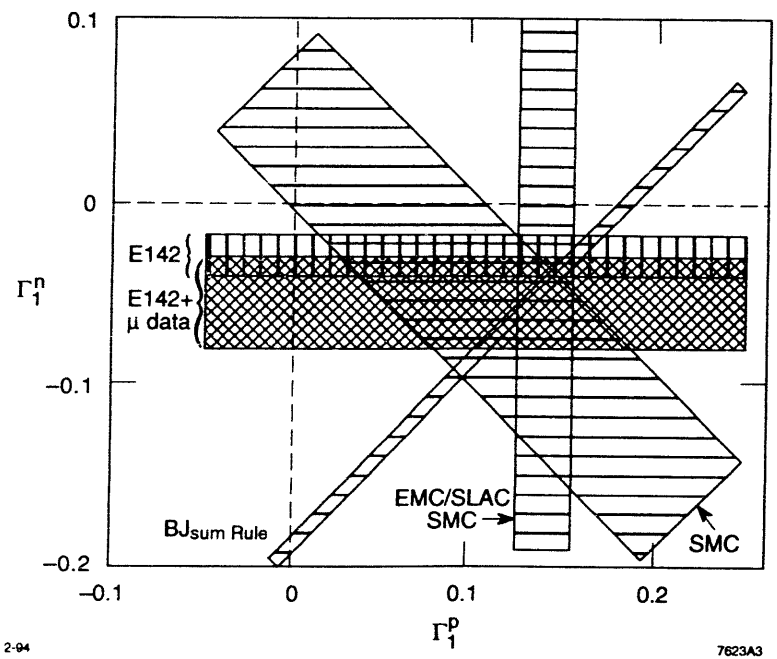

Figure 1. Experimental values for the integrals Γ_1^p and Γ_1^n of the helicity-dependent structure functions, compared with the Bjorken sum rule prediction at $Q^2 = 5$ GeV^2. From Ref. 28.

The experimental values for the sum rule integrals from the original EMC/SLAC measurements, together with the recent results from the E142 and SMC experiments are summarized in Fig. 1. The predicted value for the Bjorken sum rule is $\Gamma_1^p - \Gamma_1^n = \frac{g_A}{6} = 0.209(1)$ without radiative corrections. Taking $\alpha_s = 0.26(2)$ in $\overline{MS}$ scheme at $Q^2 = 5$ GeV^2, the leading twist radiative corrections through order α_s^3 reduce the predicted value to $\Gamma_1^p - \Gamma_1^n = 0.185(4)$ at $Q^2 = 5$ GeV^2. This prediction for the Bjorken sum rule at $Q^2 = 5$ GeV^2 appears as a diagonal band in the plot of Γ_1^p versus Γ_1^n. The recent results from E142 for the neutron asymmetry extracted from a ^{3}He target are represented as a band for Γ_1^n. The recent SMC deuteron target measurement appears as a constraint on the sum $\Gamma_1^p + \Gamma_1^n$. Within errors of order 15%, the experiments do not appear to be in conflict with the Bjorken sum rule.

However, there is an possible conflict with the leading-twist Ellis-Jaffe prediction. The preliminary value from the recent measurement of the Spin Muon Collaboration for proton targets gives $\Gamma_1^p(\mathrm{SMC} Q^2 = 10.5\,\mathrm{GeV}^2) = 0.152 \pm 0.015(\mathrm{stat}) \pm 0.018(\mathrm{syst})$, where the systematic error includes uncertainties from the Regge extrapolation to $x \to 0$. The predicted value, including the leading order correction, but neglecting strange quarks, is $\Gamma_1^p = 0.177 \pm 0.010$ at $Q^2 = 10.5$ GeV^2. The combined data from all of the experiments gives $\Gamma_1^p(\mathrm{World}) = 0.145 \pm 0.01 \pm 0.012$. This discrepancy with the predicted value $\Gamma_1^p = 0.172 \pm 0.010$ at $Q^2 = 5$ GeV^2 can be taken as evidence for a polarized strange quark contribution in the nucleon. However, as emphasized by Burkert and Ioffe, higher-twist corrections could significantly reduce the predicted value.

Figure 2 presents another representation of the data, assuming the validity of the Bjorken sum rule, as well as the constraint from hyperon decay $\Delta u + \Delta d - 2\Delta s = \Sigma - 3\Delta s = 0.59(2)$. The figure shows that the E142 measurement of the neutron asymmetry is consistent with a small strange quark polarization and a large value for the total quark polarization $\Sigma = \Delta u + \Delta d + \Delta s \simeq 0.6$, of the same order as the quark momentum fraction. (The non-relativistic three quark model predicts $\Sigma = 1$.) However, the asymmetry measured by the SMC on polarized deuteron targets implies a large and negative strange quark polarization in the nucleon: $\Delta s \sim -0.2$ and correspondingly, a small value for the total quark helicity Σ. The recent (preliminary) analysis from the SMC experiment using polarized

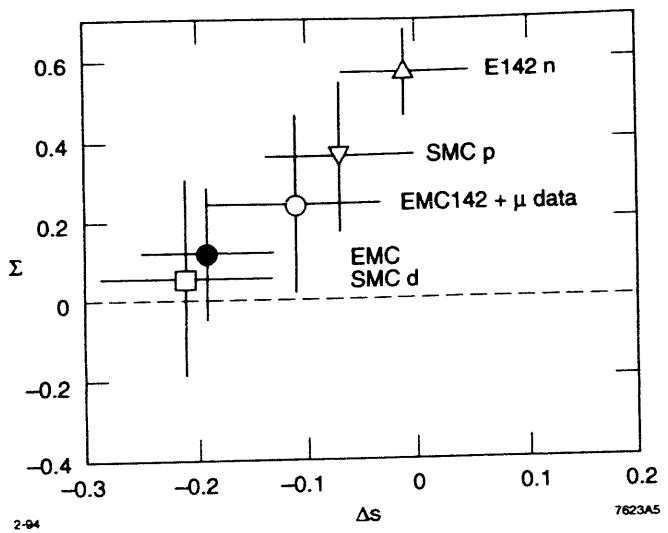

Figure 2. Experimental values for the total quark helicity Σ and the strange quark helicity Δs in the nucleon. The hyperon beta decay constraint is assumed. From Ref. 28.

muons scattering on polarized proton targets gives[28] $\Delta\Sigma = 0.36 \pm 0.21$, and

$$\Delta s = -0.07 \pm 0.06 \ . \tag{21}$$

The overall average from the SMC experiments is $\Sigma = 0.28 \pm 0.11$, and $\Delta s = -0.09 \pm 0.04$. Any apparent discrepancy between the E142 and SMC measurements could be due to different low-x extrapolations or large higher-twist corrections, corrections which would most strongly affect the lower energy data. The new HERMES gas jet target measurements planned at DESY and the higher energy $p_{\rm lab} = 50$ GeV/c E143 experiment now underway at SLAC will hopefully be able to clarify these issues. In addition, deep inelastic neutrino scattering can also provide direct information on the polarization of strange quarks in the nucleon.

6 Higher-Twist Corrections to Deep Inelastic Scattering

Power-law-suppressed $1/Q^n$ corrections to the Bjorken sum rule, as well as the structure functions themselves, are an inevitable complication to the physics of inelastic lepton-proton scattering. For example, at small values of Q^2 comparable to $1/R^2$ where R is the separation of quarks in the nucleon, the interference of amplitudes where two different quarks are struck must be taken into account. These contributions give corrections to the Bjorken sum rule of order $N_q(N_q-1)/Q^2R^2$, where N_q is the number of quark constituents in the nucleon.[30] These corrections can be labelled as *intrinsic* higher-twist effects corrections since they depend on the detailed structure of the nucleon itself. The intrinsic higher order contributions to structure functions give corrections of relative order $\Lambda^2_{QCD}/(1-x)Q^2$; *i.e.* they become very large at $x \to 1$, since the lepton can scatter on a coherent multi-quark system carrying a large fraction of the nucleon momentum. In particular, the scattering of the lepton on the two valence quark system gives a large higher twist contribution to the longitudinal structure function at large x. Such contributions have in fact been observed in the SLAC and NMC deep inelastic scattering measurements, and are taken into account in the analysis of structure function evolution.[31] Higher twist corrections are also caused by finite mass effects, finite intrinsic transverse momentum smearing, and insertions due to vacuum condensates. QCD condensate corrections to the quark and gluon propagators give *extrinsic* power-law suppressed corrections, since they are essentially target-independent. However, as emphasized by Mueller,[32] such terms are difficult to distinguish from the Borel sum of perturbative higher order contributions in $\alpha_s(Q^2)$. Thus it is difficult to identify the condensate corrections unless one first has control over the leading-twist corrections of very high order.

There is however, a reliable way to estimate the intrinsic higher-twist corrections to QCD sum rules. As shown by Ioffe *et al.*[4], the integrals over the structure functions

$$\Gamma_{p,n}(Q^2) = \frac{Q^2}{2M^2_{p,n}} \int_{Q^2/2M_{p,n}}^{\infty} \frac{d\nu}{\nu} G_{1p,n}(\nu, Q^2) \tag{22}$$

that appear in the Bjorken and Ellis-Jaffe sum rules are—up to a factor of Q^2—precisely the same integrals $I_{p,n} = (2M^2_{p,n}/Q^2)\ \Gamma_{p,n}(Q^2)$ which appear in the

Drell-Hearn Gerasimov sum rule for the proton and neutron anomalous magnetic moments: (See Section 7.)

$$I_{p,n}(0) = -\frac{1}{4}\kappa^2_{p,n}. \tag{23}$$

The G_1 structure function is equal to the polarized photoabsorption cross section at $Q^2 = 0$ and

$$\frac{\nu}{M_p}G_1(x,Q^2) \rightarrow g_1(x,Q^2) \tag{24}$$

in the Bjorken limit. The sum rule integrals $\Gamma_{p,n}(Q^2)$ must thus each change sign as Q^2 decreases. This identification provides a powerful constraint on the path of the Bjorken integral $\Gamma_p(Q^2) - \Gamma_n(Q^2)$ as Q^2 is decreased to the photoabsorption point. Figure 3, which is taken from a recent analysis by Burkert and Ioffe[4], shows that resonance contributions to the Bjorken integral are likely to give significant corrections to the leading-twist predictions at momentum transfers $Q^2 < 2$ GeV^2. It would clearly be interesting to measure the sum rule integrals in the low Q^2 domain to see this transition. Note the effect of the resonances and moment constraints at low Q^2 has a very strong effect for the Ellis-Jaffe sum rule for $\Gamma_p(Q^2)$. It would also be interesting to find similar low Q^2 constraints for the Gross-Llewellyn Smith sum rule for the charged-current structure functions.

Recently, Ji and Unrau[33] have noted that, technically, the Bjorken sum rule integral, as defined from the saturation of a current commutator, includes the elastic nucleon pole contribution at $x = 1$, whereas the DHG sum rule does not include this contribution; the DHG integration starts at the inelastic threshold $s_{\rm thresh} = (M_p + m_\pi)^2$. However, since experimentalists always define the measured sum rule integral excluding the nucleon pole contribution, this complication does not actually occur in practice.[34]

7 The Drell-Hearn-Gerasimov Sum Rule

One of the most important constraints on the spin structure of both elementary particles and composite systems is the Drell-Hearn-Gerasimov sum rule.[35,36] The DHG sum rule was originally derived as a constraint on the anomalous magnetic moment of spin-1/2 systems by writing an unsubtracted dispersion relation for the forward helicity-flip Compton amplitude and the low-energy theorem.[37] The generalization to arbitrary spin has been made in Refs. 36 and 38.

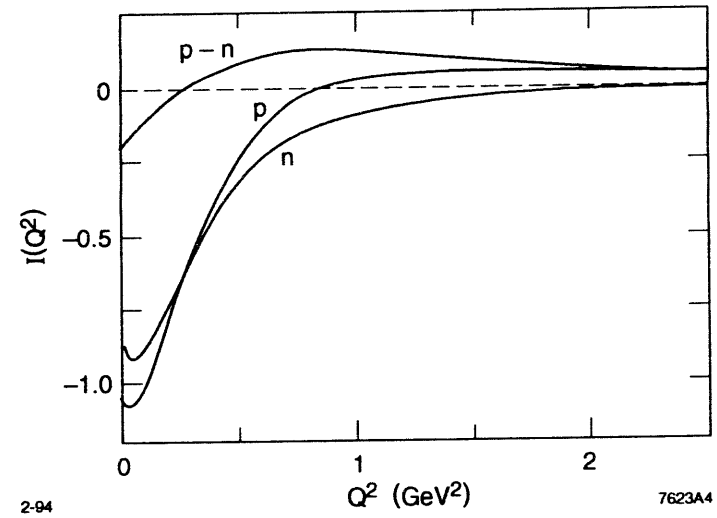

Figure 3. Connection between the Bjorken and DHG sum rule integrals $I(Q^2)$ for the proton, neutron and proton-neutron difference. At $Q^2 = 0$ the integrals are constrained by the nucleon anomalous magnetic moments. The curves include an estimate of resonance contributions up to mass 1.8 GeV. From Burkert and Ioffe, Ref. 4.

The DHG sum rule for spin-1/2 and spin-1 systems takes the form

$$\mu_a^2 = \frac{1}{\pi}\int_{\omega_{\rm th}}^{\infty}\frac{d\omega}{\omega}\left[\sigma_P(\omega) - \sigma_A(\omega)\right], \tag{25}$$

where $\mu_a = \mu_1 - \frac{e}{2M}$ and $\mu_a = \mu_1 - \frac{e}{M}$ are by definition the anomalous magnetic moment for the spin-1/2 and spin-1 systems, respectively, σ_P (σ_A) is the total cross section for absorption of a photon with spin parallel (antiparallel) to the spin of the target, and ω is the photon energy, with $\omega_{\rm th}$ the threshold energy. The result is totally general, applying to both elementary fields such as leptons, quarks, W's and Z's, as well as composite systems such as baryons, vector mesons, and nuclei. Although an experimental verification of the DHG sum rule for nucleons has been carried out,[39] it would also be interesting to verify this result for deuterons.

The extension of the DHG sum rule analysis to include the quadrupole moment of a spin-one system requires a low-energy theorem to second-order in the photon energy. At this order, the polarizability enters the Compton amplitude in addition

to the quadrupole moment. Hiller and I[40] have shown how one can use a dispersion relation due to Tung[41] in order to obtain the following sum rule for the non-forward Compton amplitude:

$$\mu_a^2 + \frac{2t}{M^2}\left(\mu_a + \frac{M}{2}Q_a\right)^2 = \frac{1}{4\pi}\int_{\nu_{\rm th}^2}^{\infty}\frac{d\nu^2}{(\nu - t/4)^3}\left(\mathcal{I}m\, f_P(s,t) - \mathcal{I}m\, f_A(s,t)\right) \quad (26)$$

where M is the mass, $Q_a = Q_1 + \frac{e}{M^2}$ defines the anomalous quadrupole moment, ν is $(s-u)/4$, and f_P (f_A) is the helicity amplitude for parallel (antiparallel) photon and target spins. The standard Mandelstam variables s, t and u are used. The optical theorem takes the form

$$\mathcal{I}m\, f_{P,A} = 2\nu\sigma_{P,A}\,. \quad (27)$$

Thus in the forward direction, this extended sum rule reduces to the DHG Sum Rule, with the use of $\omega = \nu/M$. A sum rule that relates Q_a to total cross sections does not exist.[41]

One of the most interesting consequences of the DHG sum rule occurs if we take a point-like limit such that the threshold for inelastic excitation becomes infinite while the mass of the system is kept finite. In such a case the photoabsorption cross section and the integrals that appear in the RHS of the sum rules vanish as the size $R \to 0$ or the excitation energy $\nu_{\rm th} \to \infty$. Thus in the point-like limit, the magnetic moment of a spin-half system must approach the Dirac value $\mu \to \mu_D = e/2M$ up to structure corrections of order M/Λ, [or $(M/\Lambda)^2$ if the underlying theory is chiral].[42] We can apply a similar limit for spin-one composite systems: $Q_a \to 0$ and $\mu_a \to 0$. Therefore $\mu_1 = \frac{e}{M}$ and $Q_1 = -\frac{e}{M^2}$ are the canonical moments of a spin-one system. Note that this analysis is non-perturbative. In the case of the standard model, the integrals in are higher order $\sim \mathcal{O}(\alpha^2)$; thus again $\mu_W = \frac{e}{M}$ and $Q_W = -\frac{e}{M^2}$, up to Schwinger-like radiative corrections of order α/π. Thus in the point-like limit, both the magnetic moment and quadrupole moment of any spin-one system must approach the canonical values predicted by electroweak theory for the W.[40]

Note that any spin-half or spin-one system is required to satisfy the extended DHG sum rule. Thus one cannot distinguish an elementary lepton, quark, W,

or Z from a compact composite system simply on the basis that its magnetic moment and quadrupole moment are close to those predicted by the standard model, since such behavior is also automatically attained for any composite system with size small compared to its Compton scale, *i.e.* $RM \ll 1$. Specific models for compositeness of leptons and intermediate vector bosons are discussed by Brodsky and Drell,[42] Abbott and Farhi,[43] and Claudson, Farhi, and Jaffe.[44] The DHG sum rule has also been used to place constraints on quark and lepton compositeness and excited states in the strong-coupling standard model[43] by Jaffe and Ryzak.[45]

However, the case of the axial coupling of a composite system is more subtle. As we shall show in the following section, the natural limit of g_A for a composite spin-$\frac{1}{2}$ system is $\lim_{MR\to 0} g_A = A$ not $g_A = 1$ as required for leptons and quarks in the standard model. Thus it would be necessary to enforce strict chiral symmetry if one wishes to use composite systems simulate the chiral properties of the elementary fields of the standard model.

Hiller and I[40] have also shown that the ratios of the three electromagnetic form factors $G_C : G_M : G_Q = (1 - \frac{2}{3}\eta) : 2 : -1$ are identical for elementary spin-one W's and for composite spin-one hadrons in QCD at large momentum transfer since the leading helicity-conserving amplitude is dominant. Thus at large Q^2, perturbative QCD predicts that the ratio of form factors for deuterons, $\rho^{\pm}$, etc., become identical to those of the point-like spin-one fields of the standard model.

One of the most remarkable consequences of natural magnetic moments is the prediction of null zones in exclusive radiative processes. For example the tree-graph contributions to the differential cross section

$$\frac{d\sigma}{d\Omega}(u\bar{d}\to W^+\gamma) = 0 \quad (28)$$

at the special angle $\cos\theta = e_d/e_W = 1/3$ provided that the W^+ and the quarks have natural magnetic and quadrupole moments as defined by the DHG Sum rule and its extensions.[46] More generally, the Born contribution to any radiative cross section with an arbitrary number of incident and outgoing charged lines will vanish at the photon emission angle which satisfies the null zone condition that all ratios $e_i/p_i \cdot k$ are equal. Again this occurs only if provided $\mu_a = 0$ and $Q_a = 0$. Thus all helicity amplitudes for the subprocess $u\bar{d}\to W^+\gamma$ simultaneously vanish at $\cos\theta = e_d/e_W$ provided that the W^+ and the quarks have natural moments.

The occurrence of null zones requires not only the destructive interference of radiation from all of the convection currents $p_i^\mu + p_i'^\mu$ of all of the incident and final particles, but in addition, the radiation from all of the spin currents must also cancel among themselves. This fact follows from the same reason that the precession and Larmor frequencies of a spin-$\frac{1}{2}$ particle in an external magnetic field are identical when there is no anomalous moment and the gyromagnetic ratio $g = 2$; in such a case the spin currents can be generated by a pseudo-Lorentz transformation and the spin-current contributions vanish at the same angle as the convection contributions. Thus the moments defined by the DHG sum rule and its extension in the point-like limit also are the moments that preserve null zones. A discussion of bounds on the W anomalous moment that can be obtained from present $p\bar{p}\to W\gamma X$ data is presented in Ref. 47.

The Drell-Hearn sum rule also has important consequences for the computation of the magnetic moments of baryons in QCD. Magnetic moments are often computed using the quark model formula $\vec{\mu} = \sum_{i=1}^{3} \vec{\mu}_i$. This formula is correct in the case of atoms where the mass of the nucleus can be taken as infinite. However, magnetic moment additivity cannot be correct in general: the DHG sum rule shows that in the limit of strong binding where the constituents become very massive and the hadron becomes point-like, its magnetic moment must equal the Dirac value, not zero as predicted by quark moment additivity. The flaw in the conventional quark model formula is that it does not take into account the fact that the moment of a system H is derived from the electron scattering amplitude $eH\to e'H'$ at non-zero momentum transfer q. The Dirac value in the point-like limit actually arises from the Wigner boost of the wavefunction from p to $p+q$. A detailed discussion of this and the resulting relativistic corrections to the moment are given Ref. 48. On the other hand, the overlap of light-cone Fock wavefunctions does provide a general method for the evaluation of hadronic magnetic moments and form factors.[42]

8 Regge Behavior of Deep Inelastic Structure Functions

The high energy behavior $s \gg Q^2$ behavior of the virtual photoabsorption cross sections $\sigma_{T,L}^{\gamma^* N}(s, Q^2)$ which underlay the deep inelastic structure functions is dictated by Regge theory. In general, analyticity predicts that an hadronic amplitude at high energy $s \gg -t$ has the form of a sum of terms $[1 \pm \exp(i\pi\alpha_R(t)]\beta(t)s^{\alpha_R(t)}$ where the $\pm$ sign is determined by crossing symmetry. Each Reggeon corresponds to systems of exchanged particles with specific global quantum numbers. The longitudinal virtual photoabsorption cross sections $\sigma_{T,L}(s, Q^2)$ are related by the optical theorem to the forward virtual Compton amplitude illustrated in Fig. 4(c); thus Regge theory predicts $\sigma_{T,L} \sim \sum_R s^{\alpha_R(0)-1} C_R(Q^2)$. The above form provides an empirical method for extrapolating data into the Regge regime. One should first analyze the Regge behavior of the virtual photoabsorption cross section at fixed Q^2, just as one does for hadronic cross sections such as $\sigma(\pi^+ p) - \sigma(\pi^- p)$ in order to set the domain where the Regge parameterization is applicable. The critical issue is what happens in the Bjorken scaling limit. Do the Pomeron and Reggeon contributions observed at fixed Q^2 lead to Regge behavior of structure functions $F_2(x, Q^2) = \sum_R C_R x^{1-\alpha_R(0)}$ at small x as a scaling function of $x = Q^2/2M\nu$, or do such terms decouple as Q^2 increases?

The Regge behavior of structure functions can be analysed most simply within the format of the "covariant parton model" developed by Landshoff, Polkinghorne and Short.[49] The virtual photoabsorption cross section has the space-time structure shown in Fig. 4(a).

The structure function $F_2(x, Q^2) = \Sigma_{\bar{q},q} e_q^2 x G_{q/N}(x, Q^2)$ can be thus written as an integration over quark- and antiquark-nucleon cross sections:[49]

$$x G_{q/N}(x, Q^2) \propto \frac{x^2}{1-x} \int d\hat{s} \int d^2k_\perp \; \hat{s}\, \sigma_{\bar{q}p}(\hat{s}, k^2), \tag{29}$$

where $\hat{s} = (k+p)^2$ is the subprocess energy squared and $k^2 = -\frac{x}{1-x}(\hat{s} - k_\perp^2) + xM^2 - k_\perp^2$ is the interacting quark or antiquark virtuality.

The physics of the parton model corresponds to "aligned jet" regime where $k_\perp^2$ and k^2 are of order of hadronic scales. For this domain of kinematics $\hat{s} \sim -k^2/x$ for small x. Thus if $\sigma_{\bar{q}p}(\hat{s}, k^2) \sim \hat{s}^{\alpha_n - 1}$, then the structure functions will Bjorken-scale and have the Regge behavior $F_2(x, Q^2) \sim x^{1-\alpha_n}$ at small x. Additional contributions to the structure functions also arise from the symmetric pair regime where $k^2 \sim \mathcal{O}(Q^2)$. For example, the leading twist contribution to $F_L(x, Q^2)$ which violates the Callan-Gross relation comes from this domain. However, in this case

$$F_L(x, Q^2) \sim \sum_R C_R \alpha(Q^2) \left(\frac{x}{Q^2}\right)^{1-\alpha_R} \tag{30}$$

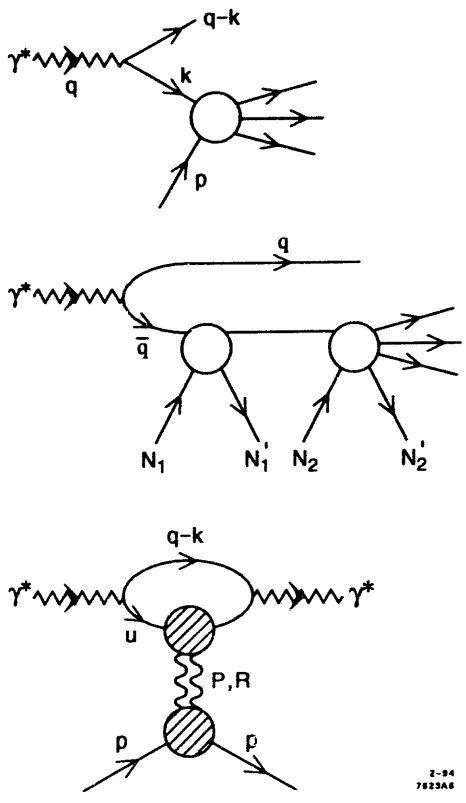

Figure 4. Space-time picture of deep inelastic scattering in the target rest-frame. (a) Contribution to the leading twist structure function from $\bar{q}p$ interactions. (b) Two-step scattering process contributing to shadowing of nuclear structure functions. (c) Regge contributions to the forward virtual Compton amplitude.

so that the Regge contributions to F_L evidently do not scale if $\alpha_R < 1$. Thus aside from the Pomeron contribution, the non-leading Reggeons decouple from the structure function contributions which arise from the $k^2 \sim \mathcal{O}(Q^2)$ symmetric jet regime.

It seems paradoxical that Regge behavior, which reflects soft hadron physics and hadron exchange processes, could be compatible with the charge and momentum sum rules of the parton model. In fact if one considers the difference of scattering of leptons on a proton and a *gedanken* "null" proton which consists of

charge-less valence quarks, the Pomeron and Reggeon contributions to the deep inelastic structure functions cancel. An analysis of this problem is discussed in Ref. 50.

9 Polarization-Dependent Nuclear Shadowing

The space-time picture of deep inelastic scattering shown in Fig. 4(a) which leads to Regge behavior of structure functions also provides the physical basis for understanding the shadowing of deep inelastic lepton-nucleus scattering cross sections.[51] In the small x domain, the $q\bar{q}$ pair with mass $\mathcal{M}^2$ has an effective lifetime $\tau = \frac{2\nu}{Q^2+M^2} = \mathcal{O}\left(\frac{1}{xM_p}\right)$ in the nuclear target rest frame. Thus at small x, the nuclear dependence of the virtual photoabsorption cross section will simply reflect the nuclear dependence of the $\sigma_{\bar{q}A}(\hat{s})$ cross section at $\hat{s} = -k^2/x$. As in ordinary Glauber theory, one must take into account "two-step" and higher multi-scattering processes in a nuclear target, such as those shown in Fig. 4(b) where the quark scatters coherently on an upstream nucleon N_1 before interacting inelastically on a nucleon N_2 further inside the nucleus. Hung Jung Lu and I have shown[51] that the Pomeron contributions to $\hat{\sigma}(\bar{q}N)$ lead to destructive interference of the one-step and multi-step scattering amplitudes, so that only the front nucleons in the nucleus see the full hadronic structure of the incoming virtual photon, thus producing shadowing of the nuclear structure functions: $\sigma^T_{\gamma^* A}(s,Q^2) < A\sigma^T_{\gamma^* N}(s,Q^2)$. Conversely, the phase of the coherent Reggeon contributions to $\hat{\sigma}(\bar{q}N)$ leads to constructive interference of the one-step and multiple step amplitudes and hence "antishadowing": $\sigma^T_{\gamma^* A}(s,Q^2) > A\sigma^T_{\gamma^* N}(s,Q^2)$ at moderate values of $x \sim 0.13$, as originally predicted by Nikolaev and Zakharov.[52] The ratio of antishadowing to shadowing contributions is fixed from the observed Pomeron and Reggeon behavior of the isospin singlet and non-singlet nucleon structure functions themselves.

Another interesting spin effect in QCD is the prediction that nuclear shadowing depends on the virtual photon polarization. In models where shadowing is due to the deformation of nucleon structure functions in the nucleus, one would not expect such any dependence on photon polarization. As noted above, nuclear shadowing (in the target rest frame) arises from the destructive interference of the multiple scattering of a quark (or antiquark) in the nucleus. The $q\bar{q}$ pair is formed at a formation time (coherence length) $\tau \propto 1/x_{\rm bj}M$ before the target. In order to get significant multiple scattering and interference one needs a coherence

length comparable to the nuclear size. However, Hoyer, Del Duca, and I found[53] that the coherence length is significantly shorter (by a factor of $1/\sqrt{3}$) for the longitudinally polarized photon than the transverse case. The reason for this is that the internal transverse momentum and hence the virtual mass and energy of the $q\bar{q}$ pair is larger by a nearly constant factor in the longitudinal case, thus shortening its lifetime. Thus the nuclear attenuation is delayed to smaller values of $x_{\rm bj}$ in the longitudinal compared to the transverse cross section. Nikolaev[54] has also recently discussed the possibility of smaller nuclear shadowing of σ_L on the grounds that the $q\bar{q}$ system has a smaller transverse size in the case of a longitudinally polarized photon, and it is thus more color transparent. In this case diminished longitudinal shadowing would persist for all $x_{\rm bj}$.

10 Connections between Global Spin Measures[55]

Light-cone quantization has a number of unique features that make it appealing for solving relativistic bound-state problems in the strong coupling regime., most notably, the ground state of the free theory is also a ground state of the full theory, and the Fock expansion constructed on this vacuum state provides a complete relativistic many-particle basis for diagonalizing the full theory.[56] The method seems therefore to be well-suited to solving quantum chromodynamics. For practical calculations one approximates the field theory by truncating the Fock space.[57] The assumption is that a few excitations describe the essential physics, and that adding more excitations only refines this initial approximation. This is quite different from the instant formulation of QCD where an infinite number of gluons is essential for formulating even the vacuum. In this paper we restrict ourselves to an effective three-quark Fock description of the nucleon. In this effective theory, all additional degrees of freedom (including zero modes) are parameterized in an effective potential.[58] In such a theory the constituent quarks will also acquire effective masses and form factors.

After truncation, one could in principle obtain the mass M and light-cone wavefunction $|\Psi\rangle$ of the three-quark bound-states (see the Introduction) by solving the Hamiltonian eigenvalue problem

$$H_{\rm LC}^{\rm effective}|\Psi\rangle = M^2|\Psi\rangle. \tag{31}$$

Given the eigensolutions $|\Psi\rangle$ one could then compute the form factors and other

properties of the baryons. Even without explicit solutions, one knows that the helicity and flavor structure of the baryon eigenfunctions must reflect the assumed global SU(6) symmetry and Lorentz invariance of the theory. However, since we do have an explicit representation for the effective potential in the light-cone Hamiltonian $H_{\rm LC}^{\rm effective}$ for three-quarks, we shall have to proceed by making an ansatz for the momentum space structure of the wavefunction Ψ. This may seem quite arbitrary, but as we will show below, for a given size of the proton, the predictions and interrelations between observables at $Q^2 = 0$, such as the proton magnetic moment μ_p and its axial coupling g_A, turn out to be essentially independent of the shape of the wavefunction.

The light-cone model given in Ref. 59 provides a framework for representing the general structure of the effective three-quark wavefunctions for baryons. The wavefunction Ψ is constructed as the product of a momentum wavefunction, which is spherically symmetric and invariant under permutations, and a spin-isospin wave function, which is uniquely determined by SU(6)-symmetry requirements. A Wigner[60] (Melosh[61]) rotation is applied to the spinors, so that the wavefunction of the proton is an eigenfunction of J and J_z in its rest frame.[62,63] To represent the range of uncertainty in the possible form of the momentum wavefunction we choose two simple functions of the invariant mass $\mathcal{M}$ of the quark:

$$\begin{aligned} \psi_{\rm H.O.}(\mathcal{M}^2) &= N_{\rm H.O.}\exp(-\mathcal{M}^2/2\beta^2), \\ \psi_{\rm Power}(\mathcal{M}^2) &= N_{\rm Power}(1+\mathcal{M}^2/\beta^2)^{-p} \end{aligned} \tag{32}$$

where β sets the scale of the nucleon size. Perturbative QCD predicts a nominal power-law fall off at large $k_\perp$ corresponding to $p = 3.5$.[58] The invariant mass $\mathcal{M}$ can be written as

$$\mathcal{M}^2 = \sum_{i=1}^{3} \frac{\vec{k}_{\perp i}^2 + m^2}{x_i} \tag{33}$$

where we used the longitudinal light-cone momentum fractions $x_i = p_i^+/P^+$ (P and p_i are the nucleon and quark momenta, respectively, with $P^+ = P_0 + P_z$). The internal momentum variables $\vec{k}_{\perp i}$ are given by $\vec{k}_{\perp i} = \vec{p}_{\perp i} - x_i\vec{P}_\perp$ with the constraints $\sum \vec{k}_{\perp i} = 0$ and $\sum x_i = 1$. The Melosh rotation has the matrix repre-

sentation[61]

$$R_M(x_i, k_{\perp i}, m) = \frac{m + x_i\mathcal{M} - i\vec{\sigma}\cdot(\vec{n}\times\vec{k}_i)}{\sqrt{(m+x_i\mathcal{M})^2 + \vec{k}_{\perp i}^2}}, \tag{34}$$

with $\vec{n} = (0,0,1)$, and it becomes the unit matrix if the quarks are collinear

$$R_M(x_i, 0, m) = 1. \tag{35}$$

Thus the internal transverse momentum dependence of the light-cone wavefunctions also affects its helicity structure.

The Dirac and Pauli form factors $F_1(Q^2)$ and $F_2(Q^2)$ of the nucleons are given by the spin-conserving and the spin-flip vector current J_V^+ matrix elements $(Q^2 = -q^2)$[42]

$$\begin{aligned} F_1(Q^2) &= \langle p+q, \uparrow | J_V^+ | p, \uparrow \rangle, \\ (Q_1 - iQ_2)F_2(Q^2) &= -2M\langle p+q, \uparrow | J_V^+ | p, \downarrow \rangle. \end{aligned} \tag{36}$$

We then can calculate the anomalous magnetic moment $a = \lim_{Q^2\to 0} F_2(Q^2)$. [The total proton magnetic moment is $\mu_p = (e/2M)(1+a_p)$.] The same parameters as in Ref. 59 are chosen; namely, $m = 0.263$ GeV (0.26 GeV) for the up- and down-quark masses, and $\beta = 0.607$ GeV (0.55 GeV) for ψ_{Power} ($\psi_{\text{H.O.}}$) and $p = 3.5$. The quark currents are taken as elementary currents with Dirac moments $e_q/2m_q$. All of the baryon moments are well-fit if one takes the strange quark mass as 0.38 GeV. With the above values, the proton magnetic moment is 2.81 nuclear magnetons, the neutron magnetic moment is -1.66 nuclear magnetons* and the radius of the proton is 0.76 fm; *i.e.* $M_pR_1 = 3.63$.[59]

In Fig. 5 we show the functional relationship between the anomalous moment a_p and its Dirac radius predicted by the three-quark light-cone model. The value of $R_1^2 = -6dF_1(Q^2)/dQ^2|_{Q^2=0}$ is varied by changing β in the light-cone wavefunction while keeping the quark mass m fixed. The prediction for the power-law wavefunction ψ_{Power} is given by the continuous line; the broken line represents $\psi_{\text{H.O.}}$. Figure 5 shows that when one plots the dimensionless observable a_p against

* The neutron value can be improved by relaxing the assumption of isospin symmetry.

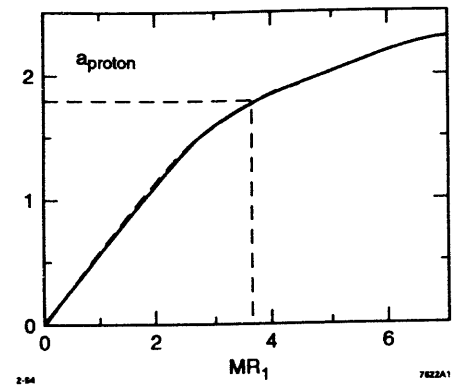

Figure 5. The anomalous magnetic moment $a = F_2(0)$ of the proton as a function of M_pR_1: continuous line, pole type wavefunction; broken line, gaussian wavefunction. The experimental value $a = 1.79$ at $M_pR_1 = 3.63$ is shown by the dotted lines. The model predictions are essentially independent of the shape of the light-cone wavefunction.

the dimensionless observable MR_1 the prediction is essentially independent of the assumed power-law or Gaussian form of the three-quark light-cone wavefunction. Different values of $p > 2$ do also not affect the functional dependence of $a_p(M_pR_1)$ shown in Fig. 5. In this sense the predictions of the three-quark light-cone model relating the $Q^2\to 0$ observables are essentially model-independent. The only parameter controlling the relation between the dimensionless observables in the light-cone three-quark model is m/M_p which is set to 0.28. For the physical proton radius $M_pR_1 = 3.63$ one obtains the empirical value for $a_p = 1.79$ (indicated by the dotted lines in Fig. 5).

The prediction for the anomalous moment a can be written analytically as $a = \langle\gamma_V\rangle a^{\text{NR}}$, where $a^{\text{NR}} = 2M_p/3m$ is the non-relativistic $(R\to\infty)$ value and γ_V is given as[64]

$$\gamma_V(x_i, k_{\perp i}, m) = \frac{3m}{\mathcal{M}}\left[\frac{(1-x_3)\mathcal{M}(m+x_3\mathcal{M}) - \vec{k}_{\perp 3}^2/2}{(m+x_3\mathcal{M})^2 + \vec{k}_{\perp 3}^2}\right]. \tag{37}$$

The expectation value $\langle\gamma_V\rangle$ is evaluated as†

† $[d^3k] = d\vec{k}_1 d\vec{k}_2 d\vec{k}_3 \delta(\vec{k}_1 + \vec{k}_2 + \vec{k}_3)$. The third component of $\vec{k}$ is defined as $k_{3i} = \frac{1}{2}(x_i\mathcal{M} - (m^2 + \vec{k}_{\perp i}^2/x_i\mathcal{M}))$. This measure differs from the usual one used in Ref. 58 by the Jacobian $\prod dk_{\perp i}/dx_i$, which can be absorbed into the wavefunction.

$$\langle \gamma_V \rangle = \frac{\int [d^3k] \gamma_V |\psi|^2}{\int [d^3k] |\psi|^2}. \tag{38}$$

We now take a closer look at the two limits $R \to \infty$ and $R \to 0$. In the non-relativistic limit we let $\beta \to 0$ and keep the quark mass m and the proton mass M_p fixed. In this limit the proton radius $R_1 \to \infty$ and $a_p \to 2M_p/3m = 2.38$ since $\langle \gamma_V \rangle \to 1$[‡]. Thus the physical value of the anomalous magnetic moment at the empirical proton radius $M_p R_1 = 3.63$ is reduced by 25% from its non-relativistic value due to relativistic recoil and nonzero $k_\perp$[§].

To obtain the ultra-relativistic limit we let $\beta \to \infty$ while keeping m fixed. In this limit the proton becomes pointlike $M_p R_1 \to 0$ and the internal transverse momenta $k_\perp \to \infty$. The anomalous magnetic momentum of the proton goes linearly to zero as $a = 0.43 M_p R_1$ since $\langle \gamma_V \rangle \to 0$. Indeed, the Drell-Hearn-Gerasimov (DHG) sum rule[35,36] demands that the proton magnetic moment becomes equal to the Dirac moment at small radius. For a spin-$\frac{1}{2}$ system

$$a^2 = \frac{M^2}{2\pi^2 \alpha} \int_{s_{th}}^{\infty} \frac{ds}{s} [\sigma_P(s) - \sigma_A(s)], \tag{39}$$

where $\sigma_{P(A)}$ is the total photoabsorption cross section with parallel (antiparallel) photon and target spins. If we take the point-like limit, such that the threshold for inelastic excitation becomes infinite while the mass of the system is kept finite, the integral over the photoabsorption cross section vanishes and $a = 0$.[42] In contrast, the anomalous magnetic moment of the proton does not vanish in the non-relativistic quark model as $R \to 0$. The non-relativistic quark model does not reflect the fact that the magnetic moment of a baryon is derived from lepton scattering at non-zero momentum transfer[48]; *i.e.* the calculation of a magnetic moment requires knowledge of the boosted wavefunction. The Melosh transformation is also essential for deriving the DHG sum rule and low energy theorems (LET) of composite systems.[48]

‡ This differs slightly from the usual non-relativistic formula $1 + a = \sum_q (e_q/e)(M_p/m_q)$ due to the non-vanishing binding energy which results in $M_p \neq 3m_q$.

§ The non-relativistic value of the neutron magnetic moment is reduced by 31%.

A similar analysis can be performed for the axial-vector coupling measured in neutron decay. The coupling g_A is given by the spin-conserving axial current J_A^+ matrix element

$$g_A(0) = \langle p, \uparrow | J_A^+ | p, \uparrow \rangle. \tag{40}$$

The value for g_A can be written as $g_A = \langle \gamma_A \rangle g_A^{\rm NR}$ with $g_A^{\rm NR}$ being the non-relativistic value of g_A and with γ_A as[64,65]

$$\gamma_A(x_i, k_{\perp i}, m) = \frac{(m + x_3 \mathcal{M})^2 - \vec{k}_{\perp 3}^2}{(m + x_3 \mathcal{M})^2 + \vec{k}_{\perp 3}^2}. \tag{41}$$

In Fig. 6 the axial-vector coupling is plotted against the proton radius $M_p R_1$. The same parameters and the same line representation as in Fig. 5 are used. The functional dependence of $g_A(M_p R_1)$ is also found to be independent of the assumed wavefunction. At the physical proton radius $M_p R_1 = 3.63$ one predicts the value $g_A = 1.25$ (indicated by the dotted lines in Fig. 6) since $\langle \gamma_A \rangle = 0.75$. The measured value is $g_A = 1.2573 \pm 0.0028$.[66] This is a 25% reduction compared to the non-relativistic SU(6) value $g_A = 5/3$, which is only valid for a proton large radius $R_1 \gg 1/M_p$. As shown by Ma and Zhang[65] the Melosh rotation generated by the internal transverse momentum spoils the usual identification of the $\gamma^+\gamma_5$ quark current matrix element with the total rest-frame spin projection s_z, thus resulting in a reduction of g_A.

Thus given the empirical values for the proton's anomalous moment a_p and radius $M_p R_1$, its axial-vector coupling is automatically fixed at the value $g_A = 1.25$. This prediction is an essentially model-independent prediction of the three-quark structure of the proton in QCD. The Melosh rotation of the light-cone wavefunction is crucial for reducing the value of the axial coupling from its non-relativistic value 5/3 to its empirical value. In Fig. 7 we plot $g_A/g_A(R_1 \to \infty)$ versus $a_p/a_p(R_1 \to \infty)$ by varying the proton radius R_1. The near equality of these ratios reflects the relativistic spinor structure of the nucleon bound state, which is essentially independent of the detailed shape of the momentum-space dependence of the light-cone wavefunction.

We emphasize that at small proton radius the light-cone model predicts not

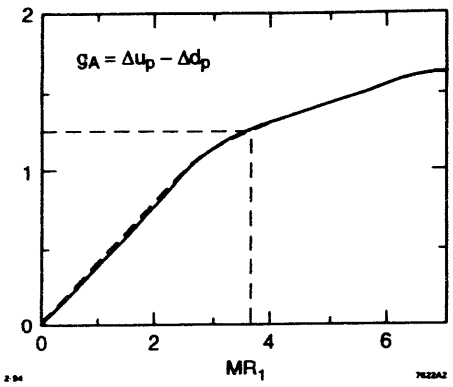

Figure 6. The axial vector coupling g_A of the neutron to proton decay as a function of M_pR_1: line code as in Fig. 5. The experimental values $g_A = 1.26$ and $M_pR_1 = 3.63$ are shown by the dotted lines.

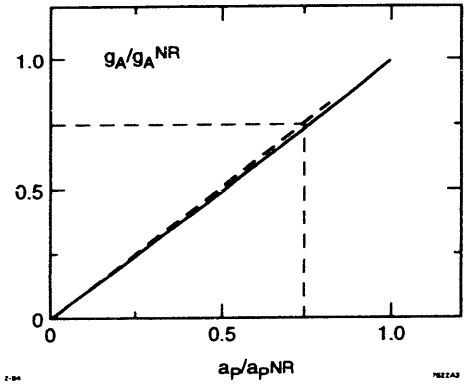

Figure 7. The ratio $g_A/g_A(R_1 \to \infty)$ versus the ratio $a_p/a_p(R_1 \to \infty)$ obtained by varying the proton radius R_1. The experimental values are indicated by the dotted lines.

only a vanishing anomalous moment but also

$$\lim_{R_1 \to 0} g_A(M_pR_1) = 0. \tag{42}$$

One can understand this physically: in the zero radius limit the internal transverse momenta become infinite and the quark helicities become completely disoriented.

This is in contradiction with chiral models which suggest that for a zero radius composite baryon one should obtain the chiral symmetry result $g_A = 1$.

The helicity measures Δu and Δd of the nucleon each experience the same reduction as g_A due to the Melosh effect. Indeed, the quantity Δq is defined by the axial current matrix element

$$\Delta q = \langle p, \uparrow | \bar{q}\gamma^+\gamma_5 q | p, \uparrow \rangle, \tag{43}$$

and the value for Δq can be written analytically as $\Delta q = \langle \gamma_A \rangle \Delta q^{NR}$ with Δq^{NR} being the non-relativistic or naive value of Δq and with γ_A given in Eq. (41).

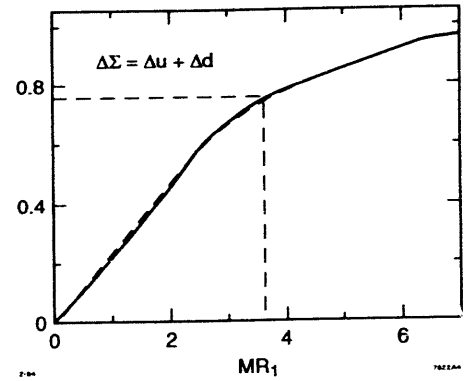

Figure 8. The quantity $\Delta\Sigma = \Delta u + \Delta d$ of the proton as a function of M_pR_1. The experimental value $M_pR_1 = 3.63$ is indicated by the dotted lines.

Figure 8 shows the prediction of the light-cone model for the quark helicity sum $\Delta\Sigma = \Delta u + \Delta d$ as a function of the proton radius R_1. The same parameters and the same line representation as in Fig. 5 are used. This figure shows that the helicity sum $\Delta\Sigma$ defined from the light-cone wavefunction depends on the proton size, and thus it cannot be identified as the vector sum of the rest-frame constituent spins. As emphasized by Ma,[65] the rest-frame spin sum is not a Lorentz invariant for a composite system. Empirically, one can measures Δq from the first moment of the leading twist polarized structure function $g_1(x, Q)$. In the light-cone and parton model descriptions, $\Delta q = \int_0^1 dx[q^\uparrow(x) - q^\downarrow(x)]$, where $q^\uparrow(x)$ and $q^\downarrow(x)$ can be interpreted as the probability for finding a quark or antiquark with

longitudinal momentum fraction x and polarization parallel or antiparallel to the proton helicity in the proton's infinite momentum frame.[58] [In the infinite momentum there is no distinction between the quark helicity and its spin-projection s_z.] Thus Δq refers to the difference of helicities at fixed light-cone time or at infinite momentum; it cannot be identified with $q(s_z = +\frac{1}{2}) - q(s_z = -\frac{1}{2})$, the spin carried by each quark flavor in the proton rest frame in the equal time formalism.

One sees from Fig. 8 that the usual SU(6) values $\Delta u^{\rm NR} = 4/3$ and $\Delta d^{\rm NR} = -1/3$ are only valid predictions for the proton at large MR_1. At the physical radius the quark helicities are reduced by the same ratio 0.75 as $g_A/g_A^{\rm NR}$ due to the Melosh rotation. Thus for $M_p R_1 = 3.63$, the three-quark model predicts $\Delta u = 1$, $\Delta d = -1/4$, and $\Delta\Sigma = \Delta u + \Delta d = 0.75$. Although the gluon contribution $\Delta G = 0$ in our model, the general sum rule[67]

$$\frac{1}{2}\Delta\Sigma + \Delta G + L_z = \frac{1}{2} \tag{44}$$

is still satisfied, since the Melosh transformation effectively contributes to L_z.

Suppose one adds polarized gluons to the three-quark light-cone model. The flavor-singlet quark-loop radiative corrections to the gluon propagator will then give an anomalous contribution $\delta(\Delta q) = -\frac{\alpha_s}{2\pi}\Delta G$ to each light quark helicity.[68] The predicted value of $g_A = \Delta u - \Delta d$ is of course unchanged. For illustration we shall choose $\frac{\alpha_s}{2\pi}\Delta G = 0.20$. The gluon-enhanced quark model then gives the values in Table 1, which agree well with the present experimental values. Note that the gluon anomaly contribution to Δs has probably been overestimated here due to the large strange quark mass.

In summary, we have shown that relativistic effects are important for understanding the spin structure of the nucleons. By plotting dimensionless observables against dimensionless observables we obtain model-independent relations independent of the momentum-space form of the three-quark light-cone wavefunctions. For example, the value of $g_A \simeq 1.25$ is correctly predicted from the empirical value of the proton's anomalous moment. For the physical proton radius $M_p R_1 = 3.63$ the inclusion of the Wigner (Melosh) rotation due to the finite relative transverse momenta of the three quarks results in a $\simeq 25\%$ reduction of the non-relativistic predictions for the anomalous magnetic moment, the axial vector coupling, and the quark helicity content of the proton.

Table 1

Comparison of the quark content of the proton in the non-relativistic quark model (NR), in our three-quark model (3q), in a gluon enhanced three-quark model (3q+g), and with experiment.[29]

Quantity	NR	3q	3q+g	Expt.
Δu	$\frac{4}{3}$	1	0.80	0.80 ± 0.04
Δd	$-\frac{1}{3}$	$-\frac{1}{4}$	-0.45	-0.46 ± 0.04
Δs	0	0	-0.20	-0.13 ± 0.04
$\Delta\Sigma$	1	$\frac{3}{4}$	0.15	0.22 ± 0.10

In the next section I will discuss theoretical constraints on the shape of the quark and gluon helicity distributions which follow from general QCD principles.

11 Perturbative QCD Constraints on the Shape of Polarized Quark and Gluon Distributions[9]

The measurements of polarization correlations in high momentum transfer reactions provide highly sensitive tests of the underlying structure and dynamics of hadrons. The most direct information on the light-cone momentum distributions of helicity-aligned and helicity-anti-aligned quarks in nucleons is obtained from deep inelastic scattering of polarized leptons on polarized targets. The recent fixed-target measurements, the SMC muon-deuteron and muon-proton experiments at CERN,[69,28] and the electron-He^3 experiments E142 and E143 at SLAC[70] are now providing important new constraints on the proton and neutron helicity-dependent structure functions.

Although the Q^2-evolution of structure functions is well-predicted by perturbative QCD, the initial shape of these distributions reflects the non-perturbative quark and gluon dynamics of the bound-state solutions of QCD. Nevertheless, it is possible to accurately predict some aspects of the shape of the nucleon structure functions from perturbative arguments alone. In fact as Burkardt and Schmidt[9] and I have recently shown, one can derive an analytic parameterization of the polarized quark and gluon distributions in the nucleons which incorporates

general constraints obtained from the requirements of color coherence of gluon couplings at $x \sim 0$ and the helicity structure of perturbative QCD couplings at $x \sim 1$. The predicted forms provide useful guides to the expected shapes of the polarized structure functions.

As discussed in the introduction and appendix, the polarized quark and gluon distributions $G_{q/H}(x,\lambda,Q)$ and $G_{g/H}(x,\lambda,Q)$ of a hadron are probability distributions determined by the light-cone wavefunctions $\psi_n(x_i,k_{\perp i},\lambda_i)$, where $\sum_{i=1}^n x_i = 1$, and $\sum_{i=1}^n k_{\perp_i} = 0_\perp$. The square of the invariant mass of an n-particle Fock State configuration in the wavefunction is $\mathcal{M}_n^2 = \sum_{i=1}^n (k_{\perp i}^2 + m_i^2)/x_i$. Thus the kinematical regime where one quark has nearly all of the light-cone momentum $x \sim 1$, and the remaining constituents have $x_i \sim 0$, represents a very far off-shell configuration of a bound state wavefunction. In the limit $x \to 1$, the Feynman virtuality of the struck parton in a bound state becomes far off-shell and space-like: $k_F^2 - m^2 = x(M_H^2 - \mathcal{M}^2) \to -\mu^2/(1-x)$, where μ is the invariant mass of the system of stopped constituents. If one assumes that the bound state wavefunction of the hadron is dominated by the lowest invariant mass partonic states, then the constituents can attain far off-shell configurations only by exchanging hard gluons; thus the leading behavior at large virtuality can be computed simply by iterating the gluon exchange interaction kernel.[71,72,58] This conforms to the usual ansatz of perturbative QCD that hard perturbative contributions dominate amplitudes involving high momentum transfer compared to the contributions arising from non-perturbative sources.

Thus, because of asymptotic freedom, the leading order contributions in $\alpha_s(k_F^2)$ to the quark and gluon distributions at $x \to 1$ can be computed in perturbative QCD from minimally connected tree graphs. For example, in the case of the nucleon structure functions, the dominant amplitude is derived from graphs where the three valence quarks exchange two hard gluons. The tree amplitude is then convoluted with the nucleon distribution amplitude $\phi(x_i,k_F^2)$ which is obtained by integrating the valence three-quark nucleon wavefunction $\psi_3(x_i,k_{\perp i},\lambda_i)$, over transverse momenta up to the scale k_F^2.[58] The $dk_\perp d\phi$ azimuthal loop integrations project out only the $L_z = 0$ component of the three-quark nucleon wavefunction. Thus, in amplitudes controlled by the short distance structure of the hadron's valence wavefunction, orbital angular momentum can be ignored, and the valence quark helicities sum to the hadron helicity.

The limiting power-law behavior at $x \to 1$ of the helicity-dependent distributions derived from the minimally connected graphs is

$$G_{q/H} \sim (1-x)^p, \tag{45}$$

where

$$p = 2n - 1 + 2\Delta S_z. \tag{46}$$

Here n is the minimal number of spectator quark lines, and $\Delta S_z = |S_z^q - S_z^H| = 0$ or 1 for parallel or anti-parallel quark and proton helicities, respectively.[71] This counting rule reflects the fact that the valence Fock states with the minimum number of constituents give the leading contribution to structure functions when one quark carries nearly all of the light-cone momentum; just on phase-space grounds alone, Fock states with a higher number of partons must give structure functions which fall off faster at $x \to 1$. The helicity dependence of the counting rule also reflects the helicity retention properties of the gauge couplings: a quark with a large momentum fraction of the hadron also tends to carry its helicity. The antiparallel helicity quark is suppressed by a relative factor $(1-x)^2$. Similarly, in the case of a splitting function such as $q \to qg$ or $g \to \bar{q}q$, the sign of the helicity of the parent parton is transferred to the constituent with the largest momentum fraction.[73] The counting rule for valence quarks can be combined with the splitting functions to predict the $x \to 1$ behavior of gluon and non-valence quark distributions. In particular, the gluon distribution of non-exotic hadrons must fall by at least one power faster than the respective quark distributions.

The counting rules for the end-point-behavior of quark and gluon helicity distributions can also be derived from duality, *i.e.* continuity between the physics of exclusive and inclusive channels at fixed invariant mass.[74] As shown by Drell and Yan,[75] a quark structure function $G_{q/H} \sim (1-x)^{2n-1}$ at $x \to 1$ if the corresponding form factor $F(Q^2) \sim (1/Q^2)^n$ at large Q^2. Recent measurements of elastic electron-proton scattering at SLAC[76] are compatible with the perturbative QCD predictions[12] for both the helicity-conserving $F_1(Q^2)$ and helicity-changing $F_2(Q^2)$ form factors: $Q^4F_1(Q^2)$ and $Q^6F_2(Q^2)$ become approximately constant at large Q^2. The power-law fall-off of the form factors corresponds to the helicity-parallel and helicity-antiparallel quark distributions behaving at $x \to 1$ as $(1-x)^3$

and $(1-x)^5$, respectively, in agreement with the counting rules. The leading exponent for quark distributions is odd in the case of baryons and even for mesons in agreement with the Gribov-Lipatov crossing rule.[8]

The counting rule predictions for the quark and gluon distributions are relevant at low momentum transfer scales $Q_0 \sim \Lambda_{QCD}$ in which the controlling physics is that of the hadronic bound state rather than the radiative corrections associated with structure function evolution. At the hadronic scale one can normalize the non-singlet quark helicity content of the proton and neutron using the constraint from β decay:[66]

$$\Delta u - \Delta d = \frac{g_A}{g_V} = 1.2573 \pm 0.0028 \ . \tag{47}$$

where $\Delta q_i(x) = q_i^+(x) - q_i^-(x)$ with $i = u, d, s$ is the difference of the helicity-aligned and helicity-anti-aligned quark distributions in the proton, and $\Delta q_i = \int_0^1 dx q_i(x)$ is the integrated moment. [In the standard notation $q^+(x,Q) = G_{q/p}(x, \lambda_q = \lambda_p, Q) + G_{\bar{q}/p}(x, \lambda_q = \lambda_p, Q)$ so that both quark and anti-quark contributions are included.] In addition, if one assumes $SU(3)$ flavor symmetry, hyperon decay also implies a polarized strange quark component in the proton wavefunction[77, 78]

$$\frac{\Delta u + \Delta d - 2\Delta s}{\sqrt{3}} = 0.39 \ . \tag{48}$$

Thus only one normalization is left undetermined.

The presence of polarized gluons in the nucleon wavefunction implies that polarized strange quarks contribute to the nucleon helicity-dependent structure functions at some level. There is also evidence from neutrino-proton elastic scattering that the proton has a significant polarized strange quark content.[77]

The helicity-dependent structure function $g_1(x, Q^2)$ measured in deep inelastic polarized-lepton polarized-proton scattering can be identified in the Bjorken scaling region with the quark helicity asymmetry:

$$g_1(x, Q^2) = \tfrac{1}{2} \sum_i e_q^2 \Delta q(x, Q^2) \ . \tag{49}$$

The first moment of the proton-neutron difference has zero anomalous dimension and satisfies the Bjorken sum rule[73] (Eq. (16)), including radiative corrections

from hard gluon interactions in the electron-quark scattering process.[79] Thus the QCD radiative corrections[80] to the helicity-dependent structure functions can modify the shape of the distributions, within the global constraint of the Bjorken sum rule.

At high Q^2, the radiation from the struck quark line increases the effective power law fall-off $(1-x)^p$ of structure functions relative to the underlying quark distributions: $\Delta p = (4C_F/\beta_1)\log(\log Q^2/\Lambda^2)/(\log Q_0^2/\Lambda^2)$ where $C_F = 4/3$ and $\beta_1 = 11 - (2/3)n_f$. The counting rule predictions for the power p thus provide a *lower bound* for the effective exponent of quark structure functions at high $Q^2 > Q_0^2$. However, in the end-point region $x \sim 1$, the struck quark is far off-shell and the radiation is quenched since one cannot evolve Q^2 below $Q_0^2 \simeq k_f^2 = -(\mu^2/(1-x))$, the Feynman virtuality of the struck parton.[81] Furthermore, the integral of the g_1 structure function is only affected by QCD radiative corrections of order $\alpha_s(Q^2)/\pi$.

Thus PQCD can give useful predictions for the power law fall-off of helicity-aligned and anti-aligned structure functions at $x \sim 1$. Higher order contributions involving additional hard gluon exchange are suppressed by powers of $\alpha_s(k_F^2)$. Further iterations of the interaction kernel will give factors of fractional powers of $\log(1-x)$ analogous to the anomalous dimensions $\log^n Q^2$ which appear in the PQCD treatment of form factors at large momentum transfer.[12] This is in contrast to super-renormalizable theories such as QCD(1+1) where the power-law behavior in the endpoint region is modified by all-order contributions.[82]

The fact that one has a definite prediction for the $x \sim 1$ behavior of leading twist structure functions is a powerful tool in QCD phenomenology, since any contribution that does not decrease sufficiently fast at large x is most likely due to coherent multi-quark correlations. As discussed in Ref. 13, such contributions are higher twist, but they arise naturally in QCD and are significant at fixed $(1-x)Q^2$. Such coherent contributions are in fact needed in order to explain the anomalous change in polarization seen in pion-induced continuum lepton-pair and hadronic J/ψ production experiments at high x_F.[83]

At large x the perturbative QCD analysis predicts "helicity retention" — *i.e.* the helicity of a valence quark with $x \sim 1$ will matches that of the parent nucleon. This result is in agreement with the original prediction of Farrar and Jackson[72] that the helicity asymmetry $\Delta q(x)$ approaches 1 at $x \to 1$. We also

predict, in agreement with Ref. 72, that the ratio of unpolarized neutron to proton structure functions approaches the value 3/7 for $x \to 1$.

In the following sections we will analyze the shape of the polarized gluon and quark distributions in the proton. First we will study the behavior of the gluon asymmetry $\Delta G(x)/G(x)$ (polarized over unpolarized distributions) at small values of x, where it turns out to be proportional to x with a coefficient approximately independent of the details of the bound-state wavefunction. We then write down a simple model for the gluon distributions which incorporates the counting rule constraints at $x \to 1$. The same is done for the up, down and strange quark distributions. The extrinsic and intrinsic strange quark distributions are also discussed, paying special attention to the inclusive-exclusive connection with the strange quark contribution to the proton form factors.

12 Helicity-Dependent Gluon Distributions

The angular momentum of a fast-moving proton has three sources, the angular momentum carried by the quarks, the angular momentum carried by the gluons, and the orbital angular momentum carried by any of the constituents. Angular momentum conservation for J_z at a fixed light-cone time implies the sum rule[2,67]

$$\frac{1}{2}(\Delta u + \Delta d + \Delta s) + \Delta G \ + \langle L_z \rangle = \frac{1}{2}. \tag{50}$$

Here $\Delta G \equiv \int_0^1 dx \Delta G(x)$ is the helicity carried by the gluons, where $\Delta G(x)$ is the difference between the helicity-aligned and anti-aligned gluon distributions $G^+(x)$ and $G^-(x)$; the unpolarized gluon distribution $G(x)$ is the sum of these two functions, $G(x) \equiv G^+(x) + G^-(x)$. The corresponding definitions for the quark distributions $\Delta q(x) = q^+(x) - q^-(x)$ and $q(x) = q^+(x) + q^-(x)$ with $q = u, d, s$. By definition, the antiquark contributions are included in $\Delta q(x)$ and $q(x)$. As emphasized in Section 10 and by Ma,[65] the helicity distributions measured on the light-cone are related by a Wigner rotation (Melosh transformation) to the ordinary spins S_i^z of the quarks in an equal-time rest-frame wavefunction description. Thus, due to the non-colinearity of the quarks, one cannot expect that the quark helicities will sum simply to the proton spin.

In this section I shall discuss model forms for the gluon distribution functions $\Delta G(x)$ and $G(x)$ for nucleons which incorporate the known large-x counting-rule

constraints:

$$G^+(x) \to C(1-x)^4 \qquad (x \to 1)\,, \tag{51}$$

$$G^-(x) \to C(1-x)^6 \qquad (x \to 1)\,; \tag{52}$$

We shall also implement a basic constraint on the behavior of the gluon asymmetry ratio $\Delta G(x)/G(x)$ for small x :

$$\left(\frac{\Delta G(x)}{G(x)}\right)_{\text{proton}} \to \frac{x}{3}\left\langle \frac{1}{y} \right\rangle \qquad (x \to 0). \tag{53}$$

This last theoretical constraint will be demonstrated below. Here $\langle 1/y \rangle$ stands for the first inverse moment of the quark light-cone momentum fraction distribution in the proton lowest Fock state. For this state we expect $\langle 1/y \rangle \simeq 3$.

A simple form for baryon gluon distributions, which incorporates the limiting behaviors presented above, is

$$\begin{aligned} \Delta G(x) &= \frac{N}{x}\,[1-(1-x)^2]\,(1-x)^4, \\ G(x) &= \frac{N}{x}\,[1+(1-x)^2]\,(1-x)^4. \end{aligned} \tag{54}$$

In this model the momentum fraction carried by the gluons in the proton is $\langle x_g \rangle \equiv \int_0^1 dx x G(x) = \frac{12}{35}N$, and the helicity carried by the gluons is $\Delta G \equiv \int_0^1 dx \Delta G(x) = (11/30)N$. Taking the momentum fraction $\langle x_g \rangle$ to be 1/2, we predict $\Delta G = 0.54$.

Such large values for the gluon momentum fraction are inconsistent with the assumption that the proton has a dominant three-quark Fock state probability; a self-consistent approach thus requires taking into account gluon radiation from the full quark and gluon light-cone Fock basis of the nucleon. Our main emphasis here is to predict the characteristic shapes of the polarized quark and gluon distributions. The large x regime is clearly dominated by the lowest particle-number Fock states. We thus expect that the qualitative features of the model to survive in a more rigorous approach; in particular, it is apparent from the structure of the model, that the gluon helicity fraction will be of the same order of magnitude as the gluon momentum fraction.

The prediction that $\Delta G \simeq 0.5$ is phenomenologically interesting. If one also accepts the experimental suggestion from EMC that the quark helicity sum $\Delta u + \Delta d$ is small, then this implies that gluons could carry a large part of the proton helicity $J_z = 1/2$. However, one then also expects significant orbital angular momentum L_z which arises, for example, from the finite transverse momentum associated with the $q \to qg$ gluon emission matrix element.

We now proceed to prove Eq. (53) for the low-x behavior of the asymmetry $\Delta G(x)/G(x)$. In this region the quarks in the hadron radiate coherently, and we must consider interference between amplitudes in which gluons are emitted from different quark lines. An analysis of this type was first presented in Ref. 84, and in this note we extend and correct some of the results of that paper.

As an example, we first analyze the helicity content of positronium, where we can ignore internal transverse momenta and non-collinearity. Consider the ortho-positronium two-fermion $J_z = 1$ Fock state in which the particles have helicities $+ +$. Following the calculation of Ref. 84, we obtain

$$\left(\frac{\Delta G(x)}{G(x)}\right)_{\text{ortho}(J_z=+1)} \simeq x\left\langle\frac{1}{y}\right\rangle \simeq 2x \qquad (x \to 0)\ . \tag{55}$$

In the case of para-positronium (and also for $J_z = 0$ ortho-positronium), in which we start with a Fock state with helicities $+ -$, the result is $\Delta G(x) = 0$. This is because for every diagram in $G^+(x)$ there is a corresponding diagram in $G^-(x)$, but with the helicities of all the particles reversed.

We now apply a similar analysis to the gluon distribution in the nucleon. We start with a three-quark Fock state in which the quarks have helicities $+ + +$ as would be appropriate for the helicity content of an isobar state Δ with $J_z = 3/2$. Then the result found in Ref. 84, *i.e.*

$$\left(\frac{\Delta G(x)}{G(x)}\right)_{\Delta(J_z=3/2)} \simeq x\left\langle\frac{1}{y}\right\rangle \tag{56}$$

follows.

In the nucleon case, however, we start with a three-quark Fock state with helicities $+ + -$. Thus clearly there is a cancellation between the squared terms in which the gluon is emitted from one of the positive helicity quarks versus

the contributions in which the gluon is emitted by a negative helicity quark. The interference terms work similarly, ensuring a finite result for both $G(x)$ and $\Delta G(x)$ at zero $k_\perp$, just as in the case of photon distributions in positronium. Then the positive helicity quarks have a dominant $G^+(x)$ and contribute positively to $\Delta G(x)$; similarly, the negative helicity quarks contribute negatively to $\Delta G(x)$. To see this more clearly, consider the photon emitted by a single electron with $J_z = +1/2$. Then $G^+_{\gamma/e}(x) = 1/x$ and $G^-_{\gamma/e}(x) = (1-x)^2/x$. Thus $\Delta G(x)/G(x) = x$ at $x \to 0$ with unit coefficient in this case. The sign reverses for an electron with $J_z = -1/2$.

The generated gluon asymmetry distribution in the nucleon at low x is then given by Eq. (53). The extra factor of $1/3$ is due to the fact that all the quarks contribute positively to $G(x)$, but they give contributions proportional to the sign of their helicity in $\Delta G(x)$. The main assumption setting the value of the gluon asymmetry at $x \to 0$ is the estimated value of the inverse moment $\langle 1/y \rangle$. For realistic wavefunctions this expectation value may receive very large (possibly divergent) contributions from near $y = 0$. However, one must be careful at this point because in deriving Eq. (53) we assumed that $x \ll y$. In order to be consistent with this assumption we will perturb around a constituent quark wavefunction which is strongly peaked around $y = \langle y \rangle = 1/3$. We have furthermore assumed for simplicity that $\langle y \rangle$ is the same for all valence quarks, although this is inconsistent with results from QCD sum rules.[85] (One could improve the estimate for $\langle 1/y \rangle$ by allowing for different momentum fractions for the helicity-up and helicity-down quarks. This would evidently reduce ΔG, since it is known that $\langle y \rangle$ is larger for helicity parallel quarks. Furthermore, in QCD we expect that higher Fock states will contribute to reduce the value of $\langle y \rangle$ away from $1/3$, which would be the expected value if only the three-quark valence Fock state was present.)

13 The Shape of Helicity-Dependent Quark Distributions

As I have discussed in the previous sections, at $x \sim 1$ PQCD predicts that the helicity-parallel quark distribution $q^+(x)$ is enhanced relative to the helicity-antiparallel quark distribution $q^-(x)$ by two powers of $(1-x)$. The property of helicity retention at large x is a direct consequence of the gauge theory couplings between quarks and gluons. For the valence quarks in a nucleon the counting rules

predict

$$q^+(x) \sim (1-x)^3 \qquad (x \to 1), \tag{57}$$

and

$$q^-(x) \sim (1-x)^5 \qquad (x \to 1). \tag{58}$$

The case of the non-valence strange quarks is somewhat more complex and will be discussed in detail in the next section. The result is

$$s^+(x) \sim (1-x)^5 \qquad (x \to 1), \tag{59}$$

$$s^-(x) \sim (1-x)^7 \qquad (x \to 1). \tag{60}$$

For $x \sim 0$ the helicity correlation disappears since the constituent has infinite rapidity $\Delta y = \log x$ relative to the nucleon's rapidity.

The strange quark distribution in a nucleon can arise from both intrinsic and extrinsic contributions. The intrinsic contribution is associated with the multiparticle Fock state decomposition of the hadronic wavefunction, and it is essentially of non-perturbative origin. This is in contrast to the extrinsic component, which arises from $s\bar{s}$ pair production from a gluon emitted by a valence quark, and is associated with the self-field of a single quark in the proton. From evolution and gluon splitting, the extrinsic strange contributions are known to behave as

$$s_e^+(x) \sim (1-x)^5 \qquad (x \to 1) \tag{61}$$

$$s_e^-(x) \sim (1-x)^7 \qquad (x \to 1)\ . \tag{62}$$

The Drell-Yan inclusive-exclusive connection relates the high Q^2 behavior of the hadronic form factors to the large x limit of the quark distribution functions; *i.e.*

$$F(Q^2) \overset{Q^2 \to \infty}{\longrightarrow} \frac{1}{(Q^2)^n} \iff G_{q/p} \overset{x \to 1}{\longrightarrow} (1-x)^{2n-1+2\Delta S_z}, \tag{63}$$

where $\Delta S_z = 0$ or 1 for parallel or antiparallel quark and proton helicities, respectively. If we naively apply this prescription to the extrinsic strange quark

component, we would predict that the strange quark contribution to the electromagnetic proton form factor should fall as $1/Q^6$, since in this case $n = 3$. But a direct calculation of the strange quark contribution to either the axial or vector form factor of the nucleon gives only a nominal $1/Q^4$ behavior, which is the same power-law fall-off as the valence quark contribution. In the leading order calculations the loop integrals connecting a hard $s\bar{s}$ loop to a valence quark all have momenta $\ell = \mathcal{O}(Q)$, thus producing radiative corrections of order $\alpha_s^N(Q)$, to the exclusive amplitude with $N = 2$ (axial) or $N = 3$ (vector), rather than extra powers of $1/Q^2$.[58] The solution to this apparent contradiction is that we should apply the inclusive-exclusive connection for the strange quark contributions to a transition form factor connecting an initial state with three quarks (uud) to a final state in which a strange pair has been created ($uuds\bar{s}$), as in the transition form factor $p \to \Lambda K$, at *fixed* final state mass. Since the internal hard-scattering matrix element T_H for $(uud) + \gamma^* \to sud u\bar{s}$ has three off-shell fermion legs, this transition form factor falls off as $(1/Q^2)^3$, and it correctly satisfies the inclusive-exclusive connection ($n = 3$).

One can also consider the case where Q^2 and the final state mass are both large, but there is a K and Λ in the final state. This again corresponds to a $\sim (1-x)^5$ structure function. In the case of the transition $p \to p\phi$, there is a color mismatch in T_H at lowest order. Thus this amplitude should be suppressed (Zweig rule) by an extra power of $\alpha_s(Q^2)$. Of course all of this holds for the analogous charm systems as well.

The intrinsic strange components are associated with Fock states having at least five particles; the distributions thus have the behavior

$$s_i^+(x) \sim (1-x)^7 \qquad (x \to 1) \tag{64}$$

$$s_i^-(x) \sim (1-x)^9 \qquad (x \to 1)\ , \tag{65}$$

which corresponds to $n = 4$ in the spectator quark counting rules. It also satisfies the inclusive-exclusive connection, since the intrinsic contribution to the form factor falls as $(1/Q^2)^4$.

For the complete parameterization we shall adopt the canonical forms:

$$u^+(x) = \frac{1}{x^\alpha}\left[A_u(1-x)^3 + B_u(1-x)^4\right], \tag{66}$$

$$d^+(x) = \frac{1}{x^\alpha}\left[A_d(1-x)^3 + B_d(1-x)^4\right], \tag{67}$$

$$u^-(x) = \frac{1}{x^\alpha}\left[C_u(1-x)^5 + D_u(1-x)^6\right], \tag{68}$$

$$d^-(x) = \frac{1}{x^\alpha}\left[C_d(1-x)^5 + D_d(1-x)^6\right], \tag{69}$$

$$s^+(x) = \frac{1}{x^\alpha}\left[A_s(1-x)^5 + B_s(1-x)^6\right], \tag{70}$$

$$s^-(x) = \frac{1}{x^\alpha}\left[C_s(1-x)^7 + D_s(1-x)^8\right], \tag{71}$$

where we require

$$A_q + B_q = C_q + D_q \tag{72}$$

to ensure the convergence of the helicity-dependent sum rules. Thus in our model, the Regge behavior of the asymmetry $\Delta q(x) \sim x^{-\alpha_R}$ is automatically one unit less than the unpolarized intercept: $\alpha_R = \alpha - 1$. Isospin symmetry at low x (Pomeron dominance) also requires

$$A_u + B_u + C_u + D_u = A_d + B_d + C_d + D_d\ . \tag{73}$$

We emphasize that these distributions include both the quark and antiquark contributions.

Our parameterization of the helicity-dependent quark distributions is close in spirit to the parameterization D_0' for the unpolarized quark and gluon distributions given by Martin, Roberts and Stirling.[86] The MRS parameterization is a good match to our unpolarized forms $q(x) = q^+(x) + q^-(x)$ since the MRS forms combine counting-rule constraints with a good fit to a wide range of perturbative QCD phenomenology. We find that choosing the effective QCD Pomeron intercept

$\alpha = 1.12$ allows good match to the unpolarized quark distributions given by the MRS parameterization D_0' at $Q^2 = 4$ GeV^2 over the range $0.001 < x < 1$. It also predicts an increasing structure function $F_2(x, Q^2)$ at small x $x < 10^{-3}$, as suggested the recent data from HERA.[87] Thus we predict $\alpha_R = 0.12$ for the helicity-changing Reggeon intercept. The momentum fraction carried by the quarks (and antiquarks), $\langle x_q \rangle = \int_0^1 dx x q(x)$, where $q(x) \equiv q^+(x) + q^-(x)$, is assumed to be ~ 0.5.

The analysis by Ellis and Karliner[1,29] combining the SLAC[88], EMC[89] and NMC[90] polarized electron-proton data provides the constraint:

$$\int dx g_1^p(x) = 0.128 \pm 0.013\ (stat) \pm 0.019\ (syst.) \tag{74}$$

at $\langle Q^2 \rangle = 10.7\ GeV^2$. As discussed in Section 1, this value together with the constraints from nucleon and hyperon decay leads to the following values for the proton helicity carried by the different quarks:[29]

$$\Delta u = 0.82 \pm 0.04, \quad \Delta d = -0.44 \pm 0.04, \quad \Delta s = -0.11 \pm 0.04\ . \tag{75}$$

The relatively small value for the total quark helicity $\Delta\Sigma = \Delta u + \Delta d + \Delta s = 0.27 \pm 0.10$ is consistent with large N_C predictions in QCD.[2] As discussed in Section 10, the prediction of a three quark relativistic model is $\Delta\Sigma \simeq 0.75$. Thus the empirical values also implies a significant contribution of the proton's helicity is carried by gluon and orbital angular momentum. For the purposes of this section I shall assume these three values as initial phenomenological inputs for the proton; the neutron distributions then follow from isospin symmetry.

It is straightforward to find parameters for the polynomial forms which are consistent with the above inputs as well as the MRS D_0' parameterization

$$A_u = 3.361, \quad A_d = 0.672, \quad A_s = 0.001, \tag{76}$$

$$B_u = -3.188, \quad B_d = -0.499, \quad B_s = 0.073, \tag{77}$$

$$C_u = 1.574, \quad C_d = 3.286, \quad C_s = 0.787, \tag{78}$$

$$D_u = -1.401, \quad D_d = -3.113, \quad D_s = -0.713 \; . \tag{79}$$

With these set of parameters, the quark helicities in the proton are:

$$\Delta u = 0.82, \quad \Delta d = -0.44 \; , \quad \Delta s = -0.11 \; , \tag{80}$$

and the respective quark momentum fractions are:

$$\langle x_u \rangle = 0.322, \quad \langle x_d \rangle = 0.214, \quad \langle x_s \rangle = 0.04 \; . \tag{81}$$

Thus the helicity carried by the quarks with this parameterization is $\Delta q = 0.27$, and the momentum carried by the quarks is then $\Sigma_q \langle x_q \rangle = 0.57$. The model predicts that the helicity carried by the strange quark is quite large and negative relative to the nucleon helicity.[91]

Note that $\Delta d(x) \equiv d^+(x) - d^-(x)$ is positive at large x, and negative at small to moderate values of x. One thus expects that $\Delta d(x)$ will change sign and go through zero at some physical value for x. With the above parameterization the zero of $\Delta d(x)$ occurs at $x = 0.507$.

We can also find a parameterization for the polarized gluon distributions which are consistent with the $x \to 0$ and $x \to 1$ helicity constraints, as well as the MRS unpolarized gluon distribution:

$$G^+(x) = \frac{1}{x^{\alpha_g}} \left[A_g (1-x)^4 + B_g (1-x)^5 \right] \; , \tag{82}$$

$$G^-(x) = \frac{1}{x^{\alpha_g}} \left[A_g (1-x)^6 + B_g (1-x)^7 \right] \; , \tag{83}$$

with $\alpha_g = 1$, $A_g = 0.2381$ and $B_g = 1.1739$. This form incorporates the coherence constraint, Eq. (53), as well as momentum conservation: $\langle x_g \rangle = 1 - \Sigma_q \langle x_q \rangle = 0.43$. The result for the unpolarized distribution $G(x) = G^+(x) + G^-(x)$ is indistinguishable from the phenomenological D_0' gluon distribution given by MRS. With these values the helicity carried by the gluon in the nucleon is $\Delta G = 0.45$.

If we require the same Pomeron intercept $\alpha_g = \alpha = 1.12$, for the gluon and quark distributions at $x \to 0$, then a fit to the MRS D_0' form gives parameters $A_g = 2$ and $B_g = -1.25$. The result for the helicity carried by the gluon, $\Delta G = 0.46$, is essentially unchanged from the $\alpha_g = 1$ case. However, the agreement with the shape of the MRS unpolarized parameterization is somewhat worse.

14 Predictions for Polarized Structure Functions

In the following we will use the model forms for $\Delta q(x)$ and $q(x)$ to calculate the polarized helicity structure functions of nucleons:

$$g_1^{ep}(x) = \frac{1}{2} \left(\frac{4}{9} \Delta u(x) + \frac{1}{9} \Delta d(x) + \frac{1}{9} \Delta s(x) \right) \tag{84}$$

and

$$g_1^{en}(x) = \frac{1}{2} \left(\frac{4}{9} \Delta d(x) + \frac{1}{9} \Delta u(x) + \frac{1}{9} \Delta s(x) \right) \; , \tag{85}$$

and compare the results to the recent experiments. (Note that $\Delta q(x)$ refers to the combined asymmetries from both quarks and antiquarks in the proton.) In the final predictions we will, as in Ref. 77, include the normalization factor $N_{QCD} = 1 - (\alpha_s/\pi) \approx 0.92$ arising from QCD radiative corrections. The Bjorken sum rule for the difference of proton and neutron quark helicities is automatically satisfied. The Ellis-Jaffe sum rule for the nucleon quark helicity is violated by the model due to the presence of the strange quark contributions Δs.

We have emphasized that the dynamics of QCD implies helicity retention: the quark with x close to 1 has the same helicity as the proton. Thus all of the structure functions asymmetries become maximal at $x \to 1$, and the ratio of unpolarized proton and neutron structure functions can be predicted.

According to the standard $SU(6)$ flavor and helicity symmetry, the probabilities to find u and d quarks of different helicities in the proton's three-quark wavefunction are: $P(u^+) = 5/9, P(d^+) = 1/9, P(u^-) = 1/9, P(d^-) = 2/9$.[92] Thus the usual expectation from SU(6) symmetry is $F_2(n)/F_2(p) = 2/3$ for all x. As Farrar and Jackson pointed out,[72] this naive $SU(6)$ result cannot apply to the local helicity distributions since the helicity aligned and helicity anti-aligned distributions have different momentum distributions. At large x u^- and d^- can be neglected relative to u^+ and d^+, and thus $SU(6)$ is broken to $SU(3)^+ \times SU(3)^-$. Our model retains the $SU(6)$ ratio $P(u^+)) : P(d^+)) = A_u : A_d = 5 : 1$, at large x so that we predict $F_2(n)/F_2(p) \to 3/7$ as $x \to 1$. The physical picture that emerges is that the struck quark carries all the helicity of the nucleon, and the spectators have $S_z = 0$, although their total helicity is a combination of 0 and 1. This wavefunction is just a piece of the full $SU(6)$ wavefunction, but since it is the

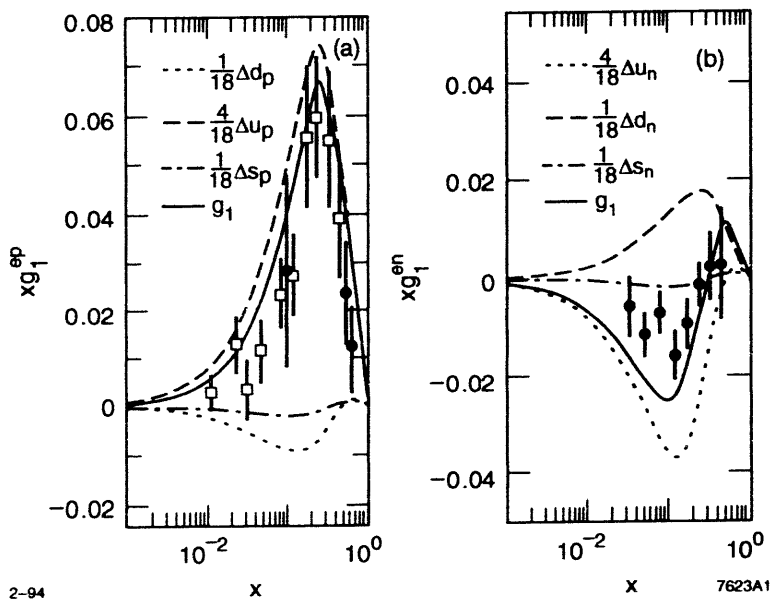

Figure 9. (a) Model prediction for the polarized helicity structure function of the proton (4.1) compared with experiment. Full line: sum of all flavors; dashed: only up quarks; dotted: only down quarks; dash-dotted: only strange quarks. The data is from the combined SLAC-EMC[88,89] analysis. (b) same as (a) but for the neutron. The data are from the SLAC E142 experiment.[70]

piece that contains the u^+ and d^+, and this part remains unchanged, the ratio $P(u^+)/P(d^+)$ is still 5/1.

Notice that the only empirical input into our model is the integrated values of the various flavors obtained from the proton data. Only the shape is determined by perturbative QCD arguments. The agreement with the shape of the SLAC and EMC experimental data for the proton is quite good. (See Fig. 9.) For the neutron we predict two new effects which are not present for the proton. First g_1^{en} tends to fall faster than g_1^{ep} for large x. This is because as in the Carlitz-Kaur[93] and Farrar-Jackson[72] models, the helicity aligned up-quark dominates the proton distribution and the helicity down quark dominates the neutron structure function at large x. A related effect is that $g_1^{en}(x)$ changes sign as a function of x. This is due to the fact that except for large x (where the helicity aligned down quark dominates) g_1^{en} is dominated by the anti-aligned up quark distribution. Since

$\int_0^1 dx\Delta u_n(x) = \int_0^1 dx\Delta d_p(x) < 0$[77] it is clear that $g_1^{en}(x)$ must be negative at small x.

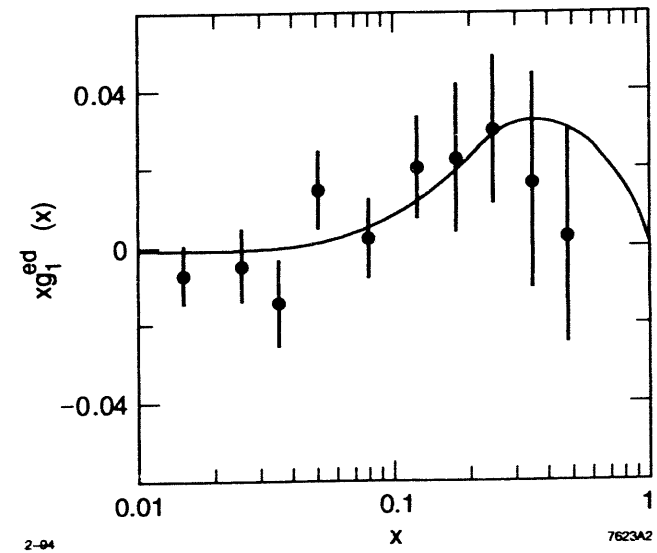

Figure 10. Polarized helicity structure function of the deuteron. The data are from Ref. 69. The prediction for the sum of proton and neutron contributions is multiplied by a D-state depolarization factor $1-(3/2)\omega_D$ with $\omega_D = 0.058$ and the PQCD correction factor $1-(\alpha_s/\pi) = 0.92$.

A comparison of our model with the recent SMC data for the polarized deuteron structure function $g_1^d(x)$ is shown in Fig. 10. The shape of the data appears to be consistent with our predictions, except possibly at the largest x point where the SMC data shows too little asymmetry. To make this prediction we have, as in Ref. 69, assumed that the deuteron structure function is half of the sum of the neutron and proton structure functions and included the D-state depolarization factor with D-state probability 0.058. The model then predicts the normalization

$$\int dx g_1^d(x) = \tfrac{1}{2}\int dx(g_1^p(x)+g_1^n(x)) = \left[\frac{5}{36}(\Delta u+\Delta d)+\frac{1}{18}\Delta s\right]\left(1-\frac{\alpha_s}{\pi}\right)\left(1-\frac{3}{2}\omega_D\right) = 0.038 \tag{86}$$

compared to the SMC result

$$\int dx g_1^d(x) = 0.023 \pm 0.020(\text{stat.}) \pm 0.015(\text{syst.}) \ . \tag{87}$$

We can also compare our model with the polarized neutron structure function extracted by the E142 from its polarized electron polarized He^3 measurements. (See Fig. 9(b).) The predicted normalization assumes an 8% radiative leading twist correction: $(1-\alpha_s/\pi) \simeq (1-0.08)$, whereas the commensurate scale relation analysis presented in the next section predicts a reduction of approximately 14% at $Q^2 = 2$ GeV^2. In addition, according to the DHG-constrained analysis of Burkert and Ioffe, higher twist corrections give a further 23% reduction to the prediction for $\Gamma_1^n(Q^2)$. The net overall reduction of 29% gives a good agreement of theory and experiment for Fig. 9(b).

The distributions presented here have applicability to any PQCD leading-twist processes which require polarized quark and gluon distributions as input. The input parameters have been adjusted to be compatible with global parameters available current experiments. The values can be refined as further and more precise polarization experiments become available. A more precise parameterization should also take into account corrections from QCD evolution, although this effect is relatively unimportant for helicity-dependent distributions. Our central observation is that the shape of the distributions is then predicted when one employs the constraints obtained from general QCD arguments at large x and small x.

A remarkable prediction of this formalism is the very strong correlations between the parent hadron helicity and each of its valence-quark, sea-quark, and gluon constituents at large light-cone momentum fraction x. Although the total quark helicity content of the proton is small, we predict a strong positive correlation of the proton's helicity with the helicity of its u quarks and gluon constituents. The model is also consistent with the assumption that the strange (and anti-strange) quarks carry 4% of the proton's momentum and -11% of its helicity. We also note that completely independent predictions based on QCD sum rules also imply that the three-valence-quark light-cone distribution amplitude has a very strong positive correlation at large x when the $u-$quark and proton helicities are parallel.[85]

15 Commensurate Scale Relations: Relating Observables in QCD without Renormalization Scale or Scheme Ambiguity[94]

One of the most serious difficulties preventing precise tests of QCD is the scale ambiguity of its perturbative predictions. Consider a measurable quantity such as $\rho = R_{e^+e^-}(s) - 3\Sigma e_q^2$ or the integral over structure functions contributing to the Bjorken sum rule: $\Gamma^{p-n} - (g_A/6)$. The PQCD prediction is of the form

$$\rho = r_0 \alpha_s(\mu) \left[1 + r_1(\mu) \frac{\alpha_s(\mu)}{\pi} + r_2(\mu) \frac{\alpha_s^2(\pi^2)}{\pi} + \cdots\right] . \tag{88}$$

Here $\alpha_s(\mu) = g_s^2/4\pi$ is the renormalized coupling defined in a specific renormalization scheme such as $\overline{\text{MS}}$, and μ is a particular choice of renormalization scale. Since ρ is a physical quantity, its value must be independent of the choice of μ as well as the choice of renormalization scheme. Nevertheless, since we only have truncated PQCD predictions to a given order in α_s^N, the predictions do depend on μ. In the specific case of $R_{e^+e^-}$, where we have predictions[95,96] through order α_s^3, the sensitivity to μ has been shown to be less than 10% over a large range of $\ell n \mu$.[96] However, in the case of the hadronic beauty production cross section $(d\sigma/d^2p_T)(\overline{p}p \to B + X)$, which has been computed to next-to-leading order in α_s, the prediction[97] for the normalization of the heavy quark p_T distribution at hadron colliders ranges over a factor of 4 if one chooses one "physical value" such as $\mu = \frac{1}{4}\sqrt{m_B^2 + p_T^2}$ rather than an equally well motivated choice $\mu = \sqrt{m_B^2 + p_T^2}$.

There is, in fact, no consensus on how to estimate the theoretical error due to the scale ambiguity, what constitutes a reasonable range of physical values, or indeed how to identify what the central value should be. Even worse, if we consider the renormalization scale μ as totally arbitrary, the next-to-leading coefficient $r_1(\mu)$ in the perturbative expansion can take on the value zero or any other value. Thus it is difficult to assess the convergence of the truncated series, and finite-order analyses cannot be meaningfully compared to experiment.

The μ dependence of the truncated prediction ρ_N is often used as a guide to assess the accuracy of the perturbative prediction, since this dependence reflects the presence of the uncalculated terms. However, the scale dependence of ρ_N only reflects one aspect of the total series. For example, consider the

ortho-positronium $J^{PC} = 1^{--}$ decay rate computed in quantum electrodynamics: $\Gamma(e^+e^-) = \Gamma_0 [1 - 10.3\ (\alpha/\pi) + \cdots]$. The large next-to-leading coefficient, $r_1 = 10.3$ shows that there is important new physics beyond Born approximation. The magnitude of the higher order terms in the decay rate is not related to the renormalization scale since the QED coupling α does not run appreciable at the momentum transfers associated with positronium decay.

Thus we have a difficult dilemma: If we take μ as an unset parameter in PQCD predictions, then we have no reliable way to assess the accuracy of the truncated series or the parameters extracted from comparison with experiment. If we guess a value for μ and its range, we are left with a prediction without an objective guide to its theoretical precision. The problem of the scale ambiguity is compounded in multi-scale problems where several plausible physical scales enter.

In fact three quite distinct methods to set the renormalization scale in PQCD have been proposed in the literature:

1. *Fastest Apparent Convergence* (FAC).[98] This method chooses the renormalization scale μ so that the next-to-leading order coefficient vanishes: $r_1(\mu) = 0$.
2. *The Principle of Minimum Sensitivity* (PMS).[99] In this procedure, one argues that the best scale is the one that minimizes the scale dependence of the truncated prediction R_N, since that is a characteristic property of the entire series. Thus in this method one chooses μ at the stationary point $dR_N/d\mu = 0$.
3. *Brodsky-Lepage-Mackenzie* (BLM).[100] In the BLM scale-fixing method, the scale is chosen such that the coefficients C_i are independent of the number of quark flavors renormalizing the gluon propagators. In practice, one chooses the scale so that N_f does not appear in the next-to-leading order coefficient. That is, if $r_1(\mu) = r_{10}(\mu) + r_{11}(\mu)N_f$, where $r_{10}(\mu)$ and $r_{11}(\mu)$ are N_f independent, then one chooses the scale μ given by the condition $r_{11}(\mu) = 0$. This prescription ensures that, as in quantum electrodynamics, vacuum polarization contributions due to fermion pairs are all incorporated into the coupling constant $\alpha(\mu)$ rather than the coefficients.

These scale-setting methods can give strikingly different results in practical applications. For example, Kramer and Lampe have analyzed[101] the application of the FAC, PMS and BLM methods for the prediction of jet production fractions

in e^+e^- annihilation in PQCD. Jets are defined by clustering particles with invariant mass less than $\sqrt{ys}$, where y is the resolution parameter and $\sqrt{s}$ is the total center-of-mass energy. Physically, one expects the renormalization scale μ to reflect the invariant mass of jets, that is, μ should be of order $\sqrt{ys}$. For example, in the analogous problem in QED, the maximum virtuality of the photon jet which sets the argument of the running coupling $\alpha(Q)$ cannot be larger than $\sqrt{ys}$. Thus one expects μ to decrease as the resolution parameter $y \to 0$. However, the scales chosen by the FAC and PMS methods both do not reproduce this behavior (see Fig. 11): The predicted scale μ rises without bound at low values for the jet fraction y. On the other hand, the BLM scale has the correct physical behavior as $y \to 0$. Since the argument of the QCD running coupling constant becomes very small, the BLM method indicates that perturbation theory QCD results are not likely to be reliable in the $y < 0.02$ domain. However, the scales chosen by PMS and FAC give no sign that the perturbative expressions break down in the soft region.

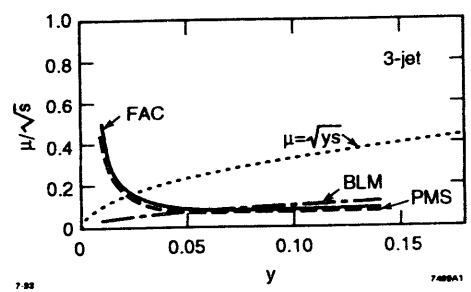

Figure 11. The scale $\mu/\sqrt{s}$ according to the BLM (dashed-dotted), PMS (dashed), FAC (full) and $\sqrt{y}$ (dotted) procedures for the three-jet rate in e^+e^- annihilation, as computed by Kramer and Lampe.[101] Notice the strikingly different behavior of the BLM scale from the PMS and FAC scales at low y. In particular, the latter two methods predict increasing values of μ as the jet invariant mass $\mathcal{M} < \sqrt{(ys)}$ decreases.

In this section we shall use the BLM method to show that all perturbatively calculable observables in QCD, including the annihilation ratio $R_{e^+e^-}(Q^2)$, the heavy quark potential, and the radiative corrections to the Bjorken sum rule can be related to each other at fixed relative scales. The "commensurate scale relation"

for observables A and B in terms of their effective charges has the form

$$\alpha_A(Q_A) = \alpha_B(Q_B)\ \left(1 + r_{A/B}\frac{\alpha_B}{\pi} + \cdots\right)\ . \tag{89}$$

The ratio of the scales $\lambda_{A/B} = Q_A/Q_B$ is chosen so that the coefficient $r_{A/B}$ is independent of the number of flavors n_F contributing to coupling constant renormalization, which guarantees that the observables A and B pass through new quark thresholds at the same physical scale. The value of $\lambda_{A/B}$ is unique at leading order. We also find that the relative scales satisfy the transitivity rule[102]

$$\lambda_{A/B} = \lambda_{A/C}\ \lambda_{C/B}\ . \tag{90}$$

This is equivalent to the group property defined by Peterman and Stückelberg[103] which ensures that predictions in PQCD are independent of the choice of an intermediate renormalization scheme C.[104] In particular, scale-fixed predictions can be made without reference to theoretically constructed renormalization schemes such as $\overline{\rm MS}$; QCD can thus be tested by checking that the observables track both in their relative normalization and commensurate scale dependence.

It is interesting that the task of setting the renormalization scale has never been considered a problem or ambiguity in perturbative QED. For example, the leading-order parallel-helicity amplitude electron-electron scattering has the form

$$\mathcal{M}_{ee\to ee}(++;++) = \frac{8\pi s}{t}\ \alpha(t) + \frac{8\pi s}{u}\ \alpha(u)\ . \tag{91}$$

Here $\alpha(Q) = \alpha(Q_0)/(1 - \Pi[Q^2, Q_0^2, \alpha(Q_0)])$ is the QED running coupling which sums all vacuum polarization insertions Π into the renormalized photon propagator. The value $\alpha(0)$ is conventionally normalized by Coulomb scattering at $t = -Q^2 = 0$. Notice that both physical scales t and u appear in the argument of the running coupling constant in the cross-section; if one chooses any other scale for the running coupling constant, in either the direct or crossed graph amplitude, then one generates a spurious geometric series in $n_f\ (\alpha/\pi)\ell n(-t/\mu^2)$ or $n_f\ (\alpha/\pi)\ell n(-u/\mu^2)$ where n_f represents the number of fermions contributing to the vacuum polarization of the photon propagator.

In general, the "skeleton" expansion of Feynman amplitudes in QED guarantees that all dependence of an observable on the variable n_f is summed into the running coupling constant; the coefficients in QED perturbation series are thus always n_f-independent once the proper scale in α has been set. Note that the variable n_f is defined to count only vacuum polarization insertions, not light-by-light loops, since such contributions do not contribute to the coupling constant renormalization.

The use of the running coupling constant $\alpha(Q)$ in QED allows one to sum in closed form all proper and improper vacuum polarization insertions to all orders, thus going well beyond ordinary perturbation theory. For example, consider the perturbative series for the lepton magnetic anomalous moment:

$$a_\ell = \frac{\alpha(Q^*)}{2\pi} + r_2\frac{\alpha^2(Q^{**})}{\pi^2} + r_3\ \frac{\alpha^3(Q^{***})}{\pi^3} + \cdots \tag{92}$$

the values $Q^* = e^{-5/4}m_\ell$, etc., can be determined either by the explicit insertion of the running coupling into integrand of the Feynman amplitude and the mean value theorem, or equivalently, by simply requiring that the coefficients C_n be independent of n_f. (Light-by-light scattering contributions are not related to coupling constant renormalization and thus enter explicitly in the order α^3 coefficient.) Thus the formula for the anomalous moment using the running coupling is form invariant, identical for each lepton e, μ, τ, since the dependence on lepton vacuum polarization insertions is implicitly contained in the dependence of the running coupling constant. These examples are illustrations of the general principle that observables such as the anomalous moments can be related tc other observables such as the heavy lepton potential $V(Q^2) = -4\pi\alpha(Q^2)/Q^2$ which can be taken as the empirical definition of the on-shell scheme usually used to define $\alpha(Q^2)$.

The same procedure can easily be adopted to non-Abelian theories such as QCD.[100] One of the most useful observables in QCD is the heavy quark potential since it can be computed in lattice gauge theory from a Wilson loop, and it can be extracted phenomenologically from the heavy quarkonium spectrum. If the interacting quarks have infinite mass, then all radiative correction are associated with the exchange diagrams, rather than the vertex corrections. It is convenient to write the heavy quark potential as $V(Q^2) = -4\pi C_F\alpha_V(Q)/Q^2$. This defines

the "effective charge" $\alpha_V(Q^2)/Q^2$ where by definition the "self-scale" $Q^2 = -t$ is the momentum transfer squared. The subscript V indicates that the coupling is defined through the potential.

In fact, any perturbatively calculable physical quantity can be used to define an effective charge[98] by incorporating the entire radiative correction into its definition; for example

$$R_{e^+e^-}(Q^2) \equiv R^0_{e^+e^-}(Q^2)\left[1 + \frac{\alpha_R(Q)}{\pi}\right] , \tag{93}$$

where R^0 is the Born result and $Q^2 = s = E^2_{cm}$ is the annihilation energy squared. An important result is that all the effective charges $\alpha_A(Q)$ satisfy the Gell-Mann-Low renormalization group equation with the same β_0 and β_1; different schemes or effective charges thus only differ through the third and higher coefficients of the β function. Thus, any effective charge can be used as a reference running coupling constant in QCD to define the renormalization procedure. More generally, each effective charge or renormalization scheme including $\overline{\rm MS}$ is a special case of the universal coupling function[105] $\alpha(Q, \beta_n)$. Peterman and Stückelberg[103] have shown that all effective charges are related to each other through a set of evolution equations in the scheme parameters β_n. Physical results relating observables must of course be independent of the choice of any intermediate renormalization scheme.

Let us now consider expanding any observable or effective charge $\alpha_A(Q_A)$ in terms of α_V :

$$\alpha_A(Q_A) = \alpha_V(\mu)\left[1 + (A_{VF}\, n_F + B)\frac{\alpha_V}{\pi} + \cdots\right] . \tag{94}$$

Since α_V sums all vacuum polarization contributions by definition, no coefficient in the series expansion in α_V can depend on n_F; *i.e.* all vacuum polarization contributions are already incorporated into the definition of α_V. Thus we must shift the scale μ in the argument of α_V to the scale[100] $Q_V = e^{3A_{VF}(\mu)}\mu$:

$$\alpha_A(Q_A) = \alpha_V(Q_V)\left[1 + r_1^{A/V}\,\frac{\alpha_V}{\pi} + \cdots\right] , \tag{95}$$

where $r_1^{A/V} = B + (33/2)\, A_{VF}$ is the next-to-leading coefficient in the expansion of the observable A in scheme V. Thus the relative scales between the two observables

$\lambda_{A/V} = Q_A/Q_V$ is fixed by the requirement that the coefficients in the expansion in α_V scheme are independent of vacuum polarization corrections. Alternatively, one can derive the same result by explicitly integrating the one loop integrals in the calculation of the observable A using $\alpha_V(\ell^2)$ in the integrand, where ℓ^2 is the four-momentum transferred squared carried by the gluon. (In practice one only needs to compute the mean-value of $\ell n \ell^2 = \ell n Q_V^2$.[106]) One can eliminate the n_F vacuum polarization dependence that appears in the higher order coefficients by allowing a new scale to appear in each order of perturbation theory. However, usually only the leading order commensurate scale is required in order to test PQCD to good precision.

We can compute other observables B and even effective charges such as $\alpha_{\overline{\rm MS}}$ as an expansion in α_V scheme:[107]

$$\alpha_B(Q_B) = \alpha_V(Q_V)\left[1 + r_1^{B/V}\,\frac{\alpha_V}{\pi} + \cdots\right] , \tag{96}$$

where $Q_V = \frac{Q_B}{\lambda_{B/V}}$ and again $r_1^{B/V}$ must be independent of vacuum polarization contributions. We can now substitute and eliminate $\alpha_V(Q_V)$:

$$\alpha_B(Q_B) = \alpha_A(Q_A)\left[1 + r_1^{B/A}\,\frac{\alpha_B}{\pi} + \cdots\right] , \tag{97}$$

where $Q_A/Q_B = \lambda_{B/A} = \lambda_{B/V}/\lambda_{A/V}$, and $r_1^{B/A} = r_1^{B/V} - r_1^{A/V}$. Note also the symmetry property $\lambda_{B/A}\lambda_{A/B} = 1$. Alternatively, we can compute the commensurate scale $Q_A = \frac{Q_B}{\lambda_{B/A}}$ directly by requiring $r_1^{B/A}$ to be n_F-independent. The result is in agreement with the transitivity rule: the BLM procedure for fixing the commensurate scale ratio between two observables is independent of the intermediate renormalization scheme. The scale-fixed relation between the heavy quark potential and $\alpha_{\overline{\rm MS}}$ is[100] $\alpha_V(Q) = \alpha_{\overline{\rm MS}}(e^{-5/6}Q)[1 - 2(\alpha_{\overline{\rm MS}}/\pi) + \cdots]$.

The transitivity and symmetry properties of the commensurate scales are the scale transformations of the renormalization "group", as originally defined by Peterman and Stückelberg.[103] The predicted relation between observables must be independent of the order one makes substitutions; *i.e.* the algebraic path one takes to relate the observables. It is important to note that the PMS method, which fixes the renormalization scale by finding the point of minimal sensitivity to μ, does not satisfy these group properties. The results are chaotic in the sense that

the final scale depends on the path of applying the PMS procedure. Furthermore, any method which fixes the scale in QCD must also be applicable to Abelian theories such as QED, since in the limit $N_C \to 0$ the perturbative coefficients in QCD coincide with the perturbative coefficients of an Abelian analog of QCD.[108]

The commensurate scale relations provide a new way to test QCD: One can compare two observables by checking that their effective charges agree both in normalization and in their scale dependence. The ratio of commensurate scales $\lambda_{A/B}$ is fixed uniquely: it ensures that both observables A and B pass through heavy quark thresholds at precisely the same physical point. Theoretical calculations are often performed most advantageously in $\overline{\rm MS}$ scheme, but all reference to such constructed schemes may be eliminated when comparisons are made between observables. This also avoids the problem that one need not expand observables in terms of couplings which have singular or ill-defined functional dependence.

Table 2

Leading Order Commensurate Scale Relations

$$\alpha_{\overline{\rm MS}}(0.435Q)$$

$$\alpha_{\eta_b}(1.67Q) \qquad \alpha_\Upsilon(2.77Q)$$

$$\alpha_\tau(1.36Q) \qquad \alpha_V(Q) \qquad \alpha_R(0.614Q)$$

$$\alpha_{GLS}(1.18Q) \qquad \alpha_{g_1}(1.18Q)$$

$$\alpha_{M_2}(0.904Q))$$

The physical value of the commensurate scale in α_V scheme reflects the mean virtuality of the exchanged gluon. However, in other schemes, including $\overline{\rm MS}$, the argument of the effective charge is displaced from its physical value. The relative scale for a number of observables is indicated in Table 2. For example, the physical scale for the branching ratio $\Upsilon \to \gamma X$ when expanded in terms of α_V is $(1/2.77)M_\Upsilon \sim (1/3)M_\Upsilon$, which reflects the fact that the final state phase space is divided among three vector systems. (When one expands in $\overline{\rm MS}$ scheme, the corresponding scale is $0.157M_\Upsilon$.) Similarly, the physical scale appropriate to the hadronic decays of the η_b is $(1/1.67)M_{\eta_b} \sim (1/2)M_{\eta_b}$.

After scale-fixing,the ratio of hadronic to leptonic decay rates for the Υ has

the form[100]

$$\frac{\Gamma(\Upsilon \to \text{hadrons})}{\Gamma(\Upsilon \to \mu^+\mu^-)} = \frac{10(\pi^2-9)}{81\pi e_b^2} \frac{\alpha^3_{\overline{\rm MS}}(0.157M_\Upsilon)}{\alpha^2_{\rm QED}} \left[1 - 14.0(5)\frac{\alpha_{\overline{\rm MS}}}{\pi} + \cdots\right] . \quad (98)$$

Thus as is the case of positronium decay, the next to leading coefficient is very large, and perturbation theory is not likely to be reliable for this observable. On the other hand, the commensurate scales for the second moment of the non-singlet structure function M_2 and the effective charges in the Bjorken sum rule (and the Gross-Llewellyn Smith sum rule) are not far from the physical value Q when expressed in α_V scheme. At large n the commensurate scale for M_n is proportional to $1/\sqrt{n}$ at large n, reflecting the fact that the available phase-space for parton emission decreases as n increases. In multiple-scale problems, the commensurate scale can depend on all of the physical invariants. For example, the scale controlling the evolution equation for the non-singlet structure function depends on $x_{\rm bj}$ as well as Q.[109]

A number of examples of commensurate scale relations between various single-scale observables based on published three-loop $\overline{\rm MS}$ calculations are given in Table 3. For simplicity we have used the leading order scale determined by eliminating the n_f dependence from the next-to-leading coefficient. We take $n_f = 3$ to fix the higher order term. We can improve these relations by requiring that all coefficients must be n_f-independent in α_V scheme. As in the example of the muon anomalous moment, the commensurate scale appearing in argument of the higher order contributions differs from the scale of the next-to-leading order term. The three-loop results[110] have a remarkable simple form: For example for $N_C = 3$

$$\frac{\alpha_{g_1}(Q^*)}{\pi} = \frac{\alpha_R(Q^*)}{\pi} - \frac{\alpha_R(Q^*)^2}{\pi} + \frac{\alpha_R(Q^{**})^3}{\pi} + \cdots . \quad (99)$$

The extension of the BLM procedure to higher orders has also been discussed recently by Grunberg and Kataev[111] and by Samuel and Surguladze.[96]

Table 3

Commensurate Scale Relations For Effective Charges to Order α_s^3

$\alpha_R(Q) = \alpha_{\overline{\rm MS}}(0.70759Q)\left[1 + (1/12)(\alpha_{\overline{\rm MS}}/\pi) - 15.7331(\alpha^2_{\overline{\rm MS}}/\pi^2) + \cdots\right]$
$\alpha_{g_1}(Q) = \alpha_{\overline{\rm MS}}(0.36788Q)\left[1 - (11/12)(\alpha_{\overline{\rm MS}}/\pi) + 0.21527(\alpha^2_{\overline{\rm MS}}/\pi^2) + \cdots\right]$
$\alpha_R(Q) = \alpha_{g_1}(1.92344Q)\left[1 + (\alpha_{g_1}/\pi) - 14.115(\alpha^2_{g_1}/\pi^2) + \cdots\right]$
$\alpha_{g_1}(Q) = \alpha_R(0.519903Q)\left[1 - (\alpha_R/\pi) + 16.115(\alpha^2_R/\pi^2) + \cdots\right]$
$\alpha_R(Q) = \alpha_\tau(2.20707Q)\left[1 + 0(\alpha_\tau/\pi) - 5.94141(\alpha^2_\tau/\pi^2) + \cdots\right]$
$\alpha_\tau(Q) = \alpha_R(0.45309Q)\left[1 + 0(\alpha_R/\pi) + 5.94141(\alpha^2_R/\pi^2) + \cdots\right]$
$\alpha_{g_1}(Q) = \alpha_\tau(1.14746Q)\left[1 - (\alpha_\tau/\pi) + 10.1736(\alpha^2_\tau/\pi^2) + \cdots\right]$
$\alpha_\tau(Q) = \alpha_{g_1}(0.87149Q)\left[1 + (\alpha_{g_1}/\pi) - 8.17363(\alpha^2_{g_1}/\pi^2) + \cdots\right]$

An interesting illustration of commensurate scale relations is the connection between the effective charge for the Bjorken sum rule for the first moment of the isospin non-singlet helicity-dependent structure functions: $\Gamma^{p-n} \equiv (g_A/6)\,[1 - (\alpha_{g_1}(Q)/\pi)]$ and the effective charge for the annihilation cross section:

$$\alpha_{g_1}(Q) = \alpha_R(0.52Q)\,\left[1 - \frac{\alpha_R}{\pi} + \cdots\right]\,. \tag{100}$$

Mattingly and Stevenson[112] have recently obtained an empirical form for $\alpha_R(Q)$ by smearing the annihilation cross section data and fitting to the three loop form using the PMS scale. Since the PMS and BLM scale are nearly coincident in this case, we can use their determination for $\alpha_R(Q)$ to predict the Bjorken sum rule corrections.[113] For example, at the scale appropriate to the E142 spin-dependent structure function measurements at SLAC, $Q^2 = 2$ GeV^2, one finds $\alpha_R(0.52Q)/\pi \simeq 0.16$ and hence $\alpha_{g_1}(1.4\,\text{GeV})/\pi \simeq 0.14$ which corresponds to $\Gamma^{p-n} = 0.180$. The predictions for the Bjorken sum rule at EMC and SMC momentum transfers $Q^2 = 10.7$ GeV^2 and $Q^2 = 4.6$ GeV^2 are $\alpha_{g_1}(3.27\text{ GeV})/\pi \simeq 0.09$ and $\alpha_{g_1}(2.14\text{ GeV})/\pi \simeq 0.11$, corresponding to $\Gamma^{p-n} = 0.190$ and $\Gamma^{p-n} = 0.186$, respectively. Alternatively, for the E142 data, we can use the commensurate scale

relation

$$\alpha_{g_1}(Q) = \alpha_\tau(1.145Q)[1 - \frac{\alpha_\tau}{\pi} + \cdots]\,, \tag{101}$$

and the empirical determination $\alpha_\tau(m_\tau) \simeq 0.19$ to find a consistent determination $\alpha_{g_1}(1.55\text{ GeV})/\pi \simeq 0.15$. The uncertainty in the PQCD radiative corrections is thus considerable smaller than usually assumed.[114]

The commensurate scale relations between observables can be tested at quite low momentum transfers, even where PQCD relationships would be expected to break down. It is likely that some of the higher twist contributions common to the two observables are also correctly represented by the commensurate scale relations. In contrast, expansions of any observable in $\alpha_{\overline{\rm MS}}(Q)$ must break down at low momentum transfer since $\alpha_{\overline{\rm MS}}(Q)$ becomes singular at $Q = \Lambda_{\overline{\rm MS}}$. (For example, in the 't Hooft scheme where the higher order $\beta_n = 0$ for $n = 2, 3, ...$, $\alpha_{\overline{\rm MS}}(Q)$ has a simple pole at $Q = \lambda_{\overline{\rm MS}}$.) The commensurate scale relations allow tests of QCD without explicit reference to schemes such as $\overline{\rm MS}$. It is thus reasonable to expect that the series expansions are more convergent when one relates finite observables to each other.

The BLM scale has also recently been used by Lepage and Mackenzie[106] and their co-workers to improve lattice perturbation theory. By using the BLM method one can eliminate $\alpha_{\rm Lattice}$ in favor of α_V thus avoiding an expansion with artificially large coefficients. The lattice determination, together with the empirical constraints from the heavy quarkonium spectra, promises to provide a well-determined effective charge $\alpha_V(Q)$ which could be adopted as the QCD standard.

After one fixes the renormalization scale μ to the BLM value, it is still useful to compute the logarithmic derivative of the observable $d\ell n R_N/d\ell n\mu$ at the BLM-determined point. If this derivative is large, or equivalently, if the BLM and PMS scales strongly differ, then one knows that the truncated perturbative expansion cannot be numerically reliable, since the entire series is independent of μ. Note that this is a necessary condition for a reliable series, not a sufficient one, as evidenced by the large coefficients in the positronium and quarkonium decay widths which appear when the scales are set correctly. In the case of the three and four-jet decay fractions, the BLM and PMS scales strongly diverge at low values of the jet discriminant y. Thus, by using this criterion, we establish that the leading-order perturbation theory must fail in the small y regime, requiring careful resummation of the $\alpha_s\ell ny$ series.

However, if we restrict the analysis to jets with invariant mass $M < \sqrt{ys}$, with $0.14 > y > 0.05$ we have an ideal situation, since both the PMS and FAC scales nearly coincide with the BLM scale when one computes jet ratios at in the $\overline{\rm MS}$ scheme. (See Fig. 11.) the renormalization scale dependence in this case is minimal at the BLM scale, and the computed NLO coefficient is nearly zero. In fact, Kramer and Lampe find that the BLM scale and the NLO PQCD predictions give a consistent description of the LEP 2-jet and 3-jet data for $0.14 > y > 0.05$. This allows a determination of α_s with remarkably small theoretical error: $\alpha_{\overline{\rm MS}}(M_z) = 0.107 \pm 0.003$, which corresponds to $\Lambda^{(5)}_{\overline{\rm MS}} = 100 \pm 20$ MeV.

The BLM method and the commensurate scale relations presented in this section can be applied to the whole range of QCD and standard model processes, making the tests of theory much more sensitive. The method should also improve precision tests of electroweak, supersymmetry and other non-Abelian theories.

16 Quark Helicity Distributions and Hadron Helicity Retention in Inclusive Reactions at Large x_F

Consider a general inclusive reaction $AB \to CX$ at large x_F where the helicities λ_C and λ_A are measured. To be precise, we shall use the boost-invariant light-cone momentum fraction $x_C = k^+_C/k^+_A = (k^0 + k^z)_C/(k^0 + k^z)_A$. Hadron helicity retention implies that the difference between λ_C and λ_A tends to a minimum at $x_C \to 1$. Hadron helicity retention follows from the helicity structure of the gauge theory interactions, and it is applicable to hadrons, quarks, gluons, leptons, or photons. For example, in QED the radiation of a photon in lepton scattering has the well-known distribution $dN/dx \propto [1 + (1-x)^2]/x$. The first term corresponds to the case where the photon helicity has the same sign as the lepton helicity; the opposite-sign helicity production is suppressed by a factor $(1-x)^2$ at $x \to 1$:[73] the projectile helicity tends to be transferred by the leading fragment at each step in perturbation theory.

One of the most important testing grounds for hadron helicity retention is J/ψ production in $\pi - N$ collisions. The helicity of the J/ψ can be measured from the angular distribution $1 + \lambda \cos^2\theta_\mu$ of one of the muons in the leptonic decay of the J/ψ. At low to medium values of x_F the Chicago-Iowa-Princeton Collaboration[115] finds that $\lambda \sim 0$. However, at large $x_F > 0.9$ the angular distribution changes markedly to $\sin^2\theta_\mu$; *i.e.* the J/ψ is produced with longitudinal polarization. The sudden change to longitudinal polarization must mean that a new heavy quark production mechanism is present at large x_F.[116] In fact, it is easy to guess the relevant process which can produce high momentum charm quark pairs. [See Fig. 12(a).] Since nearly all of the pion's momentum is transferred to the charmonium system, one needs to consider diagrams where each valence quark in the incoming pion emits a fast gluon. The two gluons then fuse to make a fast $c\bar{c}$ pair. At large momentum fraction x, each gluon's helicity tends to be parallel to the helicity of its parent quark. Thus the angular momentum J_z of the gluon pair is transferred to the $c\bar{c}$ pair. The angular momentum tends to be preserved by any subsequent gluon radiation or gluon interaction from the heavy quarks. The J/ψ then tends to have the same helicity as the projectile at high light-cone momentum fraction.

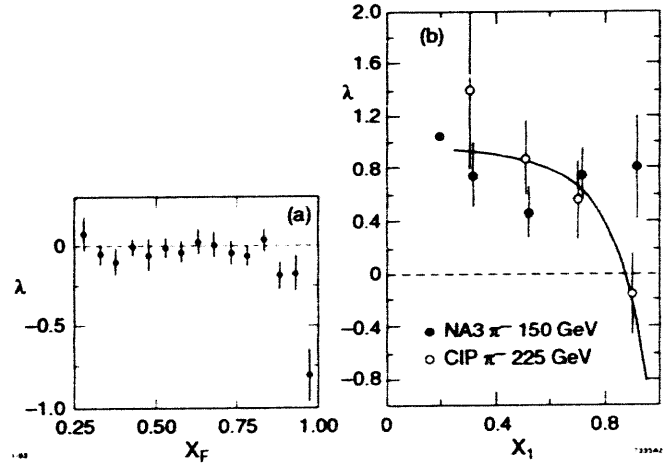

Figure 12. The x_F dependence of the polarization parameter λ for (a) J/ψ production[115] and (b) continuum lepton pair production[117] in $\pi - N$ collisions as a function of x_F.

Thus there is a natural mechanism in QCD which produces the J/ψ in the same helicity as the incoming beam hadron; the essential feature is the involvement of all of the valence quarks of the incoming hadron directly in the heavy quark production subprocess. Since such diagrams involve the correlation between the partons of the hadron, it can be classified as a higher-twist "intrinsic charm"

amplitude; the production cross section is suppressed by powers of $f_\pi/M_{Q\overline{Q}}$ relative to conventional fusion processes. Although nominally higher twist, such diagrams provide an efficient way to transfer the beam momentum to the heavy quark system while stopping the valence quarks.

The intrinsic charm mechanism also can explain other features of the J/ψ hadroproduction.[118,119,120] The observed cross section persists to high x_F in excess of what is predicted from gluon fusion or quark anti-quark annihilation subprocesses; furthermore the cross section at high x_F has a strongly suppressed nuclear dependence, $A^{\alpha(x_F)} \sim 0.7$. The nuclear dependence actually depends on x_F not x_2 which rules out leading twist mechanisms. The higher-twist intrinsic charm *e.g.* $|uudc\bar{c}\rangle$ Fock state wavefunctions have maximum probability when all of the quarks have equal velocities, *i.e.* when $x_i \propto \sqrt{m^2 + k_{\perp_i}^2}$. This implies that the charm and anti-charm quarks have the majority of the momentum of the proton when they are present in the hadronic wavefunction. In a high energy proton-nucleus collision, the small transverse size, high-x intrinsic $c\bar{c}$ system can penetrate the nucleus, with minimal absorption and can coalesce to produce a charmonium state at large x_F. Since the soft quarks expand rapidly in impact space, the main interaction in the target of the intrinsic charm Fock state is with the slow valence quarks rather than the compact $c\bar{c}$ system.[13] Thus at large x_F the interaction in the nucleus should have the A-dependence of normal hadron nucleus cross sections: $\sim A^{0.7}$. Note that at high energies, the formation of the charmonium state occurs far outside the nucleus. Thus one predicts similar $A^{\alpha(x_F)}$-dependence of the J/ψ and ψ' cross sections. These predictions are in agreement with the results reported by the E-772 experiment at Fermilab.[119]

17 Anomalous Polarization of Massive Lepton Pairs in Hadronic Collisions

One of the most surprising polarization anomalies violating perturbative QCD expectations is the strong and rapidly changing angular correlations observed in massive lepton pair hadroproduction by both the NA-10 experiment at CERN and the CIP experiment at Fermilab.[117] Both experiments measured $\pi N \to \mu^+\mu^- N$ in nuclear targets.

The angular distribution of the μ^+ in

$$\pi^- + N \to \gamma^* + X \to \mu^+ + \mu^- + X \tag{102}$$

may be parameterized in general as follows:

$$\frac{1}{\sigma}\frac{d\sigma}{d\Omega} \sim 1 + \lambda\cos^2\theta + \mu\sin 2\theta\cos\phi + \frac{\nu}{2}\sin^2\theta\cos 2\phi\ . \tag{103}$$

Here θ and ϕ are angles defined in the muon pair rest frame and λ, μ and ν are angle-independent coefficients. The parton model (Drell-Yan picture[121]) views the production of the virtual photon γ^* in Eq. (102) as originating from the annihilation of two uncorrelated constituent quarks, resulting in an angular distribution of the form $1 + \cos^2\theta$; *i.e.* $\lambda = 1$ and $\nu = \mu = 0$. This result follows simply from the fact that the virtual photon is produced transversely polarized in the annihilation of two on-shell fermions.

In order to describe the lepton pair transverse momentum distribution $d^2\sigma/dQ_T^2$ in QCD one has to take into account radiative corrections to the Drell-Yan model. The Q_T-distribution has been calculated in the QCD-improved parton model to the order of $\mathcal{O}(\alpha_s)$ with resummation of the soft gluons at the leading double logarithmic accuracy (see Ref. 122 and references therein). This approach was used in Ref. 123 to compute the angular distribution at fixed transverse momentum. The deviations from the $1 + \cos^2\theta$ behavior were found to be less than 5% in the range $0 < Q_T < 3$ GeV.[123]

However, the NA-10 and CIP measurements show a quite different behavior. In the limit where the momentum fraction x of one of the pion constituents is very close to 1 and for moderate transverse momenta of the muon pair, the value of λ turns strongly negative Ref. 117, consistent with a $\sin^2\theta$ distribution. This implies that in this kinematic limit the virtual photon is produced with longitudinal polarization, rather than transverse. Furthermore, the data[117,124,125] is observed to have a strong azimuthal modulation (nonzero μ and ν in (2)), an effect which is missing in standard QCD. The Lam-Tung sum rule,[126] $1 - \lambda - 2\nu = 0$, which follows from the approach used in Ref. 123 is also badly violated by the experimental data. Moreover, the inclusion of hard $\mathcal{O}(\alpha_s^2)$ corrections does not resolve the problem.[127] Thus the standard QCD parton model approach cannot explain the observed angular distribution.

In fact, in the large x_L region, the off-shell nature of the annihilating quark from the projectile becomes crucial, and thus the operative subprocess must involve the correlated multi-parton structure of the projectile. In effect the dominant subprocess in the off-shell domain is $Mq \to \ell\bar{\ell}q$. Berger and I have shown that this five particle amplitude gives a dominant $\lambda = -1$ longitudinal contribution at large x_F and fixed Q^2.[128] In the higher-twist subprocess diagram, Fig. 13(b), the lepton pair tends to have the same helicity as the beam hadron at large x_F. For example, consider $\pi^- N \to \mu^+\mu^- X$ at high x_F. The valence d quark emits a fast gluon which in turn makes a fast-u, slow-$\bar{u}$ pair. Because of the QCD couplings, the fast u then carries the helicity of the d. The valence $\bar{u}$ then annihilates with the fast u to make the lepton pair at $x_F \sim 1$. The lepton pair thus tends to have the helicity ($J_z = 0$) of the pion, in agreement with hadron helicity retention. A detailed calculation shows that the subprocess amplitude can be normalized to the same integral over the pion distribution amplitude $\int dx \phi(x,Q)/(1-x)$ that controls the pion form factor.[129] Thus the normalization of these processes can be interrelated.

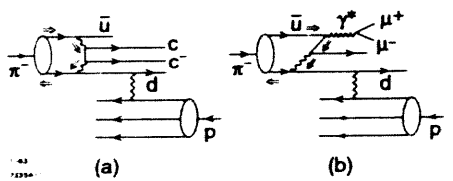

Figure 13. Higher twist mechanisms for producing (a) J/ψ and (b) massive lepton pairs at high x_F in meson-nucleon collisions.

The data from both NA-10 and CIP also show that the coefficient ν grows to values as large as 0.3 at large $\rho = Q_T/Q$; *i.e.* the azimuthal correlation $\cos 2\phi$ becomes sizeable at large lepton pair transverse momentum in strong contrast to the predictions of leading-twist PQCD. Brandenburg, Mirkes, and Nachtmann[127] have suggested an intriguing non-perturbative explanation for this anomaly. In their model the annihilating quark and antiquark interact through the chromomagnetic QCD gluon condensate and become polarized transverse to the scattering plane in much the same way that electrons become transversely polarized relative to the

plane of a storage ring. The model leads to a parameterization:

$$\nu = \nu_0 \frac{Q_\perp^2}{Q_\perp^2 + m_T^4} \tag{104}$$

with $\nu_0 = 0.34$ and $m_T = 1.5$ GeV which gives a good fit to the observed dependence of ν found by the NA-10 experiment for $\pi^- W \to \mu^+\mu^- X$ data at $p_{\rm lab} = 194$ GeV/c, and $Q = 8$ GeV.

However, it is also interesting to check the effect of the higher twist contributions. Recently, Arnd Brandenburg, Valya Khoze, Dieter Müller, and I[130] have found that large values for the azimuthal coefficients μ and ν—with the correct sign—are predicted from the $\pi q \to \ell\bar{\ell}q$ subprocess, assuming that the pion distribution amplitude has the broad two-humped shape predicted by QCD sum rules. In contrast, a very narrow pion distribution amplitude, characteristic of weak hadronic binding, predicts the wrong sign for the observed azimuthal angular coefficients μ and ν. I will briefly review this analysis here.

In order to go beyond the standard treatment we need to take into account the pion bound state effects.[128,129,131] To treat the bound state problem perturbatively, we will restrict ourselves to a specific kinematic region in which the momentum fraction x of one of the pion constituents is large, $x > 0.5$. In fact, in the large x region the off-shell nature of the annihilating quark from the projectile is crucial, and thus the operative subprocess must involve the correlated multi-parton structure of the projectile. The dominant subprocess in the off-shell domain is thus $\pi^- q \to \mu^+\mu^- q$. We resolve the pion by a single hard gluon exchange.[58] The main contribution to reaction Eq. (102) then comes from the diagrams of Fig. 14(a,b).[128,129,131] We see from diagram 1a that the $\bar{u}$ quark propagator is far off-shell, $p_{\bar{u}}^2 = -Q_T^2/(1-x_{\bar{u}})$. The second diagram is required by gauge invariance. (In a physical gauge the contribution of the second diagram is purely higher twist.)

The leading contribution to the amplitude M for the reaction

$$u + \pi^- \to \gamma^* + X \to \mu^+ + \mu^- + X \tag{105}$$

is obtained[58] by convoluting the partonic amplitude $T(u+\bar{u}d \to \gamma^* + d \to \mu^+ + \mu^- + d)$

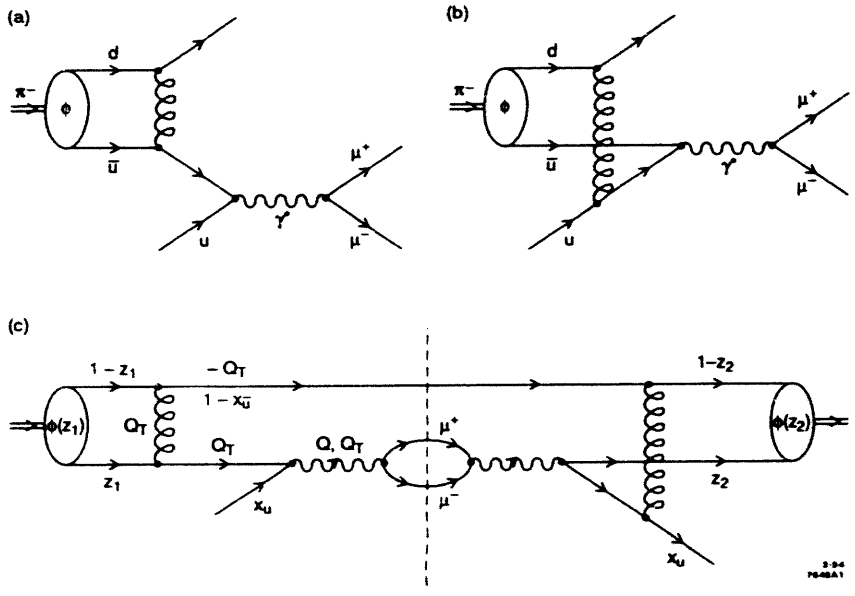

Figure 14. Diagrams (a) and (b) give the leading contribution to the amplitude of reaction (4). The cut of diagram (c) gives a typical (one out of four) contribution to the cross section.[117]

with the pion distribution amplitude $\phi(z,\widetilde{Q}^2)$,[12]

$$M = \int_0^1 dz\ \phi(z,\widetilde{Q}^2)\ T\ , \tag{106}$$

where $\widetilde{Q}^2 \sim Q_T^2/(1-x)$ is the cutoff for the integration over soft momenta in the definition of ϕ. For the hadronic differential cross section we have

$$\frac{Q^2 d\sigma(\pi^- N\to\mu^+\mu^- X)}{dQ^2 dQ_T^2 dx_L d\Omega} = \frac{1}{(2\pi)^4}\frac{1}{64}\int_0^1 dx_u G_{u/N}(x_u)\int_0^1 dx_{\bar u}\frac{x_{\bar u}}{1-x_{\bar u}+Q_T^2/Q^2}|M|^2$$

$$\delta(x_L - x_{\bar u} + x_u - Q_T^2 s^{-1}(1-x_{\bar u})^{-1})\ \delta(Q^2 - s x_u x_{\bar u} + Q_T^2(1-x_{\bar u})^{-1}) + \{u\to\bar d, \bar u\to d\}\ . \tag{107}$$

Here Q^μ is the four-momentum of γ^* in the hadronic center of mass system, $x_{u(\bar u)}$ is the light-cone momentum fraction of the $u(\bar u)$ quark and $G_{u/N}$ is the parton

distribution function of the nucleon. The longitudinal momentum fraction of the photon is defined as $x_L = 2Q_L/\sqrt{s}$ and it should be noted that its maximum value, $x_L^{\max} = 1 - s^{-1}(Q^2 + Q_T^2)$ is slightly less than 1. The second term on the right hand side of Eq. (107) is the same as the first one with quark flavors interchanged. This term gives the contribution from the nucleon sea. In Fig. 14(c) we show a typical contribution to the hadronic cross section.

We note that no primordial or intrinsic transverse momenta have been introduced. The single gluon exchange is the source of Q_T in the model discussed. We have also neglected the quark masses and the mass of the projectile which are small compared to $\widetilde{Q}$.

In analogy to Eq. (103) we parameterize the angular distribution as follows,

$$\frac{Q^2 d\sigma}{dQ^2 dQ_T^2 dx_L d\Omega}\left(\frac{Q^2 d\sigma}{dQ^2 dQ_T^2 dx_L}\right)^{-1} =$$

$$\frac{3}{4\pi}\frac{1}{\lambda+3}(1 + \lambda\cos^2\theta + \mu\sin 2\theta\cos\phi + \frac{\nu}{2}\sin^2\theta\cos 2\phi)\ , \tag{108}$$

where the angular distribution coefficients λ, μ and ν are now functions of the kinematic variables x_L, Q_T^2/Q^2 and Q^2/s.

We work in the Gottfried-Jackson frame where the $\hat z$ axis is taken to be the pion direction in the muon pair rest frame and the $\hat y$ axis is orthogonal to the $\pi^- N$ plane. Using Eqs. (106)-(108), we arrive at an expression of the form,

$$\begin{pmatrix}\lambda\\ \mu\\ \nu\end{pmatrix} = N^{-1}\int_0^1 dz_1\frac{\phi(z_1,\widetilde{Q}^2)}{z_1(z_1+\widetilde{x}-1+i\epsilon)}\int_0^1 dz_2\frac{\phi(z_2,\widetilde{Q}^2)}{z_2(z_2+\widetilde{x}-1-i\epsilon)}$$

$$\left\{z_1 z_2\begin{pmatrix}l_2\\ m_2\\ n_2\end{pmatrix} + (z_1+z_2)\begin{pmatrix}l_1\\ m_1\\ n_1\end{pmatrix} + \begin{pmatrix}l_0\\ m_0\\ n_0\end{pmatrix}\right\}\ . \tag{109}$$

where

$$N = \int_0^1 dz_1\frac{\phi(z_1,\widetilde{Q}^2)}{z_1(z_1+\widetilde{x}-1+i\epsilon)}\int_0^1 dz_2\frac{\phi(z_2,\widetilde{Q}^2)}{z_2(z_2+\widetilde{x}-1-i\epsilon)}\{z_1 z_2 r_2 + (z_1+z_2)r_1 + r_0\}\ . \tag{110}$$

and

$$\widetilde{x} \equiv \frac{x_{\bar{u}}}{1+Q_T^2/Q^2} = \frac{1}{2}\frac{x_L + \sqrt{x_L^2 + 4s^{-1}(Q^2+Q_T^2)}}{1+Q_T^2/Q^2} \,. \tag{111}$$

The variable $\widetilde{x}$ acts to resolve the distribution amplitude much like the Bjorken variable resolves the structure functions. The coefficients l_i, m_i, n_i and r_i ($i = 0,1,2$) depend only on $\widetilde{x}$ and Q_T^2/Q^2. Their explicit forms are given in Ref. 130. The factors $1/z$ in Eq. (109) come from the gluon propagators and the factors $1/(z+\widetilde{x}-1\pm i\epsilon)$ arise from the quark propagator of Fig. 14(b). In contrast to Refs. 131 and 132 we did not omit terms $\mathcal{O}(Q_T^2/Q^2(1-x_{\bar{u}}))$ and $\mathcal{O}(\ Q_T^4/Q^4(1-x_{\bar{u}})^{-1})$ and of higher orders.

We note that the internal quark line of Fig. 14(b) can go on-shell. The amplitude M of Eq. (106), however, is always regular due to the z-integration[132] for realistic choices of $\phi(z,\widetilde{Q}^2)$. This also can be read off from Eq. (109). The fact that the internal line goes on-shell does not cause a Sudakov suppression since our diagrams are the lowest order contribution of an *inclusive* process. In other words gluon emission to the final state will occur in the higher order corrections. Only when $x_{\bar{u}}$ approaches unity, where gluon emission is prohibited by kinematics, the Sudakov suppression will arise.

Our model is not to be considered as a correction to the parton model result. The diagrams of Fig. 14(a,b) give the *whole* leading order contribution in the specific kinematic region of large enough $x_{\bar{u}}$, $x_{\bar{u}} > 0.5$.[131] This is so because the gluon exchange is the resolution of the pion bound state and not a radiative correction.

In Fig. 15 we plot the predictions of the higher twist model for λ, μ, ν and $2\nu-(1-\lambda)$ versus $x_{\bar{u}}$ for $\sqrt{Q_T^2/Q^2} = 0.25$ for different choices of $\phi(z,\widetilde{Q}^2)$ together with the data of Ref. 125. The dotted line corresponds to the delta function distribution amplitude, $\phi(z) = \delta(z-1/2)$, the dashed-dotted line corresponds to the asymptotic one, $\phi(z) = 6z(1-z)$ and the dashed line shows the results for a two-humped distribution amplitude,[85] $\phi(z) = 26z(1-z)(1-50/13\ z(1-z))$. For the two-humped distribution amplitude we have chosen the evolution parameter $\widetilde{Q}^2$ to be effectively ~ 4 GeV^2.

In Fig. 16 the same quantities are shown versus $\sqrt{Q_T^2}$ for $x_{\bar{u}} = 0.6$ and $\sqrt{Q^2} = 6$ GeV. The data points in this case are averaged over intervals $4.05 < \sqrt{Q^2} < 8.55$ GeV and $0.2 < x_{\bar{u}} < 1$ and taken from Ref. 125. We would rather

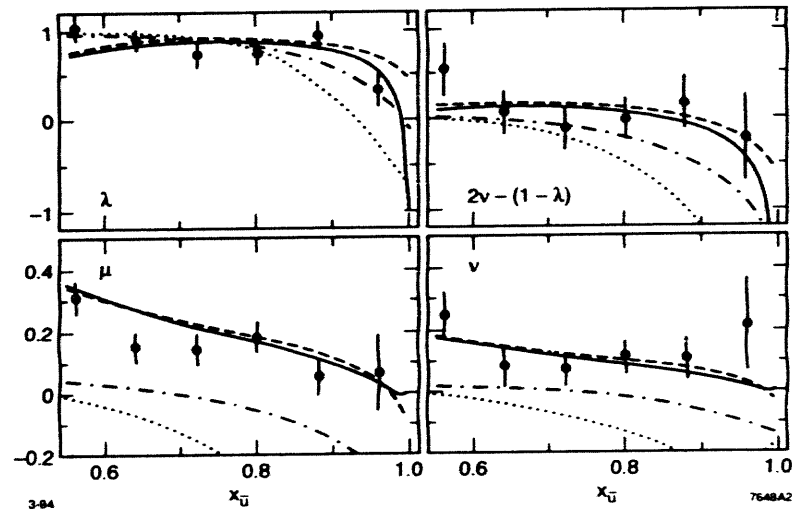

Figure 15. The angular distribution coefficients λ, μ and ν and the Lam-Tung combination, $2\nu-(1-\lambda)$, in the Gottfried-Jackson frame, versus $x_{\bar{u}}$ for $\sqrt{Q_T^2/Q^2} = 0.25$. The dotted line corresponds to $\phi(z) = \delta(z-1/2)$, the dashed-dotted line corresponds to $\phi(z) = 6z(1-z)$ and the dashed line shows the results for the two humped distribution amplitude, $\phi(z) = 26z(1-z)\cdot(1-50/13\ z(1-z))$. The solid line is the result for the two-humped $\phi(z)$ where powers of $(Q_T^2/Q^2)^{n/2}$ were dropped for $n \geq 3$. We note that corrections to our model may induce such terms; thus the difference between the dashed and the solid lines should be viewed as the uncertainty of our predictions. We also show the data points of Ref. 125 averaged in the intervals $4.05 < \sqrt{Q^2} < 8.55$ GeV and $0 < \sqrt{Q_T^2} < 5$ GeV.

prefer to use the unaveraged data which are not available. The use of the averaged-over-$x_{\bar{u}}$ data in Fig. 16 required us to fix the value $x_{\bar{u}} = 0.6$ for our theoretical prediction which is rather low for our model and pushes it to the limits of its applicability.

In principle, bound state effects require a non-perturbative analysis. The perturbative approximation makes sense only at large enough x. The contribution of soft gluons to the pion bound state is taken into account in the evolution of the distribution amplitude. The contribution of more than one hard gluon exchange will be suppressed by powers of α_s. The contribution of the higher Fock states of the pion is expected to be suppressed when x is large enough.[58]

Thus detailed measurements of the angular distribution of lepton pair in hadron-hadron collisions provides a microscope to probe the structure of hadrons at the amplitude level. It is clearly important to have detailed measurements of

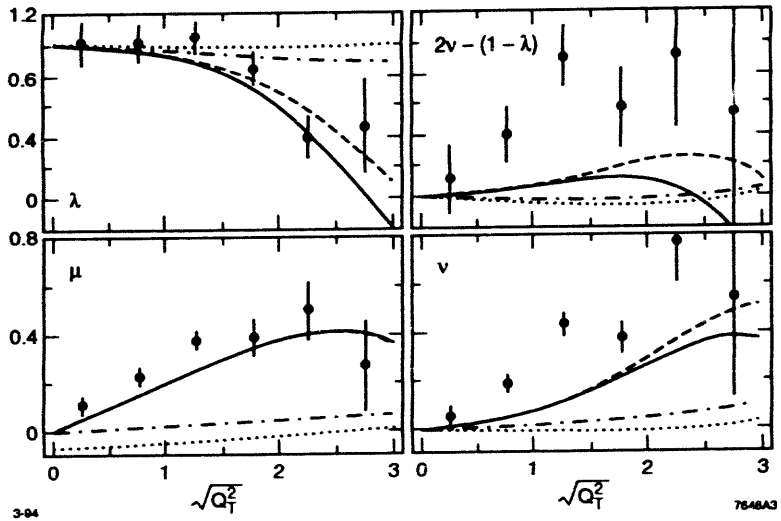

Figure 16. The same quantities as in Fig. 15 are shown. versus $\sqrt{Q_T^2}$ for $x_{\bar{u}} = 0.6$ and $\sqrt{Q^2} = 6$ GeV.

the lepton pair coefficient functions $\lambda(x_L, p_T), \mu(x_L, p_T)$, and $\nu(x_L, p_T)$ at large $x_L > 0.6$ for the reactions $Hp \to \ell\bar{\ell}X$ for the whole range of projectiles $H = \pi, K, \bar{p}, p$, and n. In each case the deviations from the parton model predictions provide a unique sensitivity to the fundamental non-perturbative structure of the projectile wavefunction. In the case of $\gamma^* p \to \ell\bar{\ell}X$, one could identify the "point-like" and "resolved" components of the distribution amplitude for both real and virtual photons.

The above analysis shows that the coefficient functions λ, μ, and ν at large $x > 0.5$ in the Drell-Yan process are very sensitive to the shape of the projectile's distribution amplitude $\phi(z, \tilde{Q}^2)$, the basic hadron wavefunction which describes the distribution of light-cone momentum fractions in the lowest-particle number valence Fock state. Measurements of meson form factors[58] and other exclusive and semi-exclusive processes[133] at large momentum transfer can only provide global constraints on the shape of $\phi(z, \tilde{Q}^2)$; in contrast, the angular dependence of the lepton pair distributions can be used to provide local measurements of the shapes of these hadron wavefunctions. Detailed measurements of the angular distribution of leptons in hadron-hadron collisions will open up a new window on the structure

of hadrons at the amplitude level.

Our analysis shows that the broad, two-humped, distribution amplitude for the pion which was predicted from QCD sum rules[85] can account for the main features of the Drell-Yan data. In contrast, narrow momentum distributions, characteristic of weak hadronic binding, predicts the wrong sign for the observed azimuthal angular coefficients μ and ν.

It is clearly important to have detailed measurements of the lepton pair distributions as a function of both x and Q_T for the reactions $Hp \to \ell^+\ell^- X$ for the whole range of fixed target beams $H = \pi, K, \bar{p}, p$, and n. In each case, the deviations from the parton model predictions will provide a unique sensitivity to the fundamental non-perturbative structure of the projectile wavefunction. In the case of $\gamma^* p \to \ell^+\ell^- X$, one can also in principle identify the "point-like" and "resolved" components of the distribution amplitude for both real and virtual photons.

We also note that if either the higher twist explanation or a more exotic non-perturbative explanation[130] of the azimuthal correlations are correct, then one expects the same type of anomalous $\cos 2\phi$ azimuthal correlation will be seen in other QCD processes such as $e^+e^- \to H^+H^- X$, $\ell p \to \ell H X$, and $pp \to H_1 H_2 X$.

18 Hadron Helicity Conservation in Hard Exclusive Reactions

There are also strong helicity constraints on form factors and other exclusive amplitudes which follow from perturbative QCD[12] At large momentum transfer, each helicity amplitude contributing to an exclusive process at large momentum transfer can be written as a convolution of a hard quark-gluon scattering amplitude T_H which conserves quark helicity with the hadron distribution amplitudes $\phi(x_i, Q)$, which are the $L_z = 0$ projection of the hadron's valence Fock state wavefunction: $\phi(x_i, \lambda_i, Q) = \int [d^2k_\perp]\ \psi(x_i, \vec{k}_{\perp i}, \lambda_i)\theta(k_{\perp i}^2 < Q^2)$ where $\psi(x_i, \vec{k}_{\perp i}, \lambda_i)$ is the valence wavefunction. Since ϕ only depends logarithmically on Q^2, the main dynamical dependence of $F_B(Q^2)$ is the power behavior $(Q^2)^{-2}$ derived from the scaling behavior of the elementary propagators in T_H.

As shown by Botts, Li, and Sterman,[134] the virtual Sudakov form factor suppresses long distance contributions from Landshoff multiple scattering and $x \sim 1$ integration regions, so that the leading high momentum transfer behavior of hard exclusive amplitudes are generally controlled by short-distance physics. Thus

quark helicity conservation of the basic QCD interactions leads to a general rule concerning the spin structure of exclusive amplitudes:[14] to leading order in $1/Q$, the total helicity of hadrons in the initial state must equal the total helicity of hadrons in the final state. This selection rule is independent of any photon or lepton spin appearing in the process. The result follows from (a) neglecting quark mass terms, (b) the vector coupling of gauge particles, and (c) the dominance of valence Fock states with zero angular momentum projection. The result is true in each order of perturbation theory in α_s.

For example, PQCD predicts that the Pauli Form factor $F_2(Q^2)$ of a baryon is suppressed relative to the helicity-conserving Dirac form factor $F_1(Q^2)$. A recent experiment at SLAC carried out by the American-University/SLAC collaboration is in fact consistent with the prediction $Q^2F_2(Q^2)/F_1(Q^2) \to$ const.[135] Helicity conservation holds for any baryon to baryon vector or axial vector transition amplitude at large spacelike or timelike momentum. Helicity non-conserving form factors should fall as an additional power of $1/Q^2$.[14] Measurements[136] of the transition form factor to the $J = 3/2$ $N(1520)$ nucleon resonance are consistent with $J_z = \pm 1/2$ dominance, as predicted by the helicity conservation rule.[14] One of the most beautiful tests of perturbative QCD is in proton Compton scattering, where there are now detailed predictions available for each hadron helicity-conserving amplitude for both the spacelike and timelike processes.[137] In the case of spin-one systems such as the ρ or the deuteron, PQCD predicts that the ratio of the three form factors have the same behavior at large momentum transfer as that of the W in the electroweak theory.[40]

Another interesting application of helicity retention in exclusive processes is the exclusive production of vector mesons in high energy electroproduction.[138] At large photon virtuality Q^2 the longitudinal couplings of the virtual photon dominate. This polarization is then retained in the diffractive production of the vector meson. The amplitude for this process can be factorized as a convolution of (a) the photon wavefunction, (b) the scattering amplitude for the quark and antiquark system to scatter through the exchange of two gluons to the target system, and (c) the vector meson distribution amplitude. Thus measurements of forward high energy diffractive leptoproduction can lead to fundamental checks on the normalization of the gluon structure function at low x, as well as moments of the vector meson wavefunction. Further details and references are given in Ref. 138.

Hadron helicity conservation in large momentum transfer exclusive reactions is a general principle of leading twist QCD. In fact, in several outstanding cases, it does not work at all, particularly in single spin asymmetries such as A_N in pp scattering, and most spectacularly in the two-body hadronic decays of the J/ψ. The inference from these failures is that non-perturbative or higher twist effects must be playing a crucial role in the kinematic range of these experiments.

The J/ψ decays into isospin-zero final states through the intermediate three-gluon channel. If $PQCD$ is applicable, then the leading contributions to the decay amplitudes preserve hadron helicity. In the case of e^+e^- annihilation into vector plus pseudoscalar mesons, Lorentz invariance requires that the vector meson will be produced transversely polarized. Since this amplitude does not conserve hadron helicity, $PQCD$ predicts that it will be dynamically suppressed at high momentum transfer. Hadron helicity conservation appears to be severely violated if one compares the exclusive decays J/ψ and $\psi' \to \rho\pi, K^*\overline{K}$ and other vector-pseudoscalar combinations. The predominant two-body hadronic decays of the J/ψ have the measured branching ratios

$$\begin{aligned} BR(J/\psi \to K^+K^-) &= 2.37 \pm 0.31 \times 10^{-4} \\ BR(J/\psi \to \rho\pi) &= 1.28 \pm 0.10 \times 10^{-2} \\ BR(J/\psi \to K^+K^{-*}) &= 5.0 \pm 0.4 \times 10^{-3} \, . \end{aligned} \tag{112}$$

Thus the vector-pseudoscalar decays are not suppressed, in striking contrast to the PQCD predictions. On the other hand, for the ψ':

$$\begin{aligned} BR(\psi' \to K^+K^-) &= 1.0 \pm 0.7 \times 10^{-4} \\ BR(\psi' \to \rho\pi) &< 8.3 \times 10^{-5} \ \ (90\%\ CL) \\ BR(\psi' \to K^+K^{-*}) &< 1.8 \times 10^{-5} \ \ (90\%\ CL) \, . \end{aligned} \tag{113}$$

From the standpoint of perturbative QCD, the observed suppression of ψ' to vector-pseudoscalar mesons is expected; it is the J/ψ that is anomalous.[139] What can account for the apparently strong violation of hadron helicity conservation? One possibility is that the overlap of the $c\bar{c}$ system with the wavefunctions of the ρ and π is an extremely steep function of the pair mass, as discussed by Chaichian and Tornqvist.[140] However, this seems unnatural in view of the similar size of the J/ψ and ψ' branching ratios to K^+K^-. Pinsky[141] has suggested that the

ψ' decays predominantly to final states with excited vector mesons such as $\rho'\pi$, in analogy to the absence of configuration mixing in nuclear decays. However, this long-distance decay mechanism would not be expected to be important if the charmonium state decays through $c\bar{c}$ annihilation at the Compton scale $1/m_c$.

Another way in which hadron helicity conservation might fail for $J/\psi \to$ gluons $\to \pi\rho$ is if the intermediate gluons resonate to form a gluonium state $\mathcal{O}$. If such a state exists, has a mass near that of the J/ψ, and is relatively stable, then the subprocess for $J/\psi \to \pi\rho$ occurs over large distances and the helicity conservation theorem need no longer apply. This would also explain why the J/ψ decays into $\pi\rho$ and not the ψ'. Tuan, Lepage, and I[139] have thus proposed, following Hou and Soni,[142] that the enhancement of $J/\psi \to K^*\overline{K}$ and $J/\psi \to \rho\pi$ decay modes is caused by a quantum mechanical mixing of the J/ψ with a $J^{PC} = 1^{--}$ vector gluonium state $\mathcal{O}$ which causes the breakdown of the QCD helicity theorem. The decay width for $J/\psi \to \rho\pi$ via the sequence $J/\psi \to \mathcal{O} \to \rho\pi$ must be substantially larger than the decay width for the (non-pole) continuum process $J/\psi \to 3$ gluons $\to \rho\pi$. In the other channels the branching ratios of the $\mathcal{O}$ must be so small that the continuum contribution governed by the QCD theorem dominates over that of the $\mathcal{O}$ pole. A gluonium state of this type was first postulated by Freund and Nambu[143] based on OZI dynamics soon after the discovery of the J/ψ and ψ' mesons. The most direct way to search for the $\mathcal{O}$ is to scan $\bar{p}p$ or e^+e^- annihilation at $\sqrt{s}$ within ~ 100 MeV of the J/ψ, triggering on vector/pseudoscalar decays such as $\pi\rho$ or $\overline{K}K^*$ and look for enhancements relative to K^+K^-. Such a search has recently been proposed for the BEPC.

19 Anomalous Spin Correlations and Color Transparency Effects in Proton-Proton Scattering

The perturbative QCD analysis of exclusive amplitudes assumes that large momentum transfer exclusive scattering reactions are controlled by short distance quark-gluon subprocesses, and that corrections from quark masses and intrinsic transverse momenta can be ignored. Since hard scattering exclusive processes are dominated by valence Fock state wavefunctions of the hadrons with small impact separation and small color dipole moments, one predicts that initial and final state interactions are generally suppressed at high momentum transfer. In particular, since the formation time is long at high energies, one predicts that

the attenuation of quasi-elastic processes due to Glauber inelastic scattering in a nucleus will be reduced. This is the color transparency prediction of perturbative QCD.[144] A test of color transparency in large momentum transfer quasielastic pp scattering at $\theta_{cm} \simeq \pi/2$ has been carried out at BNL using several nuclear targets (C, Al, Pb).[145] The attenuation at $p_{lab} = 10$ GeV/c in the various nuclear targets was observed to be in fact much less than that predicted by traditional Glauber theory. The expectation from perturbative QCD is that the transparency effect should become even more apparent as the momentum transfer rises. However, the data at $p_{lab} = 12$ GeV/c shows normal nuclear attenuation and thus a violation of color transparency.

An even more serious challenge to the PQCD predictions for exclusive scattering is the observed behavior of the normal spin-spin correlation asymmetry $A_{NN} = [d\sigma(\uparrow\uparrow) - d\sigma(\uparrow\downarrow)]/[d\sigma(\uparrow\uparrow) + d\sigma(\uparrow\downarrow)]$ measured in large momentum transfer pp elastic scattering. At $p_{lab} = 11.75$ GeV/c and $\theta_{cm} = \pi/2$, A_{NN} rises to $\simeq 60\%$, corresponding to four times more probability for protons to scatter with their incident spins both normal to the scattering plane and parallel, rather than normal and opposite.[11] In contrast, the unpolarized data is to first approximation consistent with the fixed angle scaling law $s^{10}d\sigma/dt(pp \to pp) = f(\theta_{CM})$ expected from the perturbative analysis. The onset of new structure at $s \simeq 23$ GeV^2 suggests new degrees of freedom in the two-baryon system.

Guy De Teramond and I[146] have noted that the onset of strong spin-spin correlations, as well as the breakdown of color transparency, can be explained as the consequence of a strong threshold enhancement at the open-charm threshold for $pp \to \Lambda_c Dp$ at $\sqrt{s} = 5.08\ GeV$ or $p_{lab} \sim 12\ GeV/c$. At this energy the charm quarks are produced at rest in the center of mass. Since all eight quarks have zero relative velocity, they can resonate to give a strong threshold effect in the $J = L = S = 1$ partial wave. (The orbital angular momentum of the pp state must be odd since the charm and anti-charm quarks have opposite parity.) The $J = L = S = 1$ partial wave has maximal spin correlation $A_{NN} = 1$. A charm production cross section of the order of 1 μb in the threshold region can have, by unitarity, a large effect on the large angle elastic $pp \to pp$ amplitude since the competing perturbative QCD hard-scattering amplitude at large momentum transfer is very small at $\sqrt{s} = 5\ GeV$. In fact as recently shown by Manohar, Luke, and Savage,[147] the QCD trace anomaly predicts that the scalar charmonium-nucleus interaction is

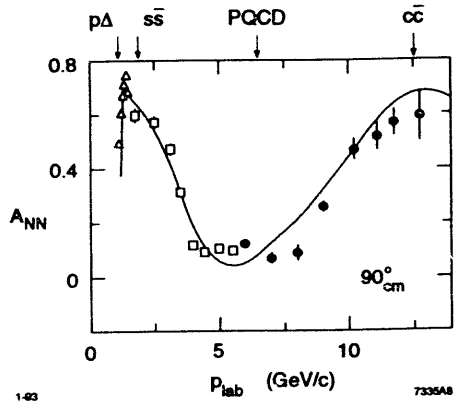

Figure 17. A_{NN} as a function of $p_{\rm lab}$ at $\theta_{cm} = \pi/2$. The data[11] are from Crosbie *et al.* (solid dots), Lin *et al.* (open squares) and Bhatia *et al.* (open triangles). The peak at $p_{\rm lab} = 1.26$ GeV/c corresponds to the $p\Delta$ threshold. The data are well reproduced by the interference of the broad resonant structures at the strange ($p_{\rm lab} = 2.35$ GeV/c) and charm ($p_{\rm lab} = 12.8$ GeV/c) thresholds, interfering with a PQCD background. The value of A_{NN} from PQCD alone is 1/3.

strongly amplified at low velocities and can lead to nuclear-bound charmonium.[148]

An analytic model which contains all of these features is given in Ref. 146. The background component of the model is the perturbative QCD amplitude with s^{-4} scaling of the $pp \to pp$ amplitude at fixed $\theta_{\rm cm}$ and the dominance of those amplitudes that conserve hadron helicity.[14] A comparison[149] of the magnitude of cross sections for different exclusive two-body scattering channels indicate that quark interchange amplitudes[150] dominate quark annihilation or gluon exchange contributions. The most striking test of the model is its prediction for the spin correlation A_{NN} shown in Fig. 17. The rise of A_{NN} to $\simeq 60\%$ at $p_{\rm lab} = 11.75$ GeV/c is correctly reproduced by the high energy J=1 resonance interfering with ϕ(PQCD). The narrow peak which appears in the data of Fig. 17 corresponds to the onset of the $pp \to p\Delta(1232)$ channel which can be interpreted as a $uuuuddq\bar{q}$ $^3F_3$ resonance. The heavy quark threshold model also provides a good description of the s and t dependence of the differential cross section, including its "oscillatory" dependence[151] in s at fixed $\theta_{\rm cm}$, and the broadening of the angular distribution near the resonances. Most important, it gives a consistent explanation for the striking behavior of both the spin-spin correlations and the anomalous energy dependence of the attenuation of quasielastic pp scattering in nuclei. A threshold

enhancement or resonance couples to hadrons of conventional size. Unlike the perturbative amplitude, the protons coupling to the resonant amplitude will have normal absorption in the nucleus. Thus the nucleus acts as a filter, absorbing the non-perturbative contribution to elastic pp scattering, while allowing the hard-scattering perturbative QCD processes to occur additively throughout the nuclear volume.[152] Conversely, in the momentum range $p_{\rm lab} = 5$ to 10 GeV/c one predicts that the perturbative hard-scattering amplitude will be dominant at large angles. It is thus predicted that color transparency should reappear at higher energies ($p_{\rm lab} \geq 16$ GeV/c), and also at smaller angles ($\theta_{\rm cm} \approx 60°$) at $p_{\rm lab} = 12$ GeV/c where the perturbative QCD amplitude dominates. If the resonance structures in A_{NN} are indeed associated with heavy quark degrees of freedom, then the model predicts inelastic pp cross sections of the order of 1 mb and 1μb for the production of strange and charmed hadrons near their respective thresholds. In fact, the neutral strange inclusive pp cross section measured at $p_{\rm lab} = 5.5$ GeV/c is 0.45 ± 0.04 mb.[153] Thus the crucial test of the heavy quark hypothesis for explaining A_{NN} is the observation of significant charm hadron production at $p_{\rm lab} \geq 12$ GeV/c.

Ralston and Pire[152] have suggested that the oscillations of the pp elastic cross section and the apparent breakdown of color transparency are associated with the dominance of the Landshoff pinch contributions at $\sqrt{s} \sim 5$ *GeV*. The oscillating behavior of $d\sigma/dt$ is then due to the energy dependence of the relative phase between the pinch and hard-scattering contributions. They assume color transparency will disappear whenever the pinch contributions are dominant since such contributions could couple to wavefunctions of large transverse size. However, the large spin correlation in A_{NN} is not readily explained in the Ralston-Pire model unless the Landshoff diagram itself has $A_{NN} \sim 1$.

20 Conclusions

In these lectures I have emphasized polarization phenomena which can provide new insights into hadron dynamics and structure. Spin physics has benefited from a remarkably close interplay between theory and experiment. A number of experiments have reported unexpectedly strong spin correlations that challenge a straightforward interpretation in quantum chromodynamics:

1. Two experiments, NA-10 at CERN and Chicago-Iowa-Princeton (CIP) at

FermiLab,[117] have reported strong deviations from leading twist perturbative QCD predictions for the polarization of the virtual photon in the Drell-Yan process $\pi N \to \mu^+\mu^- X$. The strong azimuthal and polar angular correlations observed in these experiments require the consideration of dynamical higher twist subprocesses in which the multi-quark structure of the projectile enters. Thus these measurements can provide new constraints on the structure of the pion at the amplitude level.[130]

2. The CIP collaboration[115] has also reported that the J/ψ produced in π nucleon collisions becomes strongly longitudinally polarized at large momentum fraction x_L. The result is consistent with the general principle of hadron-helicity retention and leads to new constraints on the multi-quark Fock state structure of the pion.[116]
3. The measured branching ratio for the decay of the J/ψ into $\rho\pi$ and other psuedoscalar-vector two-body exclusive decays strongly violate perturbative QCD predictions for hadron helicity conservation. No such anomaly is observed for the ψ'. The result could signal the mixing of the J/ψ with a nearby 1^{--} tri-gluonic bound state.[142,139] However, as yet there is no clear evidence for any gluonium state in this mass range.
4. A remarkably strong spin-spin correlation has been observed in wide-angle elastic polarized proton polarized proton scattering at ANL and BNL. The sudden increase in the spin correlation A_{NN} at new quark thresholds and the observed breakdown of color transparency at $\sqrt{s} \sim 5$ GeV in quasi-elastic pp scattering may reflect the strong attraction at the charm production threshold[146] predicted from the QCD trace anomaly.[147] The large values observed for the single spin asymmetry A_N may be due to higher twist corrections.

The new measurements of the polarized structure functions in deep inelastic lepton scattering from SLAC and CERN are now providing fundamental checks on QCD sum rules, as well as a detailed look at the underlying spin structure of the nucleon. The integral of the non-singlet polarized structure function $g_1^{p-n}(x,Q)$ appears compatible with the Bjorken sum rule, although a number of uncertainties due to higher twist and Regge extrapolations still remain. In these lectures I have discussed several theoretical advances which will allow more definitive tests of the QCD sum rules:

1. QCD provides important constraints on the x-dependence of the quark distributions which reflect the helicity retention properties of the underlying gauge couplings at large x and the decorrelation of helicities at small x. Measurements appear to be consistent with these constraints.
2. The leading twist perturbative QCD corrections to the Bjorken and Gross-Llewellyn Smith sum rules are identical, up to "light-by-light" scattering contributions of order $[\alpha_s(Q^2)\pi]^3$. Thus measurements the ratio of the sum rules can provide a highly precise test of QCD.[10] The extrapolation of the ratio of the truncated sum rule integrals to $x_{\rm min} \to 0$ should greatly eliminate uncertainties due to Regge behavior.
3. The leading twist perturbative QCD corrections to the Bjorken sum rule can be directly related to measurements of the annihilation cross section ratio $R_{e^+e^-}$ and other observables such as the τ hadronic width using commensurate scale relations.[10] These relations are convention independent; they have no ambiguity due to the choice of renormalization scale or scheme. The relation between the effective charges for the Bjorken sum rule and the annihilation cross section is now known to third order in $\alpha_s(Q^2)$, thus allowing precise tests of the gauge theory predictions by tracking both the relative normalization and dependence in momentum transfer.
4. Higher twist-corrections to the Bjorken and Ellis-Jaffe sum rules due to the intrinsic composite structure of the nucleons are constrained at small Q^2 by a corresponding Drell-Hearn Gerasimov sum rule.[4]
5. The relativistic corrections to the quark model are highly non-trivial and lead to a number of unexpected results.[7] The values of the magnetic moment and axial coupling g_A of the proton are strongly correlated, independent of the actual shape of the three-quark wavefunction. An important physical effect is that the Melosh transformation (Wigner rotation) of the constituent spinors to the light-cone causes a net misorientation of the quark helicities relative to their rest frame spin projection S_z. In the zero-radius limit the anomalous moment and the axial coupling of the nucleon vanish. For the physical size of the proton, relativistic binding leads to a 25% reduction of the quark helicities Δq and g_A from their naive values.

Polarization measurements thus provide some of the most stringent tests of quantum chromodynamics. An entire new class of polarization transfer measure-

ments can be carried out at the SLC using polarized electron-positron collisions. In addition to the fixed target experiments now being done at SLAC and CERN, the new polarization facilities such as HERMES at DESY, the proposed polarized proton collider at RHIC, and the highly polarized 50 GeV electron beam facility at SLAC will allow a wide range of exclusive and inclusive spin physics studies. There is also a critical need for measurements of the polarized gluon distributions in the nucleon from experiments such as direct photon production in polarized proton collisions and J/ψ production in polarized photon-polarized proton interactions.

21 Appendix A: Light-Cone Wave-Functions

A simple way to encode the properties of hadrons in terms of their quark and gluon degrees of freedom is the light-cone Fock expansion.[154] For example, a proton with momentum $\underline{P} = (P^+, \vec{P}_\perp)$ is described by expansion over color-singlet eigenstates of the free QCD light-cone Hamiltonian:

$$|\pi : \underline{P}\rangle = \sum_{n,\lambda_i} \int \overline{\prod_i} \frac{dx_i d^2\vec{k}_{\perp i}}{\sqrt{x_i} 16\pi^3} \left| n : x_i P^+, x_i \vec{P}_\perp + \vec{k}_{\perp i}, \lambda_i \right\rangle \psi_{n/\pi}(x_i, \vec{k}_{\perp i}, \lambda_i) \tag{114}$$

where the sum is over all Fock states and helicities starting with the valence three-quark state, and where

$$\begin{aligned} \overline{\prod_i} dx_i &\equiv \prod_i dx_i \, \delta\left(1 - \sum_j x_j\right) \\ \overline{\prod_i} d^2\vec{k}_{\perp i} &\equiv \prod_i d^2\vec{k}_{\perp i} \, 16\pi^3 \, \delta^2\left(\sum_j \vec{k}_{\perp j}\right). \end{aligned} \tag{115}$$

The wavefunction $\psi_{n/\pi}(x_i, \vec{k}_{\perp i}, \lambda_i)$ is the amplitude for finding partons in a specific light-cone Fock state n with momenta $(x_i P^+, x_i \vec{P}_\perp + \vec{k}_{\perp i})$ in the proton. The Fock state is off the light-cone energy shell: $\sum k_i^- > P^-$. The light-cone momentum coordinates x_i, with $\sum_{i=1}^n x_i$ and $\vec{k}_{\perp i}$, with $\sum_{i=1}^n \vec{k}_{\perp i} = \vec{0}_\perp$, are actually relative coordinates; *i.e.* they are independent of the total momentum P^+ and $P_\perp$ of the

bound state. The light-cone wavefunctions do not depend on the total momentum since x_i is the longitudinal momentum fraction carried by the i^{th}-parton ($0 \le x_i \le 1$), and $\vec{k}_{\perp i}$ is its momentum "transverse" to the direction of the meson. Both of these are frame-independent quantities. The ability to specify wavefunctions simultaneously in any frame is a special feature of light-cone quantization.

The coefficients in the light-cone Fock state expansion thus are the parton wavefunctions $\psi_{n/H}(x_i, \vec{k}_{\perp i}, \lambda_i)$ which describe the decomposition of each hadron in terms of its fundamental quark and gluon degrees of freedom. The light-cone variable $0 < x_i < 1$ is often identified with the constituent's longitudinal momentum fraction $x_i = k_i^z / P_z$, in a frame where the total momentum $P^z \to \text{inf}$. However, in light-cone Hamiltonian formulation of QCD, x_i is the boost-invariant light-cone fraction,

$$x_i \equiv \frac{k_i^+}{P^+} = \frac{k_i^0 + k_i^z}{P^0 + P^z}, \tag{116}$$

independent of the choice of Lorentz frame.

Given the light-cone wavefunctions, $\psi_{n/H}(x_i, \vec{k}_{\perp i}, \lambda_i)$, one can compute virtually any hadronic quantity by convolution with the appropriate quark and gluon matrix elements. For example, the leading-twist structure functions measured in deep inelastic lepton scattering are immediately related to the light-cone probability distributions:

$$2M\, F_1(x, Q) = \frac{F_2(x, Q)}{x} \approx \sum_a e_a^2 \, G_{a/p}(x, Q) \tag{117}$$

where

$$G_{a/p}(x, Q) = \sum_{n,\lambda_i} \int \overline{\prod_i} \frac{dx_i d^2\vec{k}_{\perp i}}{16\pi^3} |\psi_n^{(Q)}(x_i, \vec{k}_{\perp i}, \lambda_i)|^2 \sum_{b=a} \delta(x_b - x) \tag{118}$$

is the number density of partons of type a with longitudinal momentum fraction x in the proton. This follows from the observation that deep inelastic lepton scattering in the Bjorken-scaling limit occurs if x_{bj} matches the light-cone fraction of the struck quark. (The $\sum_b$ is over all partons of type a in state n.) However, the light-cone wavefunctions contain much more information for the final state of deep inelastic scattering, such as the multi-parton distributions, spin and flavor correlations, and the spectator jet composition.

The spacelike form factor is the sum of overlap integrals analogous to the corresponding nonrelativistic formula:

$$F(Q^2) = \sum_{n,\lambda_i} \sum_a e_a \int \overline{\prod_i} \frac{dx_i\, d^2\vec{k}_{\perp i}}{16\pi^3}\, \psi_n^{(\Lambda)*}(x_i, \vec{\ell}_{\perp i}, \lambda_i)\, \psi_n^{(\Lambda)}(x_i, \vec{k}_{\perp i}, \lambda_i). \quad (119)$$

Here e_a is the charge of the struck quark, $\Lambda^2 \gg \vec{q}_\perp^{\,2}$, and

$$\vec{\ell}_{\perp i} \equiv \begin{cases} \vec{k}_{\perp i} - x_i \vec{q}_\perp + \vec{q}_\perp & \text{for the struck quark} \\ \vec{k}_{\perp i} - x_i \vec{q}_\perp & \text{for all other partons.} \end{cases} \quad (120)$$

The general rule for calculating an amplitude involving wavefunction $\psi_n^{(\Lambda)}$, describing Fock state n in a hadron with $\underline{P} = (P^+, \overrightarrow{P}_\perp)$, has the form[58]

$$\sum_{\lambda_i} \int \overline{\prod_i} \frac{dx_i d^2\vec{k}_{\perp i}}{\sqrt{x_i} 16\pi^3}\, \psi_n^{(\Lambda)}(x_i, \vec{k}_{\perp i}, \lambda_i)\; T_n^{(\Lambda)}(x_i P^+, x_i \overrightarrow{P}_\perp + \vec{k}_{\perp i}, \lambda_i) \quad (121)$$

where $T_n^{(\Lambda)}$ is the irreducible scattering amplitude in LCPTh with the hadron replaced by Fock state n. The light-cone Fock expansion thus allows a definition of the parton model and wavefunctions. By using the light-cone gauge, $A^+ = 0$, only physical non-ghost degrees of freedom appear in the Fock expansion even for non-Abelian theories. Furthermore in this gauge, the numerator couplings of soft gluons inserted into hard scattering expansions remain finite in the high momentum transfer limit. Thus this formalism is ideal for proving factorization theorems, *i.e.* the isolation of hard and soft contributions at high momentum transfer.

22 Acknowledgements

Much of the work reported in these lectures is based on collaborations with colleagues. I wish to particularly thank Michael Boulware, Arnd Brandenburg, Matthias Burkardt, Lance Dixon, Vittorio del Duca, John Ellis, Leonid Frankfurt, Jack Gunion, Tom Hyer, Paul Hoyer, Marek Karliner, Valya Khoze, Peter Lepage, Hung Jung Lu, Al Mueller, Dieter Müller, Michael Peskin, Ivan Schmidt, Felix Schlumpf, Mark Strikman, Wai-keung Tang, Mikko Vanttinen, Ramona Vogt, and Kai Wong for helpful discussions.

This work was supported by the Department of Energy, contract DE-AC03-76SF00515.

References

[1] J. Ellis and M. Karliner CERN-TH-7022-93, (1993). Plenary talk at *13th International Conference on Particles and Nuclei*, PANIC '93, Perugia, Italy.

[2] S. J. Brodsky, J. Ellis, and M. Karliner, Phys. Lett. **206B**, 309 (1988). For a detailed discussion, see M. Karliner, TAUP-1932-91 (Tel-Aviv), invited talk at *International Symposium on π N Physics and the Structure of the Nucleon*, Bad Honnef, Germany, September 9–13, 1991; PRINT-89-0966 (Tel-Aviv), Lecture at *Summer School in High Energy Physics and Cosmology*, Trieste, Italy, June 26–August 25, 1989; TAUP-1730-89, (Tel-Aviv), invited talk given at *24th Rencontres de Moriond: New Research in Hadronic Interactions*, Les Arcs, France, March 12–18, 1989.

[3] Emlyn Hughes, these proceedings.

[4] V. D. Burkert and B. L. Ioffe, Phys. Lett. **B296**, 223 (1992); CEBAF preprint (1993). M. Anselimino, B. L. Ioffe, E. Leader, Sov. J. Nucl. Phys. **49,** 136 (1989). The experimental validity of the DHG sum rule for the proton-neutron difference is not clear. See R. L. Workman and R. A. Arndt, Phys. Rev. **D45**, 1789, (1992).

[5] An explicit calculation of the soft multi-gluonic Fock states for heavy quarkonium is given in A. H. Mueller, Columbia University preprint CU-TP-609, (1993).

[6] S. Dalley and I. R. Klebanov, Phys. Rev. **D47,** 2517 (1993). K. Demeterfi, I. R. Klebanov, and Gyan Bhanot, Princeton University preprint PUPT-1427 (1993).

[7] S. J. Brodsky and F. Schlumpf, SLAC-PUB-6431 (1994).

[8] V. N. Gribov and L. N. Lipatov, Sov. J. Nucl. Phys. **15**, 438 and 675 (1972).

[9] S. J. Brodsky, M. Burkardt, and I. A. Schmidt, SLAC-PUB-6068 (1994).

[10] S. J. Brodsky and H. J. Lu, SLAC-PUB-6389 (1993), published in the *Proceedings of the Leipzig Workshop on Quantum Field Aspects of High Energy Physics*, Kyffhäuser, Germany (1993).

[11] For references to the data and a review, see A. Krisch, *Proceedings of the 10th International Symposium on High-Energy Spin Physics*, Nagoya, Japan (1992).

[12] S. J. Brodsky, G. P. Lepage, in "Perturbative Quantum Chromodynamics", edited by A. H. Mueller, World Scientific Publishing Company (1989).

[13] S. J. Brodsky, P. Hoyer, A. H. Mueller, W. K. Tang, Nucl. Phys. **B369**, 519 (1992).

[14] S. J. Brodsky and G. P. Lepage, Phys. Rev. **D24**, 2848 (1981).

[15] By S. J. Brodsky, T. A. DeGrand, R. Schwitters, Phys. Lett. **79B**, 255 (1978).

[16] H. J. Lipkin, Phys. Lett. **B256**, 284-288 (1991).

[17] J. D, Bjorken, Phys. Rev. **148**, 1467 (1966); Phys. Rev. **D1**, 1376 (1970).

[18] J. Kodaira, Nucl. Phys. **B259**, 129 (1980).

[19] S. A. Larin, F. V. Tkachev, and J. A. M. Vermaseran, Phys. Rev. Lett. **66**, 862 (1991); S. A. Larin and J. A. M. Vermaseran, Phys. Lett. **259**, 345 (1991); S. G. Gorishny and S. A. Larin, Phys. Lett. **B172**, 109 (1986).

[20] S. J. Brodsky, G. P. Lepage, and P. B. Mackenzie, Phys. Rev. **D28**, 228 (1983).

[21] S. J. Brodsky and H. Lu, to be published.

[22] E. B. Zijlstra and W. L. van Neerven, University of Leiden preprint INLO-PUB-3/93.

[23] J. Ellis and R. L. Jaffe, Phys. Rev. **D9**, 1444 (1974).

[24] G. Altarelli and G. G. Ross, Phys. Lett **B212**, 391 (1988). A. V. Efremov and O. V. Teryaev, Dubna report E2-88-287 (1988), published in the *Proceedings of the International Hadron Symposium*, Bechyne, Czechoslovakia (1988). For a complete discussion and additional references, see E. Reya, *Proceedings of the Workshop on QCD - "20 Years Later"*, Aachen (1992).

[25] H. Fritzsch, *Proceedings of the Leipzig Workshop "Quantum Field Theory Aspects of High Energy Physics"*, Bad Frankenhäusen, Germany (1993).

[26] G. T. Bodwin and J. Qiu, Phys. Rev. **D41**, 2755 (1990). S. D. Bass, B. L. Ioffe, N. N. Nikolaev, and A. W. Thomas, J. Moscow Phys. Soc. **1**, 317 (1991).

[27] R. D. Carlitz, J. C. Collins, and A. H. Mueller, Phys. Lett. **B214**, 229 (1988).

[28] SMC Collaboration preliminary results, presented by V. Hughes, at the *International Workshop on Deep Inelastic Scattering and Related Subjects*, Eilat, Israel, February, 1994.

[29] For recent analyses of the data and comparisons with theory, see J. Ellis and M. Karliner, Phys. Lett. **B313**, 131 (1993); F. E. Close and R. G. Roberts, Phys. Lett. **B316**, 165 (1993); M. Karliner, *1989 Summer School in High Energy Physics and Cosmology*, Trieste (1990).

[30] For a discussion of the analogous effects in inelastic lepton-nucleus scattering, see S. D. Drell, *Proceedings of the 1992 SLAC Summer Institute.*

[31] See S. Dasu, *et al.*. SLAC-PUB-5814, (1993) and references therein.

[32] A. H. Mueller, Phys. Lett. **308** 355, (1993).

[33] X. Ji and P. Unrau, preprint MIT-CTP-2232 (1993).

[34] M. Karliner, private communication.

[35] S.D. Drell and A.C. Hearn, Phys. Rev. Lett. **16**, 908 (1966).

[36] S.B. Gerasimov, Sov. J. Nucl. Phys. **2**, 430 (1966).

[37] F. Low, Phys. Rev. **96**, 1428 (1954); M. Gell-Mann and M.L. Goldberger, Phys. Rev. **96**, 1433 (1954); see also K. Bardakci and H. Pagels, Phys. Rev. **166**, 1783 (1968).

[38] M. Hosoda and K. Yamamoto, Prog. Theor. Phys. **36**, 426 (1966); see also S. J. Brodsky and J. R. Primack, Ann. Phys. **52**, 315 (1969).

[39] I. Karliner, Phys. Rev. **D7**, 2717 (1973).

[40] S. J. Brodsky and J. R. Hiller, Phys. Rev. **D46** 2141, (1992).

[41] W.-K. Tung, Phys. Rev. **176**, 2127 (1968).

[42] S.J. Brodsky and S.D. Drell, Phys. Rev. **D22**, 2236 (1980).

[43] L. F. Abbott and E. Farhi, Phys. Lett. **101B**, 69 (1981); Nucl. Phys. **B189**, 547 (1981).

[44] M. Claudson, E. Farhi, and R. L. Jaffe, Phys. Rev. **D34**, 873 (1986).

[45] R.L. Jaffe and Z. Ryzak, Phys. Rev. **D37**, 2015 (1988).

[46] S. J. Brodsky and R. W. Brown, Phys. Rev. Lett. **49**, 966 (1982); R. W. Brown, K. L. Kowalski and S. J. Brodsky, Phys. Rev. **D28**, 624 (1984); R. W. Brown and K. L. Kowalski, *ibid.* **29**, 2100 (1984). See also K. Mikaelian, M. A. Samuel, and D. Sahdev. Phys. Rev. Lett. **43**, 746 (1979).

[47] M. A. Samuel, G. Li, N. Sinha, R. Sinha, and M. K. Sundaresan, Phys. Rev. Lett. **67**, 9 (1991) and references therein.

[48] S. J. Brodsky and J. R. Primack, Annals Phys. **52**, 315 (1969); Phys. Rev. **174**, 2071 (1968).

[49] P. V. Landshoff, J. C. Polkinghorne, and R. Short, Nucl. Phys. **B28**, 225 (1971). S. J. Brodsky, F. E. Close, and J. F. Gunion, Phys. Rev. **D8**, 3678 (1973).

[50] S. J. Brodsky and I. A. Schmidt, Phys. Rev. **D43**, 179 (1991).

[51] S. J. Brodsky and H. J. Lu, Phys. Rev. Lett. **64**, 1342 (1990).

[52] N. N. Nikolaev and V. I. Zakharov, Phys. Lett. **55B**, 397 (1975).

[53] V. Del Duca, S. J. Brodsky, P. Hoyer, Phys. Rev. **D46**, 931 (1992).

[54] N. N. Nikolaev, *Proceedings of the 10th International Symposium on High-Energy Spin Physics*, Nagoya, Japan (1992).

[55] This section is based on work done in collaboration with Felix Schlumpf, SLAC-PUB-6431 (1994).

[56] A recent review of this approach can be found in S. J. Brodsky, G. McCartor, H. C. Pauli and S. S. Pinsky, Particle World **3**, 109 (1993), and references therein.

[57] R. J. Perry, A. Harindranath and K. G. Wilson, Phys. Rev. Lett. **65**, 2959 (1990); M. Krautgartner, H. C. Pauli and F. Wolz, Phys. Rev. **D45**, 3755 (1992).

[58] G. P. Lepage and S. J. Brodsky, Phys. Rev. **D22**, 2157 (1980).

[59] F. Schlumpf, Phys. Rev. **D47**, 4114 (1993); Mod. Phys. Lett. **A8**, 2135 (1993); Phys. Rev. **D48**, 4478 (1993); J. Phys. G (to be published).

[60] E. Wigner, Ann. Math. **40**, 149 (1939).

[61] H. J. Melosh, Phys. Rev. **D9**, 1095 (1974); L. A. Kondratyuk and M. V. Terent'ev, Yad. Fiz. **31**, 1087 (1980) [Sov. J. Nucl. Phys. **31**, 561 (1980)]; D. V. Ahluwalia and M. Sawicki, Phys. Rev. **D47**, 5161 (1993).

[62] F. Coester and W. N. Polyzou, Phys. Rev. **D26** (1982) 1349; P. L. Chung, F. Coester, B. D. Keister and W. N. Polyzou, Phys. Rev. **C37**, 2000 (1988).

[63] H. Leutwyler and J. Stern, Annals Phys. **112**, 94 (1978).

[64] P. L. Chung and F. Coester, Phys. Rev. **D44**, 229 (1991).

[65] Bo-Qiang Ma, J. Phys. **G17**, L53 (1991); Bo-Qiang Ma and Qi-Ren Zhang, Z. Phys. **C58**, 479 (1993).

[66] Particle Data Group, Phys. Rev. **D45** Part 2, 1 (1992).

[67] R. L. Jaffe and A. Manohar, Nucl. Phys. **B337**, 509 (1990).

[68] A. V. Eframov and O. V. Teryaev, Czech. Hadron Symposium 1988, 302 (1988); G. Altarelli and G. G. Ross, Phys. Lett. **B212**, 391 (1988); R. D. Carlitz, J. C. Collins and A. H. Mueller, Phys. Lett. **B214**, 229 (1988).

[69] B. Adeva, *et al.*, Phys. Lett. **B302**, 533 (1993).

[70] P. L. Anthony, *et al.*, SLAC-PUB-6101 (1993).

[71] R. Blankenbecler and S. J. Brodsky, Phys. Rev **D10**, 2973 (1974); J. F. Gunion, Phys. Rev. **D10**, 242 (1974). S. J. Brodsky and G. P. Lepage, *Proceedings of the 1979 Summer Institute on Particle Physics*, SLAC, (1979). For a recent systematic analysis in scalar field theory, see D. Müller, published in the *Proceedings of the Leipzig Workshop on Quantum Field Aspects of High Energy Physics*, Kyffhäuser, Germany (1993).

[72] G. R. Farrar and D. R. Jackson, Phys. Rev. Lett. **35**, 1416 (1975).

[73] J. D. Bjorken, Phys. Rev. **D1**, 1376 (1970).

[74] E. Bloom and F. Gilman, Phys. Rev. Lett. **25**, 1140 (1970).

[75] S. D. Drell and T.-M.Yan, Phys. Rev. Lett. **24**, 181 (1970).

[76] A. Lung, *et al.*, Phys. Rev. Lett. **70**, 718 (1993).

[77] See also R. L. Jaffe and A. Manohar, Nucl. Phys. **B321**, 343 (1989); S. D. Bass, A. W. Thomas, Cavendish preprint-HEP-93-4, (1993).

[78] M. Bourquin *et al.*, Z. Phys. **C21**, 27 (1983).

[79] For recent analyses of the radiative corrections to the Bjorken sum rule see J. Ellis and M. Karliner, Refs. 1, 29, and S. Brodsky and H. J. Lu, SLAC-PUB-6389 (1993).

[80] An analysis of the evolution of the helicity-dependent quark and gluon structure functions is given in E. L. Berger and J. Qiu, Phys. Rev. **D40**, 3128 (1989).

[81] For further discussion, see S. J. Brodsky and G. P. Lepage, Ref. 71.

[82] M. B. Einhorn, Phys. Rev. **D14**, 3451 (1976).

[83] S. J. Brodsky, *Proceedings of the 10th International Symposium on High-Energy Spin Physics*, Nagoya, Japan (1992).

[84] S. J. Brodsky and I. A. Schmidt, Phys. Lett. **B234**, 144 (1990). Coherence effects are also discussed in: S. J. Brodsky and J. F. Gunion, Phys. Rev. **D19**, 1005 (1979). Applications to atomic and molecular systems are discussed in: M. Burkardt, Nucl. Phys. **B373**, 371 (1992); see also M. Kaluža,

A. G. Schneider-Neureither and H. Pirner, Universität Heidelberg preprint (1993).

[85] V. L. Chernyak and A. R. Zhitnitsky, Phys. Rept. **112**, 173 (1984).

[86] A. D. Martin, W. J. Stirling, and R.G. Roberts, Phys. Lett. **B306**, 145 (1993).

[87] ZEUS Collaboration, Phys. Lett. **B315**, 481 (1993).

[88] M. J. Alguard *et al.*, Phys. Rev. Lett. **37**, 1261 (1976); **41**, 70 (1978); G. Baum *et al.*, ibid **51**, 1135 (1983).

[89] J. Ashman *et al.*, Phys. Lett. **B206**, 364 (1988); Nucl. Phys. **B328**, 1 (1989).

[90] P. Amadruz, *et al.*, Phys. Lett. **B295**, 159 (1992).

[91] For an alternative parameterization of the strange quark distributions, see G. Preparata, P. G. Ratcliffe, and J. Soffer, Phys. Lett. **B273** 306, (1991).

[92] See for example: W. M. Gibson and B. R. Pollard, in *Symmetry Principles in Elementary Particle Physics*, Cambridge University Press (1976), page 330.

[93] R. D. Carlitz and J. Kaur, Phys. Rev. Lett. **38**, 673 (1977); J. Kaur, Nucl. Phys. **B128**, 219 (1977). For recent empirical models, see Ref. 80 and K. Kobayakawa *et al.*, Phys. Rev. **D46**, 2854 (1992).

[94] The work in this section was done in collaboration with Hung Jung Lu, Ref. 10.

[95] S. G. Gorishnii, A. L. Kataev, S. A. Larin, Phys. Lett. **B309**, 273 (1991), **B275**, 512(E) (1992).

[96] L. R. Surguladze, M. A. Samuel, Phys. Lett. **B309**, 157 (1993).

[97] P. Nason, S. Dawson, and R. K. Ellis, Nucl. Phys. **B303**, 607 (1988); Nucl. Phys. **B327**, 49 (1989).

[98] G. Grunberg, Phys. Lett. **B95**, 70 (1980); Phys. Lett. **B110**, 501 (1982); Phys. Rev. **D29**, 2315 (1984).

[99] P. M. Stevenson, Phys. Lett. **B100**, 61 (1981); Phys. Rev. **D23**, 2916 (1981); Nucl. Phys. **B203**, 472 (1982); Nucl. Phys. **B231**, 65 (1984).

[100] S. J. Brodsky, G. P. Lepage and P. B. Mackenzie, Phys. Rev. **D28**, 228 (1983).

[101] G. Kramer and B. Lampe, Zeit. Phys. **A339**, 189 (1991).

[102] S. J. Brodsky and H. J. Lu, SLAC-PUB-6000 (1993).

[103] E. C. G. Stückelberg and A. Peterman, Helv. Phys. Acta **26**, 499 (1953), A. Peterman, Phys. Rept. **53 C**, 157 (1979).

[104] We thank A. Kataev for an illuminating discussion on this point.

[105] S. J. Brodsky and H. J. Lu, Phys. Rev. **D48**, 3310 (1993).

[106] G. P. Lepage, P. B. Mackenzie, Phys. Rev. **D48**, 2250 (1993).

[107] The one-loop calculation of α_V in $\overline{\rm MS}$ scheme is given in W. Fischler, Nucl. Phys. **B129**, 157 (1977), A. Billoire, Phys. Lett. **92 B**, 343 (1980), W. Buchmuller, G. Grunberg and S. H. H. Tye, Phys. Rev. Lett. **45**, 103 (1980); **45**, 587(E) (1980).

[108] We thank Patrick Huet and Eric Sather for conversations on this point.

[109] W.-K. Wong, *et al.*, (in preparation).

[110] S. J. Brodsky and H. Lu, to be published.

[111] G. Grunberg and A. L. Kataev, Phys. Lett. **B279**, 352 (1992). G. Grunberg, Phys. Rev. **D46**, 2228 (1992). J. Chyla and A. L. Kataev, Phys. Lett. **B297**, 385 (1992). A. Kataev, CERN-TH.6485 (1992), published in the *Proceedings of the XXVIIth Recontre de Moriond*, edited by J. Tran Than Van (1992).

[112] A. C. Mattingly and P.M. Stevenson, Phys. Rev. **D49**, 437 (1994).

[113] For a comprehensive recent analysis of the radiative and higher twist corrections to the Bjorken sum rule, see M. Karliner and J. Ellis, Phys. Lett. **B313**, 131 (1993).

[114] An analysis using CSR through order α_s^3 is in preparation.

[115] C. Biino, Phys. Rev. Lett. **58**, 2523 (1987).

[116] S. J. Brodsky, W. Tang, P. Hoyer, and M. Vanttinen, in preparation.

[117] J. G. Heinrich, *et al.*, Phys. Rev. **D44**, 1909 (1991); M. Guanziroli, *et al.*, Z. Phys. **C37**, 545 (1988).

[118] J. Badier, *et al.*, Z. Phys. **C20**, 101 (1983).

[119] D. M. Alde, *et al.* Phys. Rev. Lett. **66**, 133 (1991).

[120] R. Vogt, S. J. Brodsky, P. Hoyer, Nucl. Phys. **B360**, 67 (1991).

[121] S. D. Drell and T.M. Yan, Phys. Rev. Lett. **25**, 316 (1970).

[122] G. Altarelli, R. K. Ellis, M. Greco and G. Martinelli, Nucl. Phys. **B246**, 12 (1984).

[123] P. Chiappetta and M. Le Bellac, Z. Phys. **C32**, 521 (1986).

[124] NA10 Collaboration, S. Falciano *et al.*, Z. Phys. **C31**, 513 (1986); NA10 Collaboration, M. Guanziroli *et al.*, Ref. 117.

[125] J. S. Conway *et al.*, Phys. Rev. **D39**, 92 (1989).

[126] C. S. Lam and W. K. Tung, Phys. Rev. **D21**, 2712 (1980).

[127] A. Brandenburg, O. Nachtmann and E. Mirkes, Z. Phys. **C60**, 697 (1993).

[128] E. L. Berger and S. J. Brodsky, Phys. Rev. Lett. **42**, 940 (1979).

[129] S. J. Brodsky, E. L. Berger, G. P. Lepage, SLAC-PUB-3027, published in the *Proceedings of the Workshop on Drell-Yan Processes*, Batavia, IL, (1982).

[130] A. Brandenburg, S. J. Brodsky, V. Khoze, and D. Müller, SLAC-PUB-6464 (1994)

[131] E. L. Berger, Z. Phys. **C 4**, 289 (1980).

[132] S. Matsuda, Phys. Lett. **B 119**, 207 (1982).

[133] A. V. Efremov and A. V. Radyushkin, Phys. Lett. **B94**, 245 (1980); M. K. Chase, Nucl. Phys. **B167**, 125 (1980); S. J. Brodsky and G. P. Lepage, Phys. Rev. **D24**, 1808 (1981); E. Braaten, Phys. Rev. **D28**, 524 (1983); E. Maina and G. Farrar, Phys. Lett. **B 206**, 120 (1988); T. Hyer, Phys. Rev. **D48**, 147 (1993).

[134] J. Botts, Phys. Rev. **D44**, 2768 (1991); H. Li, G. Sterman, Nucl. Phys. **B381**, 129 (1992).

[135] P. Bosted, *et al.*, Phys. Rev. Lett. **68**, 3841 (1992).

[136] V. D. Burkert, CEBAF-PR-87-006. P. Stoler, Phys. Rev. **D44**, 73 (1991).

[137] A.S. Kronfeld B. Nizic, Phys.Rev. **D44**, 3445 (1991); ibid. **D46**, 2272 (1992). T. Hyer, SLAC-PUB-5889 (1992).

[138] S. J. Brodsky, J. F. Gunion, L. Frankfurt, A. H. Mueller, and M. Strikman, SLAC-PUB-6412 (1994).

[139] S. J. Brodsky, G. P. Lepage and San Fu Tuan, Phys. Rev. Lett. **59**, 621 (1987).

[140] M. Chaichian, N. A. Tornqvist, Nucl. Phys. **B323**, 75 (1989).

[141] S. S. Pinsky, Phys. Lett. **B236**, 479 (1990).

[142] Wei-Shou Hou and A. Soni, Phys. Rev. Lett. **50**, 569 (1983).

[143] P. G. O. Freund and Y. Nambu, Phys. Rev. Lett. **34**, 1645 (1975).

[144] S. J. Brodsky, A. H. Mueller, Phys. Lett. **206B**, 685 (1988).

[145] A. S. Carroll, *et al.*, Phys. Rev. Lett. **61**, 1698 (1988).

[146] S. J. Brodsky and G. de Teramond, Phys. Rev. Lett. **60**, 1924 (1988).

[147] M. Luke, A. V. Manohar, M. J. Savage, Phys. Lett. **B288**, 355 (1992).

[148] S. J. Brodsky, I. A. Schmidt, and G. F. de Teramond, Phys. Rev. Lett. **64**, 1011 (1990).

[149] G. C. Blazey *et al.*, Phys. Rev. Lett. **55**, 1820 (1985).

[150] J. F. Gunion, R. Blankenbecler, and S. J. Brodsky, Phys. Rev. **D6**, 2652 (1972).

[151] A. W. Hendry, Phys. Rev. **D10**, 2300 (1974).

[152] J. P. Ralston and B. Pire, Phys. Rev. Lett. **57**, 2330 (1986); Phys. Lett. **117B**, 233 (1982); University of Kansas preprint 5-15-92, (1992). See also G. P. Ramsey and D. Sivers, Phys. Rev. **D45**, 79 (1992); and C. E. Carlson, M. Chachkhunashvili, and F. Myhrer, Phys. Rev. **D46**, 2891 (1992).

[153] G. Alexander *et al.*, Phys. Rev. **154**, 1284 (1967).

[154] See, e.g. Ref. 58 and S. J. Brodsky and H.-C. Pauli, SLAC-PUB-5558 (1991), published in the *Proceedings of the 30th Schladming Winter School in Particle Physics.*

DATE
FILMED
6/17/94
END